miR-33 regulates cell proliferation, cell cycle progression and liver regeneration

DISSERTATION

Zur Erlangung des akademischen Grades

Doctor rerum naturalium

(Dr. rer. nat.)

Im Fach Biologie

Eingereicht an der

Mathematisch-Naturwissenschaftlichen Fakultät I

Der Humboldt Universität zu Berlin

Von

Daniel Cirera Salinas

Präsident der Humboldt-Universität zu Berlin

Prof. Dr. Jan-Hendrik Olbertz

Dekan der Mathematisch-Naturwissenschaftlichen Fakultät I

Prof. Dr. Stefan Hecht

Gutachter/innen: 1. Prof. Dr. rer. nat. Peter-Michael Kloetzel

2. Prof. Dr. rer. nat. Franz Theuring

3. Prof. Dr. med. vet. Anja Hauser

Tag der mündlichen Prüfung: 07.03.2013

ZUSAMMENFASSUNG

Der Cholesterin-Stoffwechsel ist sehr streng auf zellulärer Ebene reguliert und ist essentiell für das Zellwachstum. Zelluläre Ungleichgewichte des Cholesterin- und Fettsäure-Stoffwechsels führen zu pathologischen Prozessen, einschließlich Atherosklerose und Metabolisches Syndrom. MicroRNAs (miRNAs), eine Klasse nicht-kodierender RNAs, wurden als kritische Regulatoren der Genexpression identifiziert und entfalten ihre Wirkung vorwiegend auf posttranskriptioneller Ebene. Aktuelle Arbeiten aus der Gruppe um Fernández-Hernando und andere haben gezeigt, dass hsa-miR-33a und hsa-miR-33b, miRNAs die in den Intronsequenzen der Gene für die Sterol-regulatorischen Element-Bindungsproteine (SREBP-2 und SREBP -1) lokalisiert sind, den Cholesterin-Stoffwechsel im Einklang mit ihren Wirtsgenen regulieren. Gleichermaßen inhibiert miR-33 Schlüsselenzyme in der Regulation der Fettsäureoxidation, einschließlich Carnitin O-octanoyltransferase (CROT), Carnitinpalmitoyltransferase 1A (CPT1A), Hydroxyacyl-CoA Thiolase-Dehydrogenase/3-ketoacyl-CoA / Enoyl-CoA Hydratase (HADHB), Sirtuin 6 (SIRT6) und AMP-aktivierte Proteinkinase (AMPK) α, genauso wie das Insulin-Rezeptor-Substrat 2 (IRS2), eine wesentliche Komponente des Insulin-Signalwegs in der Leber.

Diese Studie zeigt, dass hsa-miR-33 Familienmitglieder nicht nur Gene in Cholesterin- und Fettsäure-Stoffwechsel sowie Insulin-Signalwege regulieren, sondern zusätzlich die Expression von Genen des Zellzyklus und der Zellproliferation modulieren. miR-33 inhibiert die Expression der Cyclin-abhängigen Kinase 6 (CDK6) und Cyclin-D1 (CCND1), wodurch sowohol die Zellproliferation als auch die Zellzyklusprogression verringert wird. Die Überexpression von miR-33 induziert einen signifikanten G1 Zellzyklusarrest. Durch eine Inhibierung der miR-33 Expression mittels 2'fluoro / Methoxyethyl-modifizierte (2'F / MOE-modifiziert) Phosphorothioat-Backbone Antisense-Oligonukleotiden, wird die Leberregeneration nach partieller Hepatektomie (PH) in Mäusen verbessert, was auf eine wichtige Rolle für miR-33 in der Regulation der Hepatozytenproliferation während der Leberregeneration hinweist.

Zusammengefasst zeigen diese Daten, dass miR-33 Signalwege reguliert, die drei der Risikofaktoren des Metabolischen Syndroms, nämlich HDL, Triglyzeride und Insulin-Signaling steuern, und legen nahe, dass Inhibitoren von miR-33 bei der Behandlung dieses zunehmenden gesundheitlichen Problems nützlich sein können. Ferner könnte der Srebf/miR-33 Locus kooperieren, um Zellproliferation und Zellzyklusprogression zu regulieren, und könnte somit auch relevant für die menschliche Leberregeneration sein.

Schlagwörter: CDK6, Cyclin D1, miR-33, Zellzyklus, microRNA

ABSTRACT

Cholesterol metabolism is tightly regulated at the cellular level and is essential for cellular growth. Cellular imbalances of cholesterol and fatty acid metabolism lead to pathological processes, including atherosclerosis and metabolic syndrome. MicroRNAs (miRNAs), a class of noncoding RNAs, have emerged as critical regulators of gene expression acting predominantly at posttranscriptional level. Recent work from Fernández-Hernando´s group and others has shown that *hsa-miR-33a* and *hsa-miR-33b*, miRNAs located within intronic sequences of the sterol regulatory element-binding protein (SREBP-2 and SREBP-1) genes, respectively, regulate cholesterol metabolism in concert with their host genes. Similarly, miR-33 targets key enzymes involved in the regulation of fatty acid oxidation including carnitine O-octanoyltransferase (CROT), carnitine palmitoyltransferase 1A (CPT1A), hydroxyacyl-CoA dehydrogenase/3-ketoacyl-CoA thiolase/enoyl-CoA hydratase (HADHB), sirtuin 6 (SIRT6) and AMP-activated protein kinase (AMPK)α, likewise, the insulin receptor substrate 2 (IRS2), an essential component of the insulin-signaling pathway in the liver. This study shows that hsa-miR-33 family members not only regulate genes involved in cholesterol and fatty acid metabolism and insulin signaling, but in addition modulate the expression of genes involved in cell cycle regulation and cell proliferation. Thus, miR-33 inhibited the expression of the cyclin-dependent kinase 6 (CDK6) and cyclin D1 (CCND1), thereby reducing cell proliferation and cell cycle progression. Over-expression of miR-33 induced a significant G1 cell cycle arrest and most importantly, inhibition of miR-33 expression using 2'fluoro/methoxyethyl-modified (2'F/MOE-modified) phosphorothioate backbone antisense oligonucleotides improved liver regeneration after partial hepatectomy (PH) in mice, suggesting an important role for miR-33 in regulating hepatocyte proliferation during liver regeneration. Altogether, these data establish that miR-33 regulates pathways controlling three of the risk factors of metabolic syndrome, namely levels of HDL, triglycerides and insulin signaling, and suggest that inhibitors of miR-33 may be useful in the treatment of this growing health concern. Furthermore, *Srebf/miR-33* locus may co-operate to regulate cell proliferation, cell cycle progression and may also be relevant to human liver regeneration.

Keywords: CDK6, Cyclin D1, miR-33, cell cycle, microRNA

Table of Contents

ABBREVIATIONS

ABCA1	ATP-binding cassette sub-family A member 1
Akt	protein kinases B
AMPKα	AMP-activated protein kinase α
ApoA-1	apolipoprotein A-1
ATP	adenosintriphosphate
bp	base pair
BSA	bovine serum albumin
ºC	degree celsius
CCND	cyclin D
CDK	cyclin-dependent kinase
cDNA	complementary DNA
CPT1A	carnitine palmitoyltransferase 1A
CROT	carnitine O-octanoyltransferase
DMEM	Dulbecco´s modified Eagle medium
DMSO	dimethylsulfoxide
DNA	deoxyribonucleic acid
DNAse	deoxyribonuclease
dNTP	deoxynucleotidetriphosphate
EDTA	ethylene diamine tetraacetic acid
ES	embryonic stem
gr	gram
GFP	green fluorescent protein
GTP	guanosine-5´-triphosphate
HADHB	hydroxyacyl-CoAdehydrogenase/3-ketoacyl-CoAthiolase/enoyl-CoAhydratase
HDL	high-density lipoprotein
HEPES	N-(-hydroxymethyl) piperazin, N'-3-propansulfoneacid
hr(s)	hour(s)
IRES	internal ribosomal entry site
IRS2	insulin receptor substrate 2
kb	kilobase
LDLr	low density lipoprotein receptor
M	molarity
mRNA	messenger ribonucleic acid
miRNA	microRNA
mg	milligram
μg	microgram
ng	nanogram
ml	milliliter
μl	microliter
μm	micrometer
min	minute
N	normal
neo	neomycin resistanse
ORF	open reading frame
pA	polyadnylation signal
PAGE	polyacrylamide gel electrophoresis
PCR	polymerase chain reaction
PH	partial hepatectomy
pH	preponderance of hydrogen ions
pmol	picomol
PBS	phosphate buffered saline
RNA	ribonucleic acid
RNAse	ribonuclease
rpm	revolution per minute

RT   room temperature
RT-PCR   reverse transcriptase-PCR
SDS   sodium dodecylsulfate
SDS-PAGE   SDS-polyacrylamide gel electrophoresis
sec   second
SIRT6   sirtuin 6
SREBP   sterol regulatory element-binding protein
SV40 pA   SV40 polyadenylation site
TE   Tris-EDTA solution
TEMED   tetramethylethylene diamine
tk   viral tyrosine kinase
Tris   tris(hydroxymethyl)-aminomethane hydrohycloride
UV   ultra violet
V   voltage

Symbols of nucleic acid

A   adenine
C   cytosine
G   guanine
T   thymine
U   uridin

1 INTRODUCTION

1.1 Regulation of cholesterol metabolism

Cholesterol is an essential component of mammalian membranes and a precursor in metabolic pathways, including steroid hormones and bile acids [1-4]. Cells require cholesterol to modulate membrane fluidity and permeability, for proliferation, cell growth and division, as well as during embryonic development [1-4]. Cholesterol homeostasis thus needs to be tightly regulated, and dysregulation of lipid metabolism is a primary perturbation associated with the development of many diseases such as atherosclerosis, metabolic syndrome and type II diabetes [5, 6].

Animal cells synthesize cholesterol from acetyl coenzyme A (acetyl-CoA) in a highly regulated enzymatic pathway [7], including more than 20 enzymatic reaction steps [8]. In addition, cells obtain cholesterol from the circulation via apolipoprotein B-containing lipoproteins, such as low density lipoprotein (LDL) [1, 9]. LDL particles are internalized by the peripheral cells via the LDL receptor (LDLr), receptor-mediated endocytosis, and are hydrolyzed to free cholesterol in the lysosomes [1, 9]. Intracellular cholesterol levels are tightly controlled by feedback mechanisms that operate at both, transcriptional and posttranscriptional levels [10, 11]. When intracellular levels of cholesterol are low, the endoplasmic reticulum (ER)-bound sterol regulatory element-binding proteins (SREBPs) coordinate the transcription of 3-hydroxy-3-methylglutaryl coenzyme A reductase (HMGCoAR), a rate-limiting enzyme of the biosynthetic pathway, and almost all down-stream enzymes of the mevalonate (MVA) pathway [12]. SREBPs also activate the transcription of the LDLr, which leads to an increase in cellular cholesterol uptake [10]. In contrast, when cells accumulate excess sterols, the activity of HMGCoAR declines more than 90% and the cell surface expression of LDLr decreases [10]. The SREBP family of basic-helix-loop-helix-leucine zipper (bHLH-LZ) transcription factors consists of SREBP1a, SREBP1c and SREBP-2 proteins encoded by two unique genes, *Srebf-1 and Srebf-2*. The SREBPs differ in their

tissue-specific expression, the target genes selectivity and the relative potencies of their transactivation domains. SREBP2 preferentially controls the synthesis and uptake of cholesterol, through the regulation of both LDLr and HMGCoAR, whereas SREBP1a and SREBP1c regulate genes involved in the synthesis of fatty acids and, as more recently found, cell cycle regulation [11, 13-15]. When intracellular levels of cholesterol are high, the liver X receptor (LXr), a nuclear hormone receptor, also contributes to the cholesterol homeostasis by activating the transcription of genes involved in cholesterol efflux, including the ATP-binding cassette transporters, ABCA1 and ABCG1 [16] (**Figure 1**). These transporters promote cellular cholesterol efflux to high-density lipoprotein (HDL) and its associated apolipoprotein, ApoA-1, a crucial step in the initiation of reverse cholesterol transport to the liver for excretion into bile [17, 18]. Because HDL levels correlate inversely with the susceptibility to atherosclerosis, there is an increasing interest in studying the regulation, mechanism of action, and suitability of ABCA1 as a target to increase HDL levels for the treatment and prevention of atherosclerosis [19].

Figure 1. Regulation of cellular cholesterol homeostasis. Animal cells synthesize cholesterol from acetyl-CoA.

In addition, cells obtain cholesterol from the circulation in the form of apolipoprotein B-containing lipoproteins, particularly LDL. The circulating LDL particles carrying cholesterol and cholesterol esters are internalized through LDLr and transported to sorting endosomes. LDL particles are subsequently transported to late endosomes and lysosomes, whereas LDL receptors are recycled to the plasma membrane. Free cholesterol egress from endosomes and lysosomes in a process mediated by Niemann-Pick type C 1 and 2 proteins (NPC1 and NPC2). Under low intracellular cholesterol concentration, the SCAP-SREBP complex moves to the Golgi where the SREBP is processed to its nuclear form. The nuclear SREBP turns on genes involved in cholesterol biosynthesis (e.g. HMGCoAR) and cholesterol uptake (LDLr). Conversely, in response to cellular cholesterol excess, the oxysterols generated bind and activate the liver X receptor (LXr), which heterodimerize with retinoic X receptor (RXR) and activate the expression of ATP transporters (ABCA1 and ABCG1). ABCA1 and ABCG1 promote cholesterol efflux via apoA1 and HDL, respectively, and help to maintain intracellular cholesterol homeostasis (Modified from Moore *et al.* [20])

1.2 Regulation of the cell cycle

To ensure proper growth and maintenance of an organism, mammalian cells exhibit a rigorously controlled cycle of growth and cell division. Cell division leads, via mitosis and cytokinesis, to two equal daughter cells. Proliferation describes cell growth, accumulation of cell properties and subsequent cell division. There are four main parts of the cell cycle, the mitosis (M phase), and the three interphases, first gap (G1), synthesis (S) and second gap (G2) [21-23]. Immediately after cell division RNA and proteins start to accumulate. This period of the cell cycle between the end of mitosis and the subsequent onset of DNA synthesis is termed G1. Usually this gap takes 12 to 15 hours. Variances in cycle duration are mostly due to differences in entering and exiting G1 phase, and to an optional break in quiescence state (G0); or even entering the differentiation modus [21-23]. This is mostly influenced by growth factors in the cell's surroundings. In sufficient concentrations these extracellular signals will encourage a cell to continue progressing the cell cycle, or their absence will trigger the cell to proceed into G0. This critical decision point in the cell cycle, several hours before the end of G1, is termed restriction point (R point) [21-23]. This also resembles the point of no return, and once the cell has passed this critical point, it will proceed with the G1/S phase transition. The following S phase, during which the DNA synthesis occurs, typically requires 6 to 8 hours to reach completion. The G2 phase takes 3 to 5 hours. Finally, the M phase extends approximately one hour, and includes four distinct subphases: prophase, metaphase, anaphase, and telophase. Mitosis finishes with cytokinesis: the division of the cytoplasm [21-23]. There are several DNA damage control points in G1 and G2 phases and the spindle-assembly checkpoint in the M phase [23].

The time a cell needs to progress through the cell cycle is greatly depending on cell type and on circumjacent conditions. The indicated lengths of each phase are commonly observed in cultured cells. Hence, actively proliferating lymphocytes may double in only 5 hours, and some cells in the early embryo may do so even more rapidly [24-27].

Controlled cell cycle progression is driven mainly by protein complexes composed of two subunits: a cyclin and a corresponding cyclin-dependent kinase (CDK). CDKs are small serine/threonine kinases that require association with a cyclin subunit for their activation. Cyclin/CDKs catalyze the phosphorylation of specific target substrates. These phosphorylation events are transient and reversible. When the cyclin/CDK complex disassembles, the phosphorylated substrates are rapidly dephosphorylated by protein phosphatases [28, 29]. Active cyclin/CDK complexes lead to the activation of transcription factors, which induce the transcription of the next set of cyclins and CDKs. Consequently, there is a rapid turnover and a tight regulation, which involves controlled transcription and degradation of cyclins. Regulation also involves the activation and inhibition of the CDKs via phosphorylation/dephosphorylation events, and the control of inhibitory proteins that associate with cyclin/CDK complexes [30-32] (**Figure 2**). During G1 phase, the D-type cyclins (CCND1, CCND2, and CCND3) bind and activate CDK4 and CDK6 [33-35]. Both CDKs have similar enzymatic activities. In late G1 after the R point, CDK2 primarily interacts with E-type cyclins (CCNE1 and CCNE2) to phosphorylate specific substrates required for the initiation of DNA replication and centrosome duplication in the S phase [36-41]. When the cells enter the S phase, the A-type cyclins (CCNA1 and CCNA2) substitute CCNE1 and CCNE2 as partners of CDK2 to promote progression through the S phase. Cyclin A phosphorylates proteins involved in DNA replication, such as CDC6 [42-44]. At the end of the S phase, the A-type cyclins now associate with CDK1 (CDC2) [44-46]. Moving further into G2 phase, CDK1 largely associates to the mitotic B-type cyclins (CCNB1 and CCNB2). During G2/M transition, cyclin A activity is needed for the initiation of the prophase [47]. At the mitotic exit, the cyclin/CDK complexes are required for chromosomal alignment and progression to the anaphase [48-50]. At the onset of the M phase, the B-type cyclin/CDK1

complex triggers many of the essential procedures that constitute mitosis and end in cytokinesis [51, 52]. The levels of CDKs slightly vary during cell cycle, only the cyclins fluctuate in a cell cycle dependent manner, thereby their name. For example, cyclin B strongly increases at the onset of mitosis to associate with CDK1. At the end of the M phase, cyclin B levels drop due to rapid degradation and is undetectable at the beginning of the next cell cycle. The only exceptions in fluctuating levels are the D-type cyclins, which are constantly expressed [53, 54].
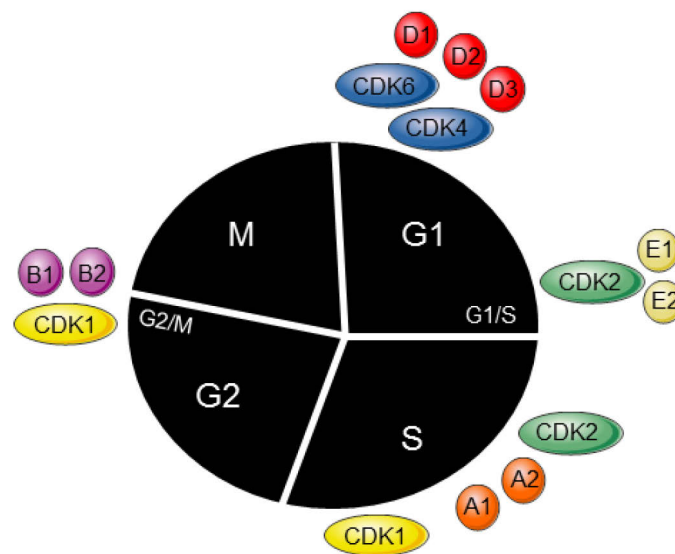
Figure 2. Mammalian cell-cycle regulation. According to classical model of cell cycle regulation Cdk4, Cdk6, Cdk2 and Cdk1 complex with phase-specific cyclins at different stages of cell cycle to coordinate initiation and progression of cell cycle. (Adapted from Satyanarayana *et al*. [55])

1.3 Mechanisms of action and biogenesis of miRNAs

In addition to the classical transcriptional regulators, members of a class of non-coding RNAs, termed microRNAs (miRNAs), have lately been identified as important post-transcriptional regulators of gene expression [56-59]. miRNAs are small (22 nucleotides), single-stranded, non-coding RNAs, which were first discovered in the nematode *Caenorhabditis elegans* [60, 61]. They are encoded in the genomes of almost all eukaryotes and some viruses [59]. miRNAs typically control the expression of their target genes by primarily acting as sequence specific inhibitors of the corresponding messenger RNA

(mRNA). This inhibitory effect can occur by either transcript destabilization, translational inhibition, or both [58, 59, 62]. Bioinformatics predictions and experimental approaches indicate that a single miRNA could target more than one hundred mRNAs [63]. Indeed, human miRNAs are predicted to control the activity of more than 60% of all protein-coding genes [59, 63, 64]. miRNAs have now been implicated in the control of a wide range of biological functions including development, differentiation, metabolism, growth, proliferation and apoptosis [65-70].

miRNAs are located through the genome within exonic and intronic portions of protein-coding genes, as well as in intergenic regions [56-59]. As illustrated in **Figure 3**, the production of functional 22 nucleotides mature miRNA involves multiple processing steps. Most animal miRNAs are transcribed in the nucleus by RNA polymerase II as stem-loop long primary transcripts (pri-miRNA) [71]. The pri-miRNAs are usually thousands of nucleotides long and contain local hairpin structures. Following transcription, they are processed sequentially in the nucleus and cytoplasm by a complex of RNase-III endonucleases: the so called Drosha and Dicer. Specifically, Drosha processes the pri-miRNA transcript to a 70-100 nucleotide stem-loop precursor RNA (pre-miRNA), which is then delivered to the cytoplasm by Exportin 5, where it is subsequently cleaved by Dicer to produce a ~22 nucleotides miRNA:miRNA* duplex (canonical pathway) [56, 58, 59]. However, a subset of intronic miRNAs called "miRtrons" can circumvent the Drosha pathway and are made by splicing and debranching of short hairpin introns [72-74]. The Dicer cleavage can alternatively be conducted by Ago2, an Argonaute protein that is part of the complex that aligns the miRNA and the mRNA [75-77]. Once in the cytoplasm, one of the duplex strand (miRNA or miRNA*) is preferentially incorporated into the RNA-induced silencing complex (RISC) in association with an Ago family member [56, 58, 59]. Within the RISC-Ago-entity, the miRNA guides the complex to its RNA target, thereby mediating its repression. In animals, miRNAs control gene expression by binding to the 3´UTR of their target genes through Watson-Crick base pairing between the target and the 5'-end of the miRNAs: representing the "seed sequence" (nucleotides 2-8) [56, 58, 59]. However, recent studies suggest that miRNAs might also repress mRNA targets by

binding to other regions including 5´UTR or protein-coding exons [78-81]. This interaction typically leads to translational repression of target mRNAs by either transcript destabilization, translational inhibition, or both [56, 58, 59].

Identifying functionally important miRNA target genes is crucial for understanding the impact of specific miRNAs on cellular function. This has been challenging, because miRNAs usually have imperfect complementarity with their targets [58]. In mammals, the most consistent requirement of miRNA-target interaction, although not always essential, is a contiguous and perfect base pairing of the miRNA at the nucleotides 2-8, the "seed sequence". In many cases, the seed seems to determine this recognition. However, in other cases, additional determinants are required, such as reasonable complementarity to the miRNA 3´half to stabilize the interaction (nucleotides 13-16). In addition, some other features of the 3´UTR sequences surrounding the target site, such as AU-rich sequences, positioned within the 3´UTR at least 50 nucleotides from the stop codon and away from the center of long UTRs, could boost miRNA efficacy [58]. The existence of multiple public miRNA target prediction algorithms has greatly facilitated the rapid identification of miRNA target genes, which however, still require validation.
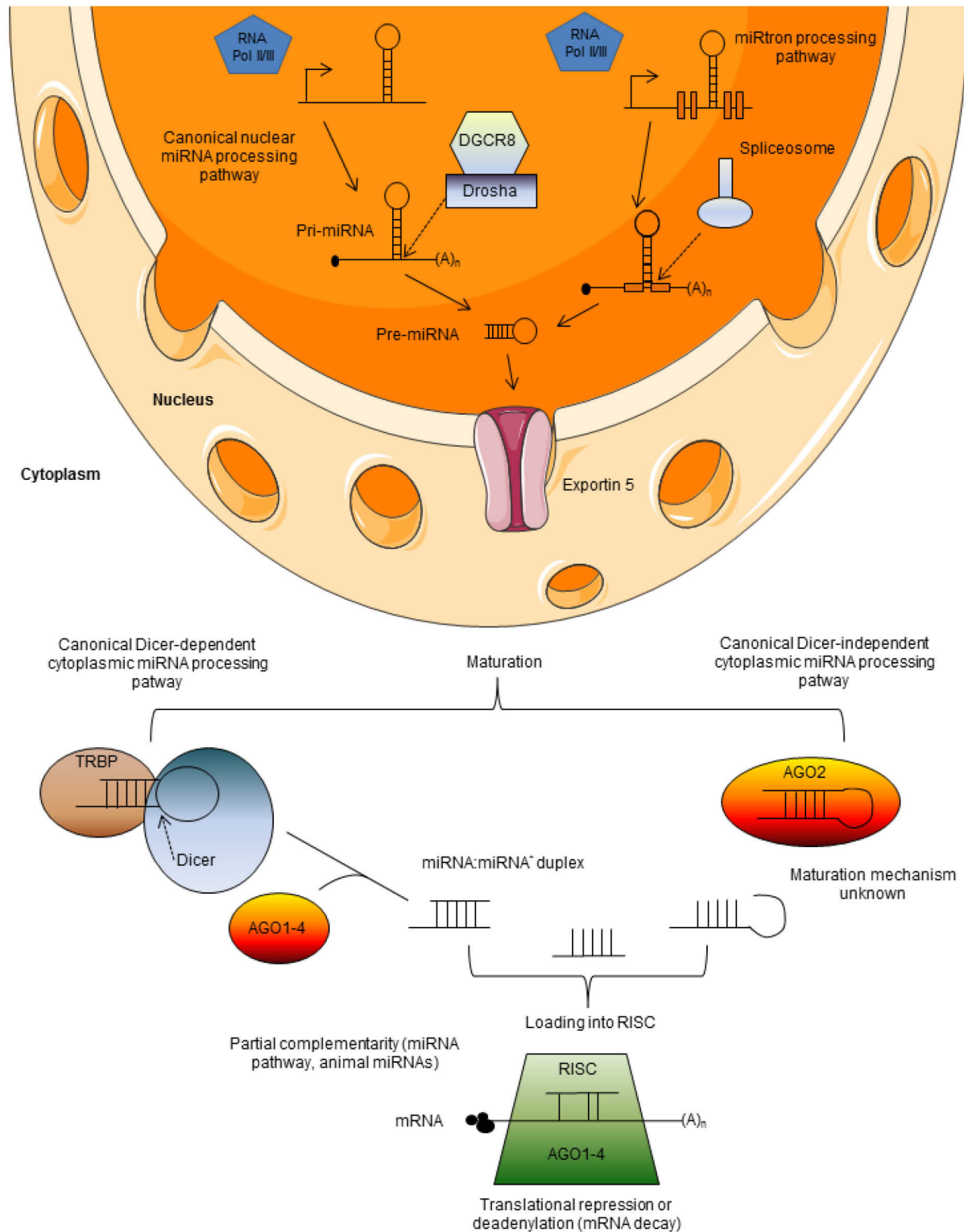
Figure 3. **miRNA biogenesis and function**. miRNAs are transcribed in the nucleus into primary transcripts (pri-miRNAs). They are transcribed from independent miRNA genes, from polycistronic transcripts or from introns of protein-coding genes. Pri-miRNAs are then processed in two steps in the nucleus and cytoplasm, catalyzed by the RNase III type endonuclease Drosha and Dicer, respectively. These enzymes function in complexes with dsRNA-binding domains proteins, DGCR8 and TRBP for Drosha and Dicer, respectively. In the canonical pathway (illustrated here) Drosha-DGCR8 processes the transcript to a stem-loop-structured precursor (pre-miRNA). A subset of miRNAs, called miRtrons, also derived from introns, is processed into pre-miRNAs by the spliceosome and the debranching enzyme. Both canonical miRNAs and miRtrons are exported to the cytoplasm via Exportin 5, where they are further processed by Dicer-TRBP to yield ≈ 20-bp miRNA duplexes. The typical Dicer cleavage product features 5′ phosphate groups and two-nucleotide overhangs at the 3′ ends. One strand is selected to function as mature miRNA and loaded into the RISC, while the partner miRNA* strand is preferentially degraded. In contrast, the precursor of miR-451 is recognized directly by Ago2. The unusual structure of the precursor (short stem, miRNA sequence spans the loop) promotes binding and cleavage by Ago2 after the 30th

nucleotide. Therefore, miR-451 is produced independently of Dicer. The miRNA is further matured by so far unknown mechanisms. The mature miRNA produced by these two mechanisms leads to translational repression or mRNA degradation. The key components of the RISC are components of the Argonaute family (Ago 1–4). Animal miRNAs usually show only partial complementarity to the target mRNA promoting translational repression (initiation and post initiation steps) or deadenylation coupled to exonucleolytic degradation of target mRNA. mRNAs repressed by deadenylation or at the translation-initiation step are moved to P-bodies for either degradation or storage (Modified from Suarez *et al*.[70]).

1.4 miRNAs and cell cycle

Deregulated miRNA expression can result from impaired miRNA processing, copy number alterations of miRNA encoding loci, or the methylation of miRNA promoter regions. Many miRNAs are located in chromosomal regions subjected to abnormalities in human cancer. Tumor suppressors maintain cell cycle checkpoint integrity and regulate apoptotic responses, so copy number loss at these loci can enhance tumorigenesis and contribute to a poor clinical outcome. Deletion of certain miRNA loci in distinct tumor types, and correlation of miRNA deletion with poor clinical prognosis has led to the prediction that miRNAs may act as tumor suppressors [67]. Croce and colleagues provided some of the first evidence that specific miRNA loci may act as human tumor suppressors [82]. For years, it has been known that deletions at chromosome 13q14 are common in chronic lymphocyte leukemia (CLL). However, despite intensive efforts, no loss of protein encoding transcript could be linked to these deletions. More recently, Calin *et al.* showed that the chromosomal region deleted in CLL contains the miRNA cluster encoding miR-15a and miR-16-1. Reduced expression of miR-15a and miR-16 was observed in 75% of CLL cases harboring this deletion. Subsequent studies showed that over-expression of the miR-15a/miR-16-1 cluster in a leukemia-derived cell line repressed levels of the anti-apoptotic protein BCL2 and induced apoptosis [83]. Another recent study suggested that miR-16 family miRNAs may directly regulate cell cycle progression and proliferation by controlling the G1 checkpoint. Over-expression of miR-16 family microRNAs led to induction of G0/G1 arrest in cultured human tumor cells [31]. Many miR-16 targets were identified, whose repression could induce G0/G1 accumulation. One of these targets was CDK6 [84], which is activated when it binds D-type cyclins in early G1 phase, as described before. CDK6/cyclin D complexes participate in the sequential hyperphosphorylation of retinoblastoma protein (RB) by CDK4/6 and CDK2 to repress RB

mediated inhibition of the transcription factor E2F, which positively regulates G1 to S phase progression.

In several neuroblastoma (NB) cell lines overexpression of miR-184 induced cell cycle arrest at G1, followed by apoptosis [85]. On the other hand, miR-34a loss has also been associated with NB. Comparative genomic hybridization demonstrated that miR-34a is located in the minimal region of 1p loss in NB tumors with 1p deletions and deletion of chromosome 1p was connected to poor NB prognosis [86]. In addition, expression of miR-34a was reduced in NB cell lines and advanced stage primary NB tumors relative to normal tissue [86]. Contrary, overexpression of miR-34a in several NB cell lines induced growth arrest followed by apoptosis [86]. E2F was identified as a putative miR-34a target, and both the activity of a luciferase-based reporter construct containing the E2F miR-34 target site in its 3' UTR and levels of endogenous E2F protein were reduced by miR-34a overexpression [86]. These data were interpreted to indicate that miR-34a exhibits the characteristics of a tumor suppressor in NB. The miR-34 family comprises three highly conserved miRNAs: miR-34a, miR-34b and miR-34c. Recently, miR-34 family members were shown to be directly regulated by the tumor suppressor p53 [87-90]. Overexpression of each miR-34 family member caused cell cycle arrest at G1, downregulation of a significant number of cell cycle related genes [87] and overlapped significantly with genes regulated by DNA damage [86]. These observations suggest that the miR-34 family plays a role in the p53-mediated DNA damage checkpoint by downregulating cell cycle genes and eliciting G1 arrest. He *et al*. validated several of the downregulated genes as direct targets by showing miR-34 regulation of reporters engineered to contain the 3' UTRs of the respective targets. These target genes included CDK4, CCNE2, and a receptor tyrosine kinase (MET) [87].

In addition, Liu *et al*. identified miR-137 as a potential regulator of *Cdc42* expression, one of the best characterized members of the Rho GTPase family upregulated in several human tumors. Expression of miR-137 in colorectal cancer cell lines inversely correlated, both at the mRNA and the protein level, with *Cdc42* expression and the transfection with the miRNA could significantly suppress *Cdc42* 3'UTR luciferase-reporter activity. Finally, the

downregulation of Cdc42 by miR-137 inhibited proliferation inducing G1 cell cycle arrest and blocked the invasion of colorectal cancer cells, whereas anti-miR-137 expression induced the opposite effect [91].

In summary, accumulating evidence suggests that other miRNAs may also directly regulate cell cycle checkpoints and cellular proliferation.

1.5 Cholesterol and cell cycle

The requirement of cholesterol for cell growth and cell division of mammalian cells has been known for many years [2, 3, 92], but whether this is just a consequence of its use for membrane formation or whether it also plays a regulatory role during cell cycle has not yet been clarified. Cholesterol is also required for cell cycle progression, and its deficiency leads to cell cycle arrest in G2/M [93]. Moreover, other non-mevalonate derivates are essential for the G1-S transition, thus confirming the relationship between the cholesterol synthesis pathway and cell cycle progression [94, 95]. SREBPs have also been implicated in the regulation of cell cycle [96]. Bengoechea-Alonso *et al*. have demonstrated that siRNA-mediated silencing of SREBP1 in human HeLa, U2OS and MCF-7 cells lead to an accumulation of cells in late G1 phase, prior to the G1/S transition [96]. By contrast, SREBP1-a overexpression, activated the transcription of p21WAF1/CIP1, a universal cyclin-dependent kinase inhibitor, leading to cell growth inhibition and G1 cell cycle arrest [97]. In addition to p21WAF1/CIP1, SREBP-1a activation also increased the accumulation of other CDK inhibitors, including p27 and p16, leading to reduced CDK2 and CDK4 activities and hypophosphorylation of RB protein [98]. Interestingly, SREBP-1a transgenic mice exhibited impaired liver regeneration after partial hepatectomy [98].

1.6 miR-33 is a key regulator of cholesterol metabolism

Most recently, several independent groups including Fernández-Hernando´s laboratory, have identified miR-33a and miR-33b, intronic miRNAs located within the *Srebf-2* and *Srebf-1* genes, respectively [99-101]. The same metabolic pathways that activate the expression of

Srebf-2 and *Srebf-1* lead to an increased expression of miR-33a and miR-33b respectively, suggesting a coregulation between the host genes and the corresponding miRNAs. Moreover, Horie *et al.* recently cloned fragments of the mouse *Srebf-2* gene including miR-33a (Exon 16-17) and showed that miR-33a is coordinately expressed when *Srebf-2* is activated [102]. miR-33a target genes were found to be involved in cholesterol trafficking, including ABCA1, ABCG1, and Niemann-Pick type C1 protein (NPC1) [99-101, 103]. Interestingly, ABCA1, a transporter responsible for the movement of cholesterol out of the cell, was among the top predicted target genes for miR-33a. miR-33a overexpression strongly repressed ABCA1 expression and decreased cellular cholesterol efflux to ApoA-1. Conversely, antagonism of endogenous miR-33 upregulated ABCA1 expression *in vitro* and *in vivo*, and promoted cholesterol efflux to ApoA-1, further confirming the physiological effects of miR-33 [99-101, 103]. Similar results were observed in mouse peritoneal macrophages isolated from miR-33 null mice [102]. miR-33 also targets ABCG1, but only in rodents [101]. Accordingly, miR-33 repressed cholesterol efflux to mature HDL in mouse cells but not in human cells [101]. Together, these findings establish a reciprocal pathway in which, during sterol-poor conditions, miR-33a is coincidentally generated with SREBP-2 and increases cellular cholesterol levels by downregulating ABCA1 and ABCG1 and thus, limits cholesterol efflux (**Figure 4**).

As mentioned above, ABCA1 plays a key role in regulating HDL biogenesis *in vivo*. Remarkably, antagonists of miR-33 *in vivo* using locked nucleic acid (LNA)-modified oligonucleotides, lentivirus and adenovirus significantly increased the expression of ABCA1 in the liver and the plasma HDL levels. Similar results were observed in miR-33 knockout mice [102]. Low levels of HDL correlated with increased cardiovascular disease risk, thereby the regulation, mechanism of action, and suitability of ABCA1 are a target to increase HDL levels for the treatment and prevention of atherosclerosis [102]. To assess whether or not anti-miR-33 therapy increases reverse cholesterol transport and promotes regression of atherosclerosis, Rayner and colleagues treated LDLr-/- mice with established atherosclerotic plaques with anti-miR-33 oligonucleotides. Interestingly, mice treated with anti-miR-33

oligonucleotides presented smaller plaques with increased fibrous caps and reduced necrotic cores, phenotypic characteristics of stable plaques and less severe atherosclerosis [104].

1.7 miR-33 coordinates genes regulating fatty acid and glucose metabolism

In addition to the cholesterol transporter genes, ABCA1, ABCG1 and NPC1, two independent studies have recently shown that miR-33a and miR-33b binding sites are highly conserved in the in the 3´UTR of genes involved in fatty acid oxidation including, *Cpt1a*, *Crot*, *Hadhb*, and *Ampk* [103]. Gerin´s and Fernández-Hernando´s groups have demonstrated that miR-33 decreased the expression of CPT1a, CROT, and HADHB at the mRNA and the protein level [101,103]. Furthermore, overexpression of miR-33a and miR-33b reduced fatty acid oxidation and lead to the accumulation of triglycerides in human Huh7 hepatic cells and in the fat body of miR-33 transgenic flies [105]. Moreover, miR-33 was shown to inhibit the expression of AMPK, a cellular energy sensor that coordinates hepatic lipid metabolism at the transcriptional and post-transcriptional level. In the liver, activation of AMPK promoted fatty acid oxidation, while inhibiting cholesterol and triglyceride synthesis [106]. Taken these results together, miR-33a and miR-33b appear to be fundamental modulators of lipid metabolism by limiting cellular cholesterol efflux and fatty acid degradation upon SREBP induction (**Figure 4**).

Previous work from Fernández-Hernando´s laboratory also revealed an interesting role for miR-33 in glucose metabolism, as miR-33 overexpression inhibited IRS2, an essential docking molecule that mediates the effects of insulin [105]. Consistent with these findings, miR-33 overexpression reduced insulin-induced 2-deoxyglucose (2-DOG) uptake in hepatic cells [105]. In addition, miR-33 inhibited SIRT6, which has been involved in regulating fatty acid and glucose homeostasis. Indeed, hepatic-specific disruption of SIRT6 in mice resulted in the formation of "fatty liver" because of enhanced glucolysis and triglyceride synthesis [105]. More work needs to be done to elucidate the function of miR-33 concerning glucose metabolism, but unpublished data strongly suggest an essential role of miRNA-33 as a modulator of lipid, cholesterol and carbohydrate metabolism.
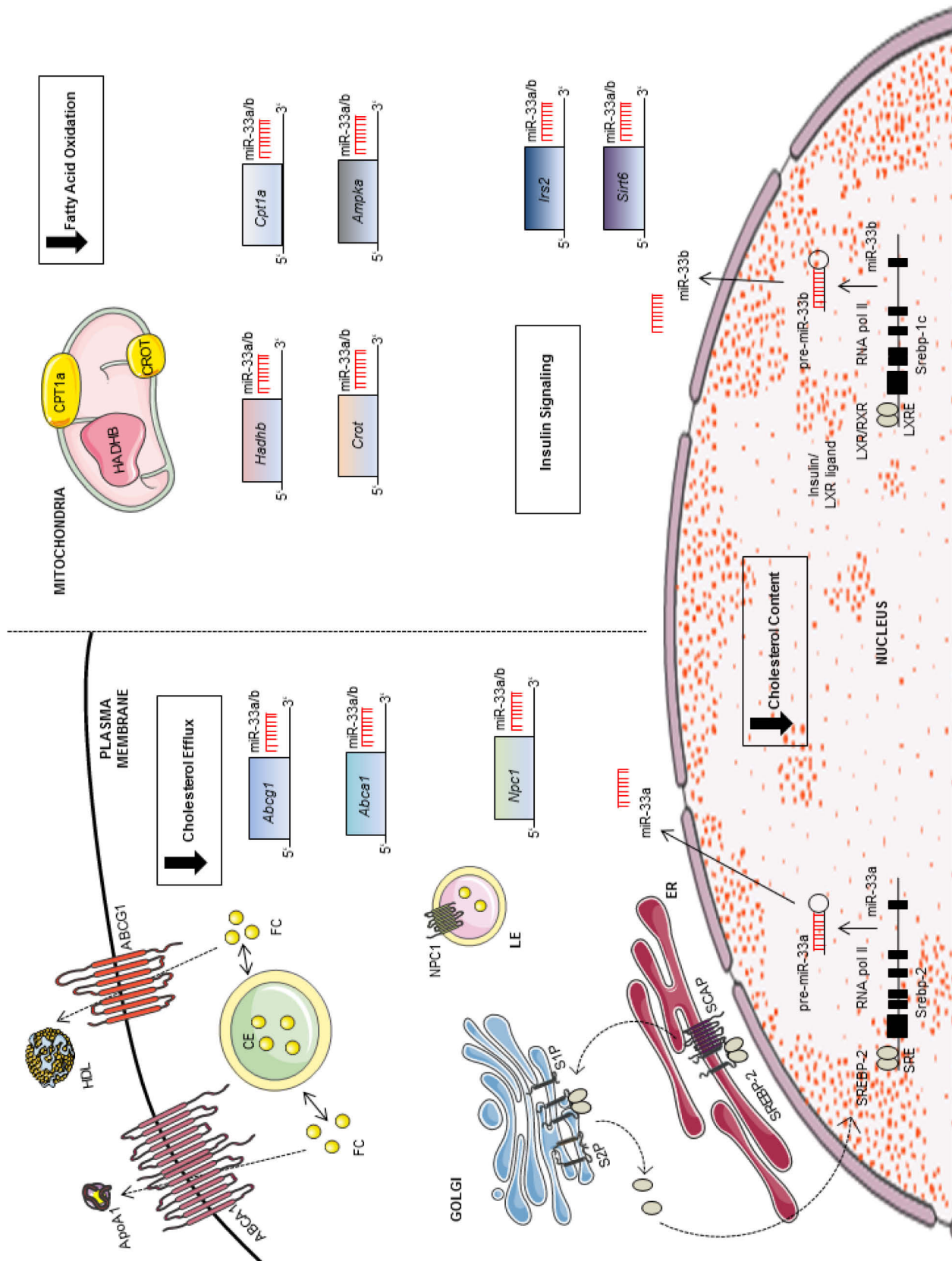
Figure 4. Maintenance of cholesterol, fatty acid and carbohydrate metabolism by sterol regulatory element binding proteins (SREBPs) and miR-33a and -b in hepatocytes. In hepatocytes, when intracellular cholesterol levels are low, SREBP-2 is sequentially cleaved in the Golgi by two membrane-bound proteases, site-1 protease (S1P) and site-2 protease (S2P). The N-terminal fragment is released and translocates to the nucleus, where it acts as a transcription factor to regulate genes containing a sterol response element (SRE), including Srebp-2. Conversely, the Srebp-1c promoter contains a liver X receptor (LXR) binding site that activates SREBP-

1c transcription in the presence of LXR agonists or insulin. Activation of SREBP-2 or SREBP-1 results in the cotranscription of miR-33a and miR-33b, respectively. These miRNAs simultaneously inhibit the expression of genes involved in cholesterol transport (ABCA1, ABCG1, and NPC1) and fatty acid oxidation (CROT, CPT1a, HADHB, and AMPK), thereby decreasing reverse cholesterol transport and reducing fatty acid β-oxidation. miR-33a and miR-33b also contribute to the regulation of glucose metabolism, by targeting IRS2 and SIRT6.
HDL, high density lipoprotein; ABCA1, ATPbinding cassette transporter A1; ABCG1, ATP-binding cassette transporter G1; FC, free cholesterol; CE, cholesteryl ester; NPC1, Niemann-Pick disease, type C1; LE, late endosome; ER, endoplasmic reticulum; SCAP, SREBP cleavage activating protein; RXR, retinoid X receptor; LXRE, liver X receptor element; CPT1a, carnitine palmitoyltransferase 1A ; CROT, carnitine Ooctanoyltransferase; HADHB, hydroxyacyl-CoA dehydrogenase/3-ketoacyl-CoA thiolase/enoyl-CoA hydratase (trifunctional protein), beta subunit; IRS2, insulin receptor substrate 2; SIRT6,sirtuin 6 (Modified from Ramírez *et al*. [107]).

1.8 A role for miR-33 in cell cycle regulation

Recently, Herrera-Merchán *et al*. reported that in super-p53 mice (sp53), which carry one extra gene dose of p53, the miR-33 is downregulated in hematopoietic stem cells (HSCs) and highly expressed in multipotent progenitors. Transplantation assays of miR-33-transduced sp53 HSC resulted in a significant acquisition of repopulating capacity and a decrease of recipients' survival. Moreover, high levels of miR-33 repressed the endogenous level of p53 protein in murine embryonic fibroblasts (MeFs), lead both to neoplastic transformation and anchorage independent growth of MeFs, and provoked a decrease of apoptotic response using tumor-derived cell lines. Accordingly, it was demonstrated that miR-33-mediated downregulation of p53 is dependent on the binding of miR-33 to two conserved motifs in the 3'UTR of p53 [108].

Likewise, a group in Marburg also newly established miR-33a as a miRNA with potential tumor suppressor activity, acting through inhibition of the proto-oncogene serine/threonine-protein kinase (Pim)-1[109]. A screen for miRNA expression in K562 lymphoma, LS174T colon carcinoma and several other cell lines revealed generally low endogenous miR-33a levels relative to other miRNAs. After transfection of K562 and LS174T cells with miR-33a a substantially reduced Pim-1 levels were observed. Seed mutagenesis of the Pim-1 3′UTR region in a luciferase reporter construct and in a Pim-1 cDNA expressed in Pim-1-deficient Skov-3 cells demonstrated specific and direct downregulation of Pim-1 by the miR-33a mimic [109]. The persistence of this effect was comparable to that of a small interfering RNA-mediated knockdown of Pim-1, resulting in decelerated cell proliferation. In conclusion, the potential of miR-33a to act as a tumor suppressor miRNA, which suggests miR-33a

replacement therapy through delivery of miRNA mimics as a novel therapeutic strategy, was demonstrated [108-109].

Similarly to Srebp/miR-33 locus, the α-mysion heavy chain (alphaMHG) gene, in addition to encoding a major cardiac contractile protein, regulates cardiac growth and gene expression in response to stress and hormonal signaling through miR-208 [110]. Altogether, the observations strongly suggest that intronic miRNAs work in conjunction with host genes to regulate similar cellular processes.

1.9 Aim of the project

Previous experiments in our laboratory clearly showed miR-33a to be cotranscribed with its host gene *Srebf-2* like many intronic miRNAs. Among other genes regulated by miR-33a are: ABCA1, which is involved in cholesterol export and efflux to Apo-A1; ABCG1, which is reducing cholesterol efflux to nascent HDL; and NPC1, which is regulating endolysosomal cholesterol transport. This regulatory function of miR-33a ensures that the cell is protected under low sterol conditions from additional sterol loss. Thus, miR-33 appears to regulate both HDL biogenesis in the liver and cellular cholesterol efflux.

In addition to this role in maintaining cholesterol homeostasis, the group also showed that miR-33a and miR-33b also regulate fatty acid metabolism and insulin signaling. Putative binding sites for miR-33 in the 3′UTR of CROT, CPT1a, HADHB, AMPKα and IRS2 were identified and it was demonstrated that miR-33a and miR-33b specifically inhibit the expression of these genes. The physiological relevance of this targeting is revealed by miR-33 overexpression in hepatic cells, were both fatty acid oxidation and insulin signaling are reduced. Furthermore, inhibition of endogenous miR-33 increased the expression of CROT, CPT1a, HADHB, AMPKα, and IRS2 and upregulated fatty acid oxidation and insulin signaling. Together, these data suggest that feedback loops involving SREBPs, miR-33a and miR-33b balance cholesterol metabolism, fatty acid oxidation, and insulin signaling; three of the major risk factors of metabolic syndrome.

Since SREBPs regulate cellular proliferation and cell cycle progression, in the current study, we tested the role of miR-33 in regulating these cellular functions. We identified putative binding-sites for miR-33 in the 3´UTR of cyclin-dependent kinases (CDK6, CDK8, and CDK19), CCND1 and CCND2, p53, Pten, Myc and mitogen-activated protein kinases (Map3k1, Map3k7, Mapk1, Mapk3, Mapk6, Mapk10 and Mapk14). The potential targets of miR-33 were validated analyzing the mRNA and the protein levels by *in vitro* overexpression and inhibition of the miR-33 in HeLa, Huh7 and A549 cell lines. Moreover, the binding sites in the 3´UTR of two predicted genes were confirmed by luciferase assay. Further, the role of miR-33 during proliferation and cell cycle progression was studied *in vivo* in a liver regeneration model after partial hepatectomy in mice. Finally, the conditional miR-33 knockout mouse model was designed and generated. This tool enables us to knockout miR-33 in a controlled and specific manner by using inducible mouse models, in order to further investigate the biological role of miR-33 in different tissues.

2 MATERIAL AND METHODS

Standard protocols for various techniques in molecular biology were mainly performed according to *Molecular Cloning* (3rd Edition, Sambrook & Russel, Cold Spring Harbor Laboratory Press, 2001).

2.1 Cloning

Overview tables of all constructs and primers are placed in section 2.8.2 and 2.8.3.

2.1.1 Bacterial *E. coli* strains

Chemically competent DH5α (Invitrogen, California, USA) were used for the propagation of standard vectors and routine subcloning. Chemically competent and electrocompetent Top10 (Invitrogen, USA) and chemically competent Stbl2 (Invitrogen, USA) were used to amplify special constructs bigger than 5000bp. Chemically XL10-Gold ultracompetent cells (Stratagene, USA) were used to amplify the point mutated constructs. Bacteria were propagated in standard LB medium (MP Biomedicals, USA) or LB agar (MP Biomedicals, USA) at 37°C in a shaking incubator (Thermo Scientific Heraeus Series 6000 Incubators, Thermo Scientific, USA) unless noted.

2.1.2 Polymerase chain reaction (PCR)

PCR reactions for cloning approaches were performed with Phusion Hot Start High-Fidelity DNA polymerase (Finnzymes, Colorado, USA), since this enzyme possesses proofreading exonuclease activity. If 3'-A overhangs were necessary (e.g. for TOPO-TA cloning) Taq DNA polymerase (Biolabs, UK) was used. Analytical PCR reactions were conducted with standard Taq DNA Polymerase (Eppendorf, Germany). Standard reactions were performed after an initial denaturation (95°C, 5 min) for 30-35 cycles of denaturation (95°C, 30 sec), annealing

(55-65°C, 30 sec), and extension (72 °C, 30-180 sec) followed by a final extension step in a

MJ Research PTC-200 thermo cycler (MJ Research, USA).

2.1.3 Agarose gel electrophoresis

DNA molecules were separated by gel electrophoresis in standard electrophoresis grade 0,5-

2% agarose gels (Invitrogen, USA). If gel extraction of the DNA fragment was required for

cloning purposes, gels were prepared with TopVision Agarose (Fermentas, Canada). The

electrophoresis was performed in a custom system (Bächler Feintech, Germany) at 80 V for

30-60 min in TBE-Buffer (45 mM Tris-borate, 1 mM EDTA, pH 8.3) in case of analytical gels

and TAE-Buffer (40 mM Tris-acetate, 1 mM EDTA, pH 8.0) for cloning approaches. Ethidium

bromide (0.5µg/ml) was included in the buffer and gel to visualize DNA bands by UV light

(Syngene, USA).

2.1.4 Plasmid isolation

For small scale plasmid isolations (max 1µg), 3ml LB medium including 100 µg/ml ampicillin

or kanamycin antibiotics, depending on the plasmid resistance, were inoculated with one

colony and cultured overnight at 37°C while shaking (225 rpm, Thermo Scientific Heraeus

Series 6000 Incubators, Thermo Scientific, USA). Cells grown in overnight culture were

pelleted and plasmids were isolated using the QIAprep Spin Miniprep Kit (QIAGEN,

Germany) according to the manufacturer´s protocol and eluted in 50 µl ddH$_2$O. If larger

amounts (max 500 µg) of plasmid DNA were desired, 100-200 µl of the overnight cultures

were used to inoculate 50-100 ml LB medium. On the next day, plasmids were isolated with

the QIAGEN Plasmid Maxi Kit (QIAGEN, Germany) according to the instruction manual. In

the case of the BAC clones (BACPAC Resources Center, Oakland, USA), a BAC clone

colony was inoculated into LB medium including 12,5 µg/ml chloramphenicol antibiotic and

cultured overnight at 37°C while shaking (225rpm, Thermo Scientific Heraeus Series 6000

Incubators, Thermo Scientific, USA). The next day the BAC DNA was recovered using the

PhasePrep BAC DNA kit (Sigma, USA).

2.1.5 PCR purification and gel extraction

PCR products were purified by QIAquick PCR Purification kit (QIAGEN, Germany) and eluted in 30 µl ddH$_2$O. Restricted DNA fragments were separated from linearized vectors by gel electrophoresis (see 2.1.3), cut from the gel, extracted using the QIAquick Gel Extraction Kit (QIAGEN, Germany), and eluted in 30 µl ddH$_2$O.

2.1.6 Ligation

DNA inserts and linearized vectors were ligated by T4 DNA ligase (Biolabs, UK) and Rapid DNA Ligation Kit (Roche, Switzerland) according to the manufacturer's protocol. Ligations were incubated overnight at 16 °C or at room temperature (depending on selected ligase) before transformation.

2.1.7 Transformation of electro- and chemically competent bacteria

Electrocompetent Top10 cells (50 µl) were thawed on ice and mixed with 1-2 µl plasmid DNA (50-100 ng) or diluted ligation reaction (50-1000 ng). The reaction was transferred into a pre-chilled 0.1 cm electroporation cuvette (BioRad, USA) and pulsed in an electroporator (EquiBio, France). The cells were resuspended in 1 ml Super Optimal broth with Catabolite repression (SOC) medium (Invitrogen, USA), incubated at 37 °C for 1 h while shaking 225 rpm (Thermo Scientific Heraeus Series 6000 Incubators, Thermo Scientific, USA) and plated onto selection agar plates. For transformation of chemically competent cells, 50 µl cell suspension was mixed with 1 µl plasmid DNA (50-100 ng) or diluted ligation reaction (50-1000 ng). The reaction was chilled on ice for 30 min, heat-shocked for 45 sec at 42 °C in a water bath or Thermomixer (Eppendorf, Germany), and placed on ice for additional 2 min. Subsequently, 0.250 ml SOC medium was added. Cells were regenerated at 37 °C for 1 h while shaking 225 rpm (Thermo Scientific Heraeus Series 6000 Incubators, Thermo Scientific, USA) and plated onto selection agar plates.

2.1.8 Site-directed mutagenesis

The QuickChange Multi Site-Directed Mutagenesis Kit (Stratagene, USA) allowed a rapid and reliable method for site-directed mutagenesis of plasmid DNA. A single oligonucleotide carrying the mutated basepair was designed to mutagenize each site, using a double-stranded DNA template. The three steps method consisted in a first step of a thermal cycling procedure to achieve multiple rounds of mutant strand synthesis (supercoiled double-stranded DNA template), by using two or more synthetic oligonucleotide primers depending on the sample containing the desired mutations and the kit-provided enzyme blend featuring *PfuTurbo* DNA polymerase (6-fold higher fidelity in DNA synthesis than *Taq* DNA polymerase). In the second step, the thermal cycling reaction products were treated with the restriction endonuclease *DpnI* (specific for methylated DNA to digest parental DNA template). Finally, the reaction mixture, enriched for multiply mutated single stranded DNA, was transformed into XL10-Gold ultracompetent cells, where the mutant closed circle single stranded-DNA was converted into duplex form *in vivo*. Plasmids isolated from the transformants were then sent to sequence to identify clones bearing each of the desired mutations.

2.2 Conditional miR-33 knockout mice

2.2.1 Construction of miR-33 conditional knockout mice vectors.

The generation of the miR-33 targeting vector was constructed based on pEZ-Frt-lox-DT vectors for conditional gene targeting, which contains a neomycin resistance gene driven by the promoter of the yeast gene encoding the glycolytic enzyme phospho-glycerate kinase (pGK promoter), flanked by FLP recognition target (FRT) sites, and a diphtheria toxin gene cassette. The strategy was designed to clone the loxP sites flanking the pre-miR-33 sequence and the neomycin resistance cassette flanked by FRT sites. For the targeting vector a 4 kb fragment (5' arm) extending upstream of the miR-33 coding region was digested with *ClaI* (Fermentas, Canada) and *NotI* (Fermentas, Canada) and ligated into the

pEZ-Frt-lox-DT. A 3.5 kb fragment (3' arm) immediately downstream from the miR-33 was digested with *XhoI* (Fermentas, Canada) and ligated downstream of the loxP sites. The genomic fragment encompassing the mir-33 coding region (75bp) was digested with *SacI* (Fermentas, Canada) and ligated into the vector between the neomycin resistance, the loxP and the Frt-flanked cassettes. The targeting vectors were linearized with *ScaI* and electroporated into JM8.N4 C57BL/6 -derived embryonic stem (ES) cells (KONP, USA).

2.2.2 Generation of miR-33 conditional KO mice

Four hundred ES cell clones were isolated and analyzed for homologous recombination. Targeted ES clones carrying the properly miR-33 flanked allele were identified by PCR screening analysis (PCR primer sequences are listed in Table 2) with several primer sets using a special polymerase (Elongase Enzyme Mix, Invitrogen, USA) and one was used for injection into 3.5 days C57BL/6 blastocyst. High-percentage chimeric male mice were crossed to C57BL/6 females to achieve germline transmission of the targeted alleles. The resulting chimeric mice were bred to C57BL/6 females to obtain germline transmission of the mutant allele. Heterozygous miR-33-neo/+ mice were intercrossed with deletor mice transgenic for *Cre* recombinase to remove the neomycin resistance cassette *in vivo* [111].

2.3 Mammalian cell culture

2.3.1 Cell lines

Cell lines HeLa, A549, Huh7, HEK293, MCF-7 and COS-7 were obtained from American Type Tissue Collection (USA) and cultured in Dulbecco's Modified Eagle Medium (DMEM, GIBCO, USA) containing 10% fetal bovine serum (FBS, GIBCO, USA) including 1% antibiotics (100 U/ml penicillin and 100 µg/ml streptomycin, Biochrom, Germany) and 2mM L-glutamine (GIBCO, USA) in a humidified with 5% CO_2 at 37ºC in an incubator (Thermo Scientific Heraeus Series 6000 Incubators, Thermo Scientific, USA). Lipoprotein depleted serum (LPDS, GIBCO, USA) media contained 200ml DMEM and 20ml filtered LPDS, 2ml L-

glutamine and 2ml penicillin/streptomycin (P/S). To synchronize the culture, cells were treated with Nocodazole (250 ng/ml, Sigma, USA) 24h post-transfection or with 2mM Thymidine (GIBCO, USA) for 18h. Stable miR-33 overexpressing cell lines were generated upon transduction with lentiviral vectors and selection with puromycin antibiotic (2 μg/ml) (GIBCO, USA). Briefly, murine miR-33 was amplified from genomic DNA and cloned into pSicoR, as described in Marquart *et al*. [99]; the green flourescent protein (GFP) cassette in pSicoR was then swapped with puromycin resistance cassette. Lentiviruses were obtained by cotransfection in HEK293 cells of empty or miR-33 pSicoR-Puro. Supernantants were collected 48h after transfection and used to transduce a variety of cell lines.

2.3.2 Transfections

Mammalian cell lines were either transfected with Lipofectamine 2000 Reagent (Invitrogen, USA) or Lipofectamine RNAiMAX (Invitrogen, USA). For transfection with Lipofectamine 2000 Reagent, the cells were seeded 12 h prior transfection at a confluency of around 70-75%. For transfections in 12-well plates, 2 μl Lipofectamine 200 Reagent was diluted in 582 μl serum free medium (OptiMEM, Gibco, USA) and incubated for 5 min at room temperature. Plasmid DNA (1 μg/μl) was then added, vortexed, and incubated for at least 15 min at room temperature. Finally the transfection complex was added to the cell culture vessel in a drop wise manner while swirling. The expression of transfected constructs was assayed 24, 48 or 72 h later. A549, HeLa and Huh7 cells were transfected with 40 nM mi*RIDIAN* miRNA mimics (miR-33) or with 60 nM mi*RIDIAN* miRNA inhibitors (inh-miR-33) (Dharmacon, USA) utilizing Oligofectamine (Invitrogen, USA). Oligofectamine is indicated for the transfection of oligonucleotides and short interfering RNA (siRNA) into eukaryotic cells. All experimental control samples were treated with an equal concentration of a non-targeting control mimic sequence (CM) or an inhibitor negative control sequence (CI) to control for non-sequence-specific effects in all miRNA experiments.

2.3.3 3'UTR luciferase reporter assay

cDNA fragments corresponding to the entire 3'UTR of *Ccnd1* and the three predicted miRNA target sites of *Cdk6* were amplified by reverse transcription polymerase chain reaction (RT-PCR) from total RNA extracted from A549 cells with *XhoI* (Fermentas, Canada) and *NotI* (Fermentas, Canada) linkers. The PCR products were directionally cloned downstream of the *Renilla* luciferase open reading frame (ORF) of the psiCHECK2^{TM} vector (Promega, USA) that also contained a constitutively expressed firefly luciferase gene, which was used to normalize transfections. Point mutations in the "seed region" of predicted miR-33 sites within the 3'UTR of *Ccnd1 and Cdk6* were generated using Multisite-QuickChange (Stratagene, USA) according to the manufacturer's protocol. All constructs were confirmed by sequencing. COS-7 cells were plated into 12-well plates (Costar, USA) and co-transfected with 1µg of the indicated 3'UTR luciferase reporter vector and the miR-33 mimic or negative control miRNA mimic (CM) (Dharmacon, USA) using Lipofectamine 200 Reagent (Invitrogen, USA). Luciferase activity was measured using the Dual-Glow Luciferase Assay System (Promega, USA). *Renilla* luciferase activity was normalized to the corresponding firefly luciferase activity and plotted as a percentage of the control (cells co-transfected with the corresponding concentration of the control mimic sequence, CM).

2.3.4 Cell cycle analysis

Cells, cultured in DMEM supplemented with antibiotics (100 units of penicillin/ml and 100 µg/ml of streptomycin) at 37°C in a humified atmosphere containing 5% CO_2, were synchronized with 250 ng/ml Nocodazole (Sigma, USA) 24 h post transfection. 2 h before harvesting the culture, 5′Bromo-2′Deoxy-Uridine (BrdU) (B-5002, Sigma, USA) was added to the culture. At the end of the incubation the cells were washed twice with ice-cold phosphate-buffered saline (PBS) and fixed in 70% ethanol. After two additional washes with PBS, the pellet was resuspended first with 2N HCL to denaturize the DNA, then with 0.1 M

Na2B4O7·10 H$_2$O pH 8.4 and finally blocked for 15 min at room temperature with PBS-0.5% Tween 20 (Sigma, USA) 1% Normal Goat Serum (NGS, Vector, USA). After blocking, the pellet was incubated with PBS-0.5% Tween 20 1% NGS and α-BrdU-FITC antibody (Anti-BrdU-FITC Becton-Dickinson, USA) for 2 h at room temperature at dark. Finally, the cells were treated with 100 µg/ml Ribonuclease A (Roche, Switzerland) and labeled with 50 µg/ml propidium iodide (PI) for 1 h at 37°C. The cells were analyzed by flow cytometry (FACScalibur, Becton-Dickinson, USA) using selective gating to exclude the doublets of cells, and subjected to MODFIT analysis (Verity Software House, USA).

2.3.5 Plasmid constructs and production of adenovirus

A fragment containing miR-33 flanked by 150 bp upstream and 150 bp downstream of the genomic sequence was amplified by PCR using *Platinum Pfx* enzyme (Invitrogen, USA) from mouse genomic DNA obtained from tail biopsy specimens from C57BL/6 mice. The reverse primer used in the PCR contained the appropriate terminator sequence for RNA-pol-III (TTTTTCT). This fragment was cloned into the HpaI-XhoI sites of pSicoR-GFP (Addgene, USA), which provided a U6 promoter to control the expression of the transgene (and a GFP cassette under control of a cytomegalovirus promoter), thus generating pSicoR-miR33. The integrity of the clones was analyzed by sequencing. Adenoviruses were produced using the AdEasy Adenoviral System (Stratagene, USA) by cloning a XbaI-XhoI fragment containing the U6 promoter with or without the miR-33 sequences from the pSicoR vectors into pAdTrack (which also contains a GFP cassette). The pAdTrack and pAdTrack-miR33 vectors were electroporated into pAdeasy-1 cells to generate the final adenoviral vectors. Recombinant vectors were identified by the presence of a 4.5-kb PacI restriction fragment. These final vectors were transfected individually into AD293 cells (Stratagene, USA) for the production and amplification of the adenoviral particles. The adenoviruses were purified by caesium chloride (CsCl) gradient ultracentrifugation, and the titers were calculated to be 1 × 10^{12} plaque-forming units (pfu/µL) for Ad-GFP and 1 × 10^{11} pfu/µL for Ad-miR33.

2.3.6 Cell proliferation assay

Huh7, A549 and HeLa cells were grown in DMEM supplemented with 10% LPDS and transfected with control mimic (CM), miR-33, control miR inhibitor (CI) and antisense inhibitor of miR-33 (inh-miR-33). At the indicated times (24h, 48h and 72h), the viable cells were counted by trypan blue dye exclusion hemocytometer.

2.3.7 Crystal violet staining

After treatment, the medium was removed and the 24-well dishes were washed with PBS, fixed with 1% glutaraldehyde for 15 min, washed twice with PBS and stained with 100 µl of 0.1% aqueous crystal violet solution for 20 min. Dishes were rinsed four times in tap water and allowed to air dry. If cell mass estimation was desired 100 µl of 10% acetic acid was added, and the content of each well was mixed before reading the absorbance at 595 nm.

2.3.8 MTT assay

MCF-7 cell viability was assessed by adding 20 µl of filter sterilised 3-(4,5-Dimethylthiazol-2-yl)-2,5-diphenyltetrazolium bromide (MTT, 5 mg/ml in PBS) (R&D, USA) to each plate. Following a 5 h incubation period with MTT, medium was removed with a needle and syringe and the blue formazan crystals, trapped in the cells, was dissolved in 100 µl sterile dimethyl sulfoxide (DMSO) by incubating at 37 °C for 30 min. The absorbance at 550 nm was measured with a plate reader (Model 680 Microplate Reader, BioRad, Germany). The growth curve was obtained from the absorbance related to the time course (DMSO as blank).

2.4 Protein extraction and Immunoblotting

Information regarding the applied antibodies is provided in the materials section 2.8.1.

2.4.1 Protein extraction from cell lysates

Cells were lysed in ice-cold lysis buffer (50 mM Tris-HCl pH 7.5, 125 mM NaCl, 1% NP-40, 5.3 mM NaF, 1.5 mM Na4P2O7 and 1mM orthovanadate, 175 mg/ml octylglucopyranoside), 1 mg/ml of protease inhibitor cocktail (Roche, Switzerland) and 0.25 mg/ml 4-(2-Aminoethyl) benzenesulfonyl fluoride hydrochloride (AEBSF, Roche, Switzerland). After 5 min incubation on ice, cells lysates were sonicated (Sonicator3000, Qsonica LL, USA) for 20 sec (4x for 5 sec) on ice and left rotating at 4°C for 1 h before the insoluble material was removed by centrifugation at 12000xg for 10 min. Protein supernatant was stored at -20°C till further use.

2.4.2 Protein extraction from tissue lysates

Briefly, liver tissue of wildtype as well as miR33-ASO and Control-ASO mice was homogenized in liquid nitrogen. Pulverized tissue (50 mg) was placed in a cooled dounce homogenizer (7 ml tight grinder, Wheaton, USA) and 1 ml ice cold lysis buffer (50 mM Tris-HCl pH 7.5, 125 mM NaCl, 1% NP-40, 5.3 mM NaF, 1.5 mM Na4P2O7 and 1mM orthovanadate, 175 mg/ml octylglucopyranoside), 1 mg/ml of protease inhibitor cocktail (Roche, Switzerland) and 0.25 mg/ml AEBSF (Roche, Switzerland)) were added. The lysate was grinded 15x to disrupt the cells and protein solution was obtained after centrifugation (see 2.4.1) and stored at -20°C.

2.4.3 Sodium dodecyl sulfate-polyacrylamide gel electrophoresis (SDS-PAGE)

For SDS-PAGE, the protein samples were mixed with 4x SDS loading buffer (300 mM Tris pH 6.8, 12% SDS, 0.6% bromphenol blue, 60% glycerol, 12% fresh β-mercaptoethanol) and denatured by cooking or not. 50 µg protein were loaded onto a polyacryl-amide gel composed of a 4% stacking gel and a 7,5-12% separating gel, and separated by gel electrophoresis (BioRad, Germany) in Running buffer (25 mM Tris, 192 mM glycine, 0.1% SDS, pH 8.3) at 80 V until the sample focused in the stacking gel and then at 120 V until the dye ran off the gel.

2.4.4 Immunoblotting

The separated proteins were transferred onto a nitrocellulose membrane in transfer buffer (25 mM Tris, 192 mM glycine, 10% methanol) using a wet blotter (BioRad, Germany). The transfer was conducted at 90 V for 3 h at 4°C. The membrane was blocked in Tris-Buffered Saline (TBST) and Tween 20 solution (125 mM Tris-HCl, 625 mM NaCl, 0.05% Tween 20, pH 8.0) containing 5% bovine serum albumin (BSA) for 30 min and incubated with the primary antibody dissolved in blocking buffer (aforementioned TBST containing 5% BSA) for 1 h at room temperature or at 4 °C over night while shaking. The membrane was washed 3x in TBST for 10 min each and incubated with the secondary antibody diluted in TBST for 1 h at room temperature. After incubation, the membranes were washed 3x in TBST for 10 min. The immune complexes were detected with the LICOR Biotechnology detection system according to the manufacturer's protocol (Oddyssey Infrared Imaging System, USA). Heat shock protein 90 (HSP90) was used to ensure equal loading. Densitometry analysis of the gels was carried out using the ImageJ software (NIH, USA, htt://rsbweb.nih.gov/ij/).

2.5 Histology

Information concerning the used antibodies is provided in the materials section 2.8.1.

2.5.1 Frozen sections

Liver samples of wildtype as well as 2'-O-methoxyethyl (2'MOE) phosphorothioate ASO (miR33-ASO) and control anti-sense oligonucleotides (Control-ASO) mice were fixed in 4% paraformaldehyde (PFA) at 4°C overnight and submerged in 30% sucrose at 4 °C during 5 h. Tissues were then embedded in cryomolds in Tissue Tek OCT compound (Sakura, Japan), snap frozen on dry ice, and stored at -80ºC. Frozen blocks were cut in eight μm thick sections (CM 1900, Leica, Germany), mounted on slides (Menzel, Germany), dried at room temperature for 30 min, and stored in airtight containers at -80ºC. The slides were warmed up to room temperature in closed containers for further immunohistochemical analysis.

2.5.2 Oil-Red-O staining

Eight μm frozen sections were rehydrated and lipid droplets deposition was detected by Oil-Red-O staining (Sigma, USA). Sections were rinsed with 60% isopropanol and stained for 20 min with filtered freshly prepared Oil-Red-O solution (0.5% in isopropanol followed by a 60% dilution in distilled water). After two rinses with 60% isopropanol and distilled water, slides were counterstained with hematoxylin for 4 min, rinsed with water and mounted. Randomly digital images per section were taken with a Leica DM 4000B microscope (Leica, Germany).

2.5.3 Immunohistofluorescence: Ki67 staining

Frozen sections of eight μm thickness were rehydrated, blocked with 5% normal goat serum (NGS), and incubated with mouse anti-Ki67 (1:100, Abcam, USA) and counterstained with DAPI (0.2 ng/μl) (eBioscience, USA). Controls without primary antibodies were used as negative controls. Binding sites of the primary antibodies were revealed with Alexa-597 goat-anti-mouse IgG (1:1000, Invitrogen, USA). Samples were analyzed with a fluorescence microscope at 597 nm (Nikon Eclipse E600, Kawasaki, and Kanagawa, Japan).

2.6 Animals

2.6.1 Mice

C57BL/6J mice (Jackson Laboratories, USA) were kept in a pathogen-free animal facility with controlled humidity (50 ± 5 %), 12/12 hours light and dark cycle at 21°C. Mice were fed ad libitum a standard diet. Twenty six weeks old male C57BL/6 mice were randomized into 3 groups (n= 20 mice): no treatment (PBS, n=4), Control-ASO (n=8) or miR-33-ASO (n=8). The mice received a weekly subcutaneous injection of PBS, 10mg/Kg Control-ASO or miR-33-ASO for 4 weeks. Animal experiments followed the German Ethical Committee for the Use and Care of Laboratory Animals, in accordance to the recommendations of the Society for Laboratory Animal Science (GV-SOLAS) and the Federation of European Laboratory Animal

Science Associations (FELASA). Likewise, all animal experiments were approved by the Institutional Animal Care Use Committee of New York University Medical Center.

2.6.2 Surgical procedure

All operations were performed under Isoflurane (DeltaSelect, Germany) anesthesia. A 70% partial hepatectomy (2/3 PH) was performed according to the technique described by Higgins and Anderson (Higgins 1931), revised by Mitchell and Willenbring in 2008 [112]. The mice were place into a plexiglas chamber for induction of anesthesia with 2% isoflurane and 2 liters/min oxygen flow for a wild-type mouse of 25 g body weight. The abdomen was opened via midline incision and two thirds of the liver (median and left lobes) were removed. After the 2/3 PH, the weights of regenerating liver were measured and the hepatic tissue was preserved for future processing at the following time points: 3, 8, 24 and 48 hours in the case of untreated mice and 5 days in the case of treated mice. The percentage of liver regeneration was calculated as a ratio between the weight of non removed lobes and the weight of total liver, and further normalized to the total body weight of the animal.

2.7 Quantitative Real-Time PCR (qRT-PCR)

2.7.1 Total RNA and miRNA isolation

Mouse tissues were withdrawn immediately after sacrification and washed in ice-cold Hank's balanced salt solution, flash-frozen in liquid nitrogen, pulverized and stored at -80ºC. Total RNA of individual tissues was isolated in parallel from no treatment, Control-ASO and miR-33-ASO using RNeasy Kit (QIAGEN, Germany) according to the manufacturer's protocol. Standard RNA isolation from cell lines was performed using RNeasy Kit (QIAGEN, Germany) and miRNeasy Kit (QIAGEN, Germany). The concentration and integrity of total RNA was measured using a NanoDrop 2000 (Thermo Scientific, USA).

2.7.2 cDNA-synthesis

1000 ng total RNA was reverse transcribed using the Taqman RT Kit (Applied Biosystems, USA) in 20 µl reactions; following the manufacture's protocol. Reactions were carried out at 25°C for 10 min, 48°C for 30 min, and 95°C for 5 min. For miRNA quantification, 1000 ng total RNA was reverse transcribed using the RT2 miRNA First Strand kit (SABiosciences, USA) in 10 µl reactions, following the manufacture's protocol. Reactions were carried out for 2 hours at 37°C, 5 min at 95°C to degrade the RNA and to inactivate the reverse transcriptase, and 40 µl of ddH20 were added to each reaction prior storage at -20°C.

2.7.3 qRT-PCR

qRT-PCR reactions were performed in triplicates using the iQ SYBR green Supermix (BioRad, Germany) in a iCycler Real-Time Detection System (BioRad, Germany). The mRNA levels were normalized to glyceraldehyde 3-phosphate dehydrogenase (GAPDH) as a housekeeping gene Gene-specific primers were designed using the Primer 3 software (Rozen, 200). The primer sequences used are listed in Table 2. Primers specific for human miR-33a, miR-33b, miR-16 (SABiosciences, USA) were used and values were normalized to human SNORD38b as housekeeping gene.

No template and no reverse transcriptase were included and product quality was analyzed by gel electrophoresis and inspection of dissociation curves. PCR efficacy was determined for single reactions using DART-PCR Version 1.0 (Peirson, 2003) and mean PCR efficacy of gene-specific reactions was used for data analysis. Normalization and error propagation were calculated as described at the geNORM website (Vandesompele, 2002). The relative quantity of a specific transcript was calculated as:

$$Q = E^{(Min(\text{mean Ct of all samples}) - Ct)}$$

E: mean PCR efficiency

Ct: threshold cycles

Normalized expression levels of target genes were calculated by dividing the corresponding relative quantity by the normalization factor. Statistical significance was assessed using two-tailed t test assuming unequal variance of the biological replicated.

2.8 Materials

2.8.1 Chemicals

Chemicals were obtained from Sigma (USA) unless otherwise noted.

2.8.2 Antibodies

Table 1. Primary and secondary antibodies

Antibody	Company	Dilution
Primary antibodies		
Mouse monoclonal anti-CDK6	Cell Signaling	1:1000
Mouse monoclonal anti-PCNA	Cell Signaling	1:1000
Rabbit monoclonal anti-CCND1	Cell Signaling	1:1000
Rabbit monoclonal anti-cleaved caspase-3 (Asp175)	Cell Signaling	1:500
Mouse monoclonal anti-HSP90	BD Bioscience	1:1000
Mouse monoclonal anti-ABCA1	Abcam	1:1000
Mouse monoclonal anti-Rb	Cell Signaling	1:1000
Rabbit monoclonal anti-Phospho-Rb (Ser795)	Cell Signaling	1:500
Mouse monoclonal anti-Ki67	Abcam	1:100
Secondary antibodies for immunofluorescence		
Alexa-597 goat-anti-mouse IgG1	Invitrogen	1:1000
Secondary antibodies for Immunoblotting		
Secondary fluorescently-labeled anti-mouse	Invitrogen	1:5000
Secondary fluorescently-labeled anti-rabbit	Invitrogen	1:5000

2.8.3 Vectors and Constructs

The generation of conditional transgenic and luciferase constructs is described in section

2.1.8 and 2.3.3, respectively

Table 2. Vectors and Constructs

Plasmids	marker	description
Empty vectors		
BAC Chori: RP24	Chloramphenicol	miR-33conditional mice
pEZ-Frt-lox-DT	Neomycin	miR-33conditional mice
psiCHECK™-2	Ampicillin	Luciferase Assay
pCR™ 2.1-TOPO®	Ampicillin	Cloning Routine
pCR™ II- TOPO®	Ampicillin	Cloning Routine
pCR®-XL-TOPO®	Kanamycin	Difficult cloning routine
pCMV-Sport 6	Ampicillin	Eukaryotic expression
pSicoR-GFP	Ampicillin	Lentiviral packaging
Constructs		
psiCHECK™-2- 3´UTR CDK6 BS1 + point mutation		
psiCHECK™-2- 3´UTR CDK6 BS2 + point mutation		
psiCHECK™-2- 3´UTR CDK6 BS3 + point mutation		
psiCHECK™-2- 3´UTR CDK6 CCND1 + point mutation		
pEZ-Frt-loxP-DT - miR-33 – SA – LA		
pSicoR-GFP-miR-33		

2.8.4 Synthetic oligonucleotide primers

All primers were obtained from IDT (Integrated DNA Technologies) in 25 nmole DNA scale

and resuspended in H20 to 100 pmol/µl (100mM) stock concentration.

Table 3. Primer sequences

Gene	Sequence
ABCA1 Fwd	5'-GGTTTGGAGATGGTTATACAATAGTTGT-3'
ABCA1 Rev	5'-CCCGGAAACGCAAGTCC-3'
ABCG1 Fwd	5'-TCACCCAGTTCTGCATCCTCTT-3'
ABCG1 Rev	5'-GCAGATGTGTCAGGACCGAGT-3'
GAPDH Fwd	5'-AACTTTGGCATTGTGGAAGG-3'
GAPDH Rev	5'-ACACATTGGGGGTAGGAACA-3'
SREBP2 Fwd	5'-GCGTTCTGGAGACCATGGA-3'
SREBP2 Rev	5'-ACAAAGTTGCTCTGAAAACAAATCA-3'
SREBP1c Fwd	5'-ACTTCCCTGGCCTATTTGACC-3'
SREBP1c Rev	5'-GGCATGGACGGGTACATCTT-3'
HMGCR Fwd	5'-CTTGTGGAATGCCTTGTGATTG -3'

HMGCR Rev	5'-AGCCGAAGCAGCACATGAT-3'
CDK6 Fwd	5'-ACC TTC GAG CAC CCC AAC GT-3'
CDK6 Rev	5'-ACC ACA GCG TGA CGA CCA CT-3'
CDK8 Fwd	5'-GCC AGT TCA GTTACCTCGGGGA-3'
CDK8 Rev	5'-GGGCAA AGCCCATGTCAGCAAT-3'
CDK19 Fwd	5'-TTT GCC GGC TGCCAG ATT CC-3'
CDK19 Rev	5'-AGG CGA GAACTG GAG TGC TGA-3'
CyclinD1 Fwd	5'-TCG TTG CCC TCT GTG CCA CA-3'
CyclinD1 Rev	5'-AGG CAG TCC GGG TCACACTT-3'
CyclinM1 Fwd	5'-CAC CCG CTT CTA CAA CCG GC-3'
CyclinM1 Rev	5'-AGG GCT CCACTTCTGTGGCC-3'
ABCA1Not1	5'-AGCGGCCGCTTTCTGTAGACCAACAGAACTGTCA-3'
ABCA1Xho1	5'-AACTCGAGAGAATCCTGTTCATACGGGG-3'
CDK6PM1 F	5'-CGCCTAGTTTACTGTTTTGAAATCTTTGCAAGAGTGATTGCAGCTTTAT-3'
CDK6PM1 R	5'-ATAAAGCTGCAATCACTCTTGCAAAGATTTCAAAACAGTAAACTAGGCG-3'
CDK6PM2 F	5'-TCATTTCTTATTTACTCCCTTTCTATATCTTTGCAATTCACAACCCAATTT-3'
CDK6PM2 R	5'-GATGTATTAAAATTGGGTTGTGAATTGCAAAGATATAGAAAGGGAGTAA-3
CDK6PM3 F	5'-ACCCTTACTTGAAAGTTTCTAATCTTAAGTTTTATGATTTGCAATAATATGTA-3'
CDK6PM3 R	5'-CTAGCTGATACATATTATTGCAAATCATAAAACTTAAGATTAGAAACTTTCAA-3'
CCND1PM F	5'-GGATGTTCATAAGGCCAGTATGATTTATATTTGCAATCTCCCCTTG-3'
CCND1PM R	5'-CAAGGGGAGATTGCAAATATAAATCATACTGGCCTTATGAACATCC-3'
miR-33 Fwd	5'-TCGACCTGTGGTGCATTGTAGTTGCATTGCATGTTCTGGCAATACCTGTGCA-3'
miR-33 Rev	5'-CAGGTATTGCCAGAACATGCAATGCAACT ACAATGCACCACAGG-3'
miR-33 LA Fwd	5'-AAAGCGGCCGCAGGCCTGCCCTGACTGCC-3'
miR-33 LA Rev	5'-AAAATCGATGTGGGTGGAGGCCCAGGT-3'
miR-33 SA Fwd	5'-AAACTCGAGGGCCGAGCCTGGGGTCTT-3'
miR-33 SA Rev	5'-AAACTCGAGCTGCCCGCCAGGAGGTGT-3'
neo Fwd	5'-AGACAATCGGCTGCTCTGAT-3'
neo Rev	5'-ATACTTTCTCGGCAGGAGCA-3'

2.9 Statistics

Experiments were performed in triplicates and repeated at least three times (3 biological and 3 independent technical replicates). Data are presented as mean ± standard error of the mean (SEM) and number of replicates (n) is stated in the figure legends. Statistical significances were evaluated with the Student´s t-test (Excel-Office, Microsoft, USA) and differences were considered significant at the level of $p<0.05$.

2.10 Computer analysis

For the analysis of the nucleotide sequences, BLAST, BLAST2, MEGABLAST and NCBI (www.ncbi.nlm.nih.gov) were used. Mouse genome sequences, transcripts and putative proteins were downloaded from Ensembl (www.ensembl.org).

3 RESULTS

3.1 miR-33 has predicted target genes involved in cell cycle and proliferation

Since SREBPs regulate cellular proliferation and cell cycle progression and miR-33 is cotranscribed with SREBPs, in the current study, we decided to test the role of miR-33 in regulating these cellular functions. When looking at the Diana mirPath Software, designed to cover the need of a quick and easy interpretation of the involvement of a series of genes in biological processes, miR-33 was found to target genes involved in proliferation and cell cycle progression. As previously described by Fernández-Hernando's laboratory and others, miR-33 was as well found to regulate cholesterol and fatty acid homeostasis by targeting other genes involved in these pathways (**Table 4**).

Table 4. miR-33 predicted pathways. KEGG Pathways enrichment in hsa-miR-33 target genes. Prediction software: TS5- using a score threshold (Predicted Target Genes: 240, Found in pathways: 50).

| KEGG Pathway	Gene Name	Found Genes	- ln (p-value)
ABC-transporters - General	ABCA1	1	13.32
Glioma	PDGFRA, CDK6, CAMK2G, PIK3R3, CCND1	5	10.67
Non-small cell lung cancer	PDPK1, CDK6, PIK3R3, CCND1	4	7.57
Fatty-acid metabolism	ACADSB, HADHB, ALDH3A2	3	7.27
Prostate cancer	PDGFRA, PDPK1, CREB5, PIK3R3, CCND1	5	7.01
Focal adhesion	PDGFRA, VCL, PDPK1, RAC1, LAMC1, PIK3R3, CCND1	7	5.36
Melanoma	PDGFRA, CDK6, PIK3R3, CCND1	4	5.3
Pancreatic cancer	CDK6, RAC1, PIK3R3, CCND1	4	5.19

To further determine potential miR-33 targets involved in cell proliferation and cell cycle, a combination of bioinformatics tools for miRNA target prediction, such as TargetScan (http:/www.targetscan.org), miRanda (http:/www.microrna.org), DIANAmt (http://diana.cslab.ece.ntua.gr), miRDB (http://mirdb.org), miRWalk (http://www.ma.uni-heidelberg.de/aps/zmf/mirwalk) and PITA (http://genie.weizmann.ac.il) were used. This analysis confirmed that the 3'UTR of the cyclin dependent kinases (*Cdk6*, *Cdk8* and *Cdk19*), *Ccnd1* and Ccn*d2*, *p53*, *Pten*, *Myc* and mitogen-activated protein kinases (*Map3k1*, *Map3k7*, *Mapk1*, *Mapk3*, *Mapk6*, *Mapk10* and *Mapk14*) have predicted binding sites for miR-33 (**Table 5**).

Table 5. **miR-33 predicted target genes.** Gene target prediction based on TargetScan, miRanda, DIANAmt, miRDB and PITA. The five algorithms were applied to databases of 3'UTR sequences. The potential predicted targets for miR-33 are marked according to the algorithm used.

Gene	DIANAmT	miRanda	miRDB	miRWalk	PITA	TargetScan
ABCA1	✓	✓	✓	✓	✓	✓
CDK6	✓		✓	✓	✓	✓
CDK8	✓	✓		✓	✓	✓
CDK19	✓	✓		✓	✓	✓
CCND1		✓		✓	✓	✓
CCND2		✓		✓	✓	✓
MAP3K1	✓	✓	✓	✓	✓	✓
MAP3K7	✓	✓		✓		
MAPK1	✓	✓		✓		
MAPK3	✓	✓		✓		
MAPK6	✓	✓		✓	✓	✓
MAPK10	✓	✓		✓	✓	
MAPK14	✓	✓	✓	✓	✓	✓
p53	✓	✓		✓	✓	✓
PIK3R3	✓	✓		✓	✓	✓
PTEN		✓		✓	✓	✓
MYC		✓		✓	✓	✓

3.2 miR-33 regulates posttranscriptionally CDK6 and CCND1 expression

To determine the effect of miR-33 on the mRNA expression of *CDK6*, *CDK8*, *CDK19*, *CCND1*, *CCNM1*, three different cell lines were transfected with miR-33 or a control sequence. Transfection of Huh7 cells with miR-33 (40-fold increased expression, data not shown) significantly inhibited the mRNA levels of *CDK6* and *ABCA1*, a previous identified target of miR-33 (**Fig. 5A**). However, mRNA levels of *CDK8*, *CDK19*, *CCND1* and *CCNM1* were not significantly downregulated. Similar results were observed in A549 and HeLa cells transfected with miR-33 or control (**Fig. 5C** and **5E,** respectively). To enhance the activity of miR-33, HeLa cells were further cultivated in absence of cholesterol (LPDS medium) to avoid endogenous repression of the miR-33. As seen in **Fig. 5F**, *CDK6* and *ABCA1* mRNA levels were significantly decreased. Notably, endogenous inhibition of *miR-33* using anti-miR-33 oligonucleotides (2.5-fold decrease, data not shown) increased mRNA expression of *CDK6*
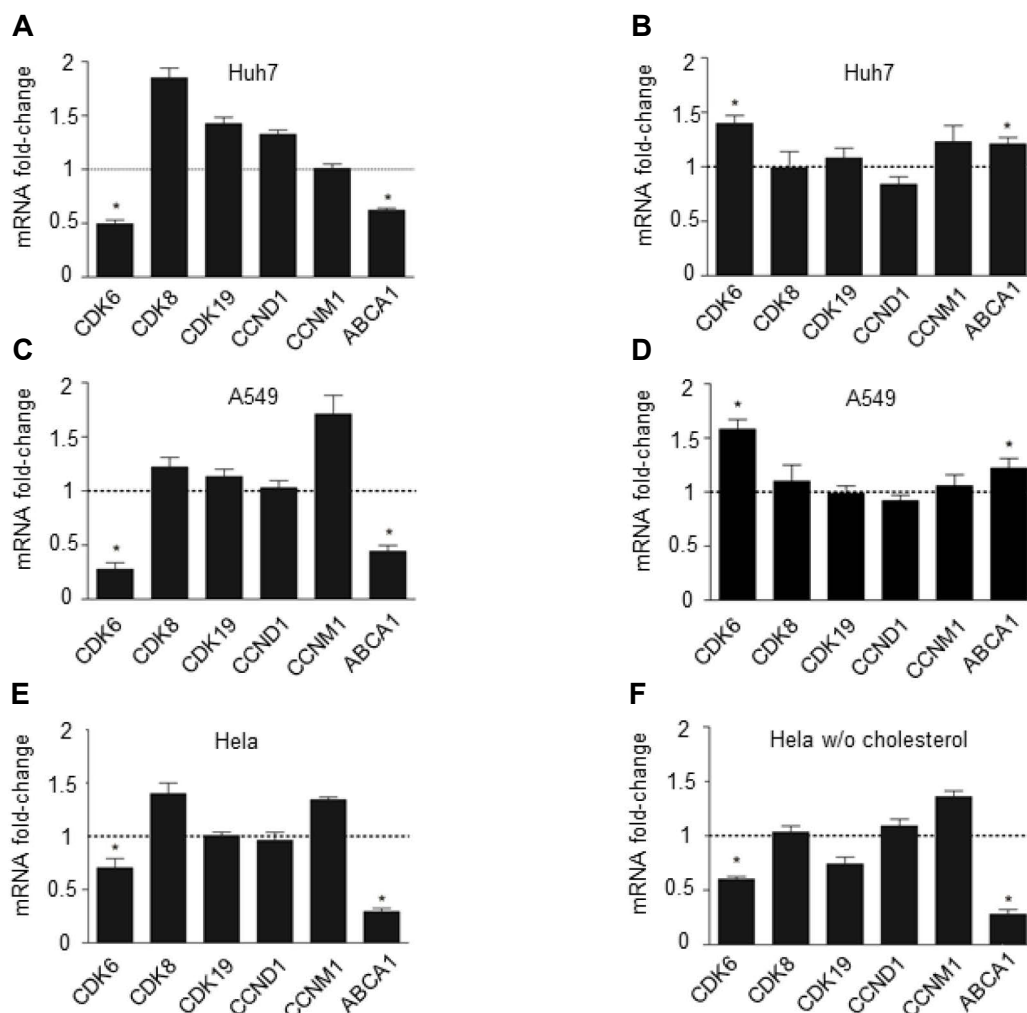
and *ABCA1* in Huh7 and A549 cell lines (**Fig. 5B** and **5D**).

Figure 5. **Post-transcriptional regulation of cell cycle genes and ABCA1 by miR-33**. Quantitative RT-PCR expression profile of selected miR-33 predicted target genes: *Cdk6*, *Cdk8, Cdk19, Ccnd1*, *Ccnm1* and *Abca1* in (**A**) human liver Huh7 cell line overexpressing miR-33, (**B**) human liver Huh7 cell line overexpressing anti-miR-33, (**C**) human lung A549 cell line overexpressing miR-33, (**D**) human lung A549 cell line overexpressing anti-miR-33, (**E**) human cervical HeLa cell line overexpressing miR-33 and (**F**) human cervical HeLa cell line overexpressing miR-33 cultured in cholesterol free medium. Dotted lines at 1 indicate value corresponding to control-miR or control inhibitor (random sequence molecules that have been extensively tested in human and mouse cell lines and tissues and validated to produce no identifiable effects on known miRNA function). Data are the mean ± SEM and are representative of ≥ 3 experiments. * p ≤ 0.05.

Since the expression level of CCND1 and CCNM1 varies along the cell cycle, Huh7 and A549 cells were synchronized in the G1 phase using a double thymidine block, which arrested the cells in the early S phase (**Fig. 6A**). As seen in **Fig. 6B**, transfection of Huh7 (upper panel) and A549 (lower panel) with miR-33 significantly inhibited *CDK6, CCND1* and *ABCA1* mRNA levels.
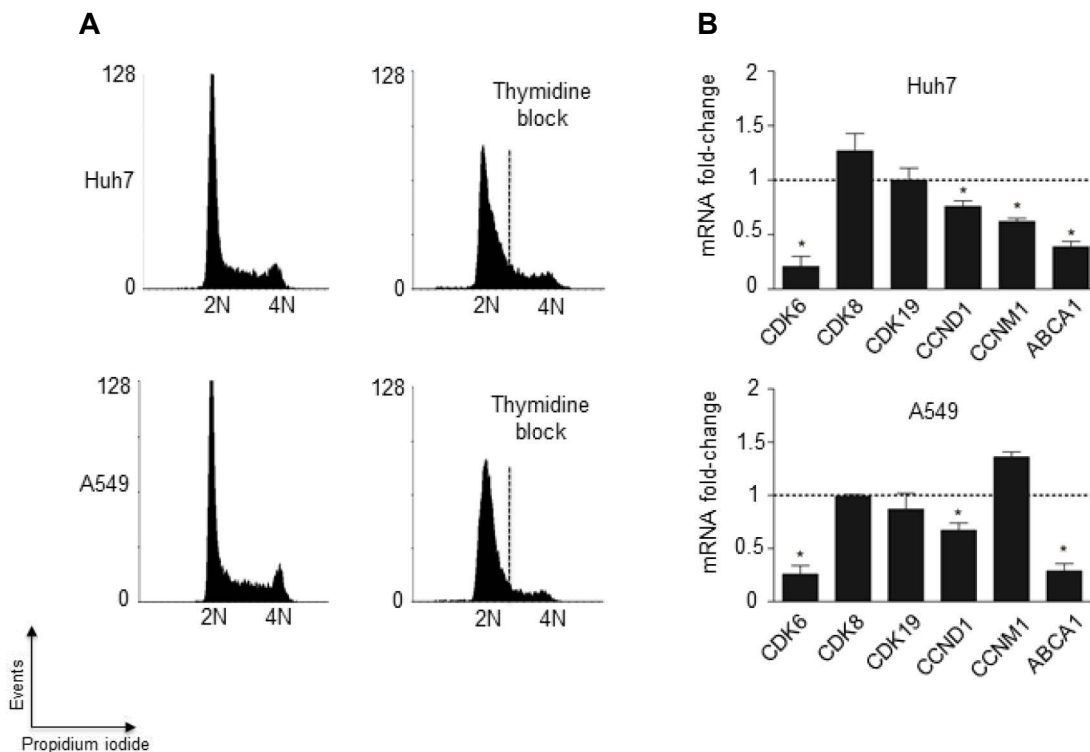

Figure 6. **Posttranscriptional regulation of cell cycle genes and ABCA1 by miR-33 in synchronized Huh7 and A549 cells**. (**A**) Flow cytometry analysis of Huh7 cells (upper panels) and A549 cells (bottom panels) synchronized using double thymidine block (right panels). (**B**) Quantitative RT-PCR analysis of selected miR-33 predicted targets in Huh7 and A549 cells transfected with control-miR (CM) or miR-33 after thymidine block synchronization. Dotted lines at 1 indicate value corresponding to CM. Data are the mean ± SEM and are representative of ≥ 3 experiments. * p ≤ 0.05.

3.3 miR-33 regulates CDK6 and CCND1 protein levels in Huh7 and A549 cells

Huh7 cells were transfected with control-miR (CM) or miR-33 (Fig. 7, upper panel) and protein content was analyzed by Western Blot after 48 h upon transfection. Cells transfected with miR-33 showed significantly decreased protein levels of ABCA1, CDK6 and CCND1 (Fig. 7, upper panel). Conversely, when cells were transfected with the inhibitor of miR-33 (Inh-miR-33) (Fig.7, bottom panel) the content of the proteins increased significantly when compared to the control inhibitor (CI) (Fig.7, bottom panel).
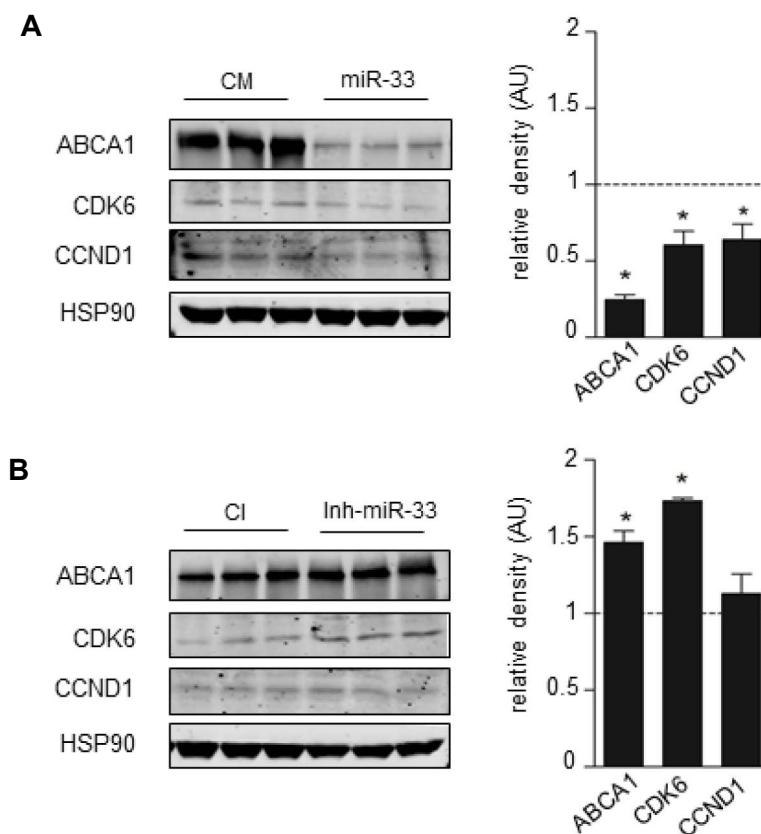
Figure 7. **miR-33 overexpression inhibits CDK6 and CCND1 protein expression in Huh7 cells**. Western Blot analysis of CDK6, CCND1 and ABCA1 expression from Huh7 cells transfected with CM or miR-33 (**A**) or control-inhibitor (CI) and Inh-miR-33 (**B**). Heat shock protein (HSP)90 bands are the loading control. Dotted lines at 1 indicate value corresponding to CM or CI. Data are the mean ± SEM and are representative of ≥ 3 experiments * $p \leq 0.05$.

In a time course experiment, A549 cells were transfected for 24, 48 and 72 h with either CM or miR-33 and protein content was similarly analyzed by Western Blot at the indicated time

points after transfection (**Fig. 8**). In **Fig. 8A** a downregulation of CDK6 and CCND1 is illustrated and confirms the results shown in **Fig. 7**.

To further ascertain that downregulation of CDK6 and CCND1 have a functional role on the phosphorylation of their downtream signaling molecule, the reinoblastoma protein (RB), and thus on cell cycle progression, the total and phosphorylated RB levels were measured. As seen in **Fig. 8** downregulation of CDK6/CCND1 provoked by miR-33 transfection also provoked a downregulation of phosphorylated RB.
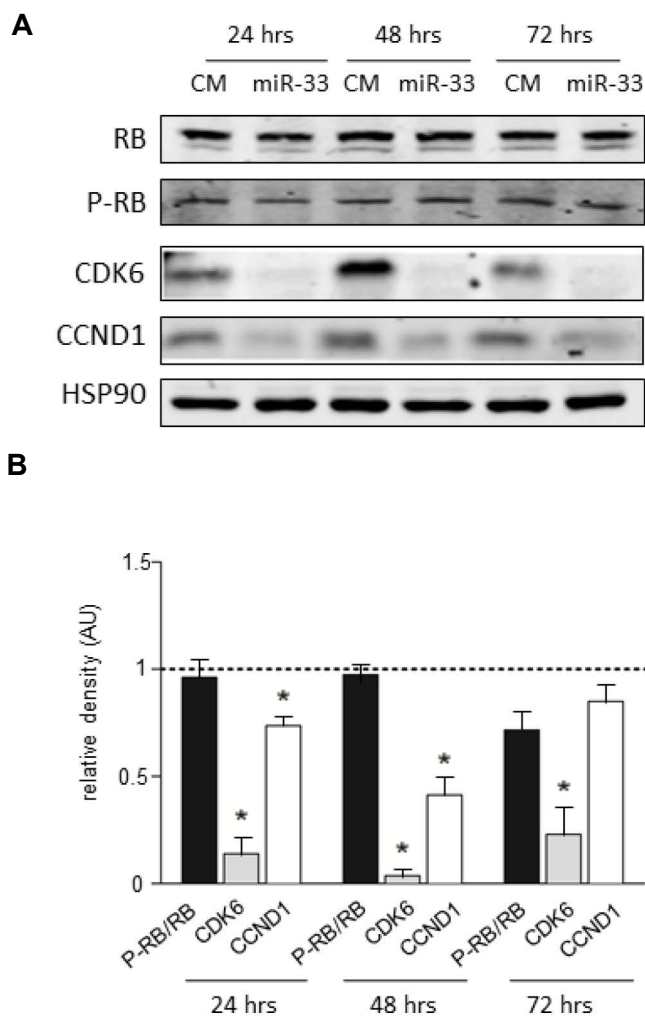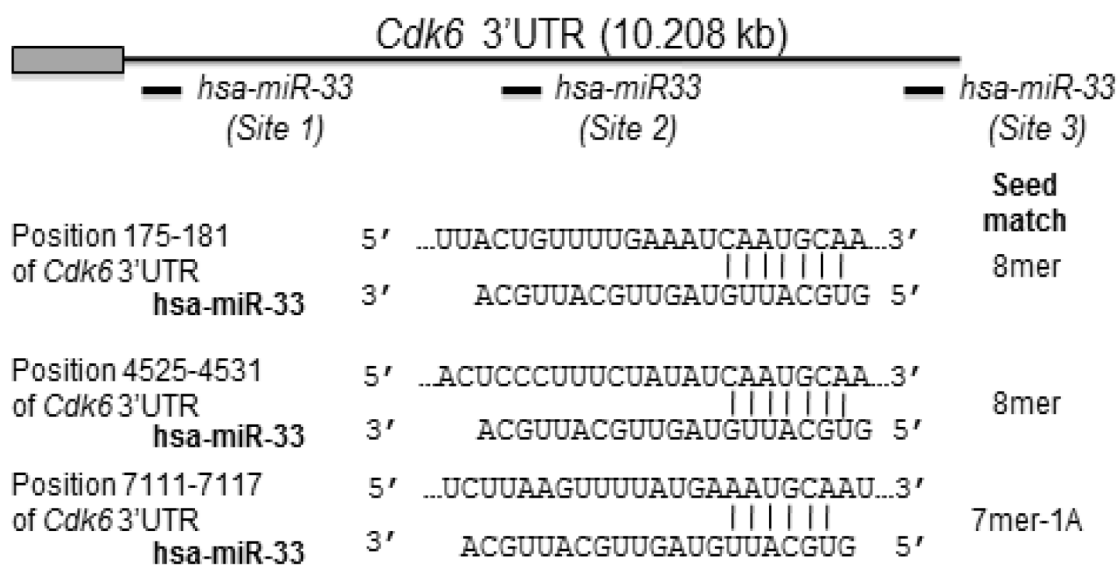

Figure 8. **miR-33 regulates CCND1/CDK6 signaling in A549 cells**. Western Blot analysis of RB, P-RB, CDK6 and CCND1 expression from Á549 cells transfected with CM and miR-33 for 24, 48 and 72 h. After transfection miR-33 impairs CCND1/CDK6 signaling by reducing RB phosphorylation in A549 cells. Dotted lines at 1 indicate value corresponding to CM. Data are the mean ± SEM and are representative of ≥ 3 experiments. * $p \leq 0.05$

Phosphorylation of RB by the CDK6/CCND1 complex allows the cell cycle progress through

G1 into S phase. Decreased phosphorylation of RB by miR-33 transfection indicates a

possible role of miR-33 in the cell cycle progression. Altogether, the mRNA and the protein

data strongly suggest that miR-33 coordinates genes regulating cell cycle progression.
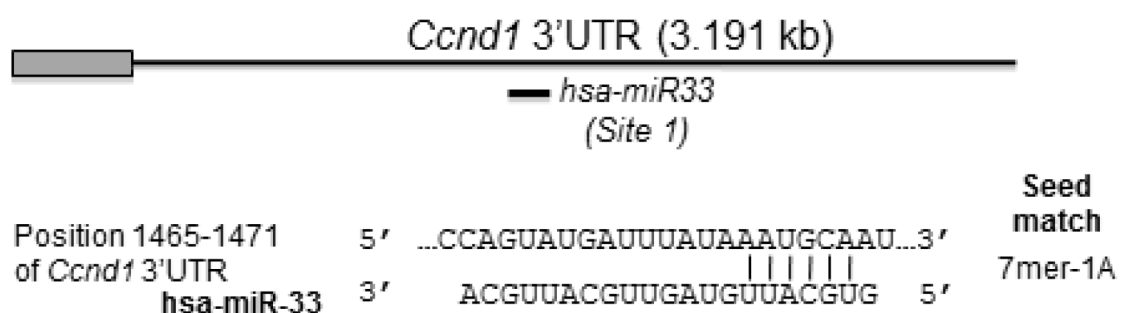
3.4 miR-33 directly targets the 3'UTR of *Cdk6* and *Ccnd1*

The human *Cdk6* and *Ccnd1* 3'UTR have three and one computationally predicted miR-33

binding sites respectively (**Fig. 9A** and **9B**). All the predicted binding sites are evolutionary

conserved (**Fig. 9C** and **9D**).

A

B

C   **D**

Cdk6 3'UTR (10.208 kb)   *Ccnd1* 3'UTR (3.191 kb)

Site 1 (175-181)   Site 1 (1465-1471)
Hsa 5'–AAAUCAAUGCAAGAG...   Hsa 5' UAUAAAUGCAAUCUC...
Ptr 5'–AAAUCAAUGCAAGAG...   Ptr 5' UAUAAAUGCAAUCUC...
Mmu 5'–AGAUCAAUGCAAGGG...   Mmu 5' AAGCAAUGUGAUCUC...
Rno 5'–AGAUCAAUGCAAGAG...   Rno 5' AAGCAAUGUGAUCUU...
Ocu 5'–AAAUCAAUGCAAGAG...   Ocu 5' GAGCGAUGCCGUCCC

Site 2 (4525-4531)
Hsa 5' AUCAAUGCAAUU...
Ptr 5' AUCAAUGCAAUU...
Mmu 5' CUCAGUCCAGUU...
Rno 5' UUCAGUCCAGUU...
Ocu 5'——————————AGUU...

Site 3 (7111-7117)
Hsa 5' AUGAAAUGCAAUAAU...
Ptr 5' AUGAAAUGCAAUAAU...
Mmu 5' AUGAAAUGCAAUAAC...
Rno 5'AUGGAAUGCAAUAAC...
Ocu 5' ACAAAAUGCAAUAAC...

Figure 9. **Putative 3´UTR target sites of CDK6 and CCND1 regulated by miR-33 and conservation among species**. Sequence alignment of the human hsa-miR-33 mature sequence with the binding sites of the human CDK6 3'UTR (**A**) and human CCND1 3'UTR (**B**). Relative position of the binding sites is indicated (-). CDK6 (**C**) and CCDN1 (**D**) miR-33 mature sequence binding site conservation between species. Hsa=human; Ptr=chimpanzee; Mmu=mouse; Rno=rat; Ocu=cat).

To directly assess whether miR-33 directly targets *CDK6* and *CCND1*, reporter constructs with the luciferase coding sequence fused to the 3'UTR of these genes were generated. In the case of CDK6 3'UTR, due to the long fragment of the sequence (more than 10 kB), the sequence was splitted into three parts, each of them containing one of the predicted binding sites for miR-33. miR-33 markedly repressed the luciferase reporter activity of the *Cdk6* and *Ccnd1* 3'UTR constructs (**Fig. 10A** and **10B**, respectively). Mutation of the miR-33 target sites relieved miR-33 repression of *CDK6* and *CCND1* 3'UTR activity, clearly demonstrating the direct interaction of miR-33 with these predicted sequences (**Fig. 10A** and **10B**, respectively).

A

Cdk6-3'UTR (WT)	5' ...TTACTGTTTTGAAATCAATGCAA ...
Cdk6-3'UTR (PM1)	5' ...TTACTGTTTTGAAATC**TT**TGCAA...

Site 1

Cdk6-3'UTR (WT)	5' ...ACTCCCTTTCTATATCAATGCAA ...
Cdk6-3'UTR (PM2)	5' ...ACTCCCTTTCTATATC**TT**TGCAA...

Site 2

Cdk6-3'UTR (WT)	5' ...TCTTAAGTTTTATGAAATGCAAT...
Cdk6-3'UTR (PM3)	5' ...TCTTAAGTTTTATGA**TT**TGCAAT...

Site 3

B

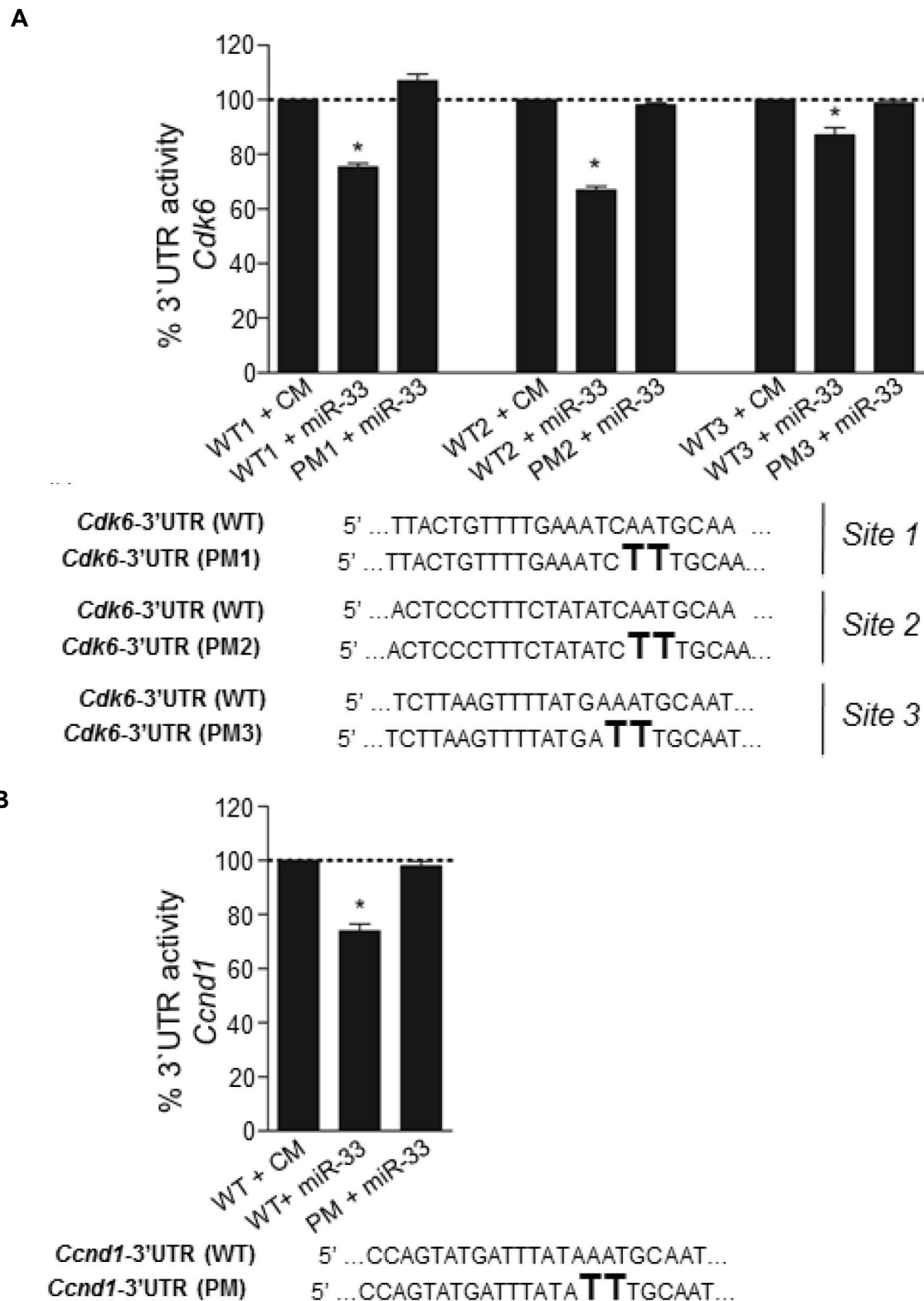|	
Ccnd1-3'UTR (WT)	5' ...CCAGTATGATTTATAAATGCAAT...
Ccnd1-3'UTR (PM)	5' ...CCAGTATGATTTATA**TT**TGCAAT...

Figure 10. **miR-33 specifically targets the 3'UTR of *Cdk6* and *Ccnd1*.** Luciferase reporter activity in COS-7 cells transfected with CM or miR-33 of the Cdk6 (**A**) and Ccnd1 (**B**) 3'UTR containing the indicated point mutations (PM) in the miR-33 target sites. Data are expressed as mean % of the 3'UTR activity of control miR ± SEM and are representative of ≥ 3 experiments. * $p \leq 0.05$

3.5 miR-33 regulates cell proliferation and cell cycle progression

To asses the role of miR-33 in regulating cell proliferation, Huh7, A549 and HeLa cells were transfected with miR-33 or CM and the viable cell number was measured at different time points. As seen in **Fig. 11A** and **11C**, overexpression of miR-33 inhibited cell growth in Huh7 and A549 cells compared to CM. Contrary, when treated with an antagonist of endogenous miR-33, increased cell proliferation in Huh7 and A549 cells was observed compared to CI (**Fig. 11B** and **11D**). However, the inhibition of cell proliferation through miR-33 overexpression took place independently from cholesterol content in the medium (**Fig. 11E** and **11F**).
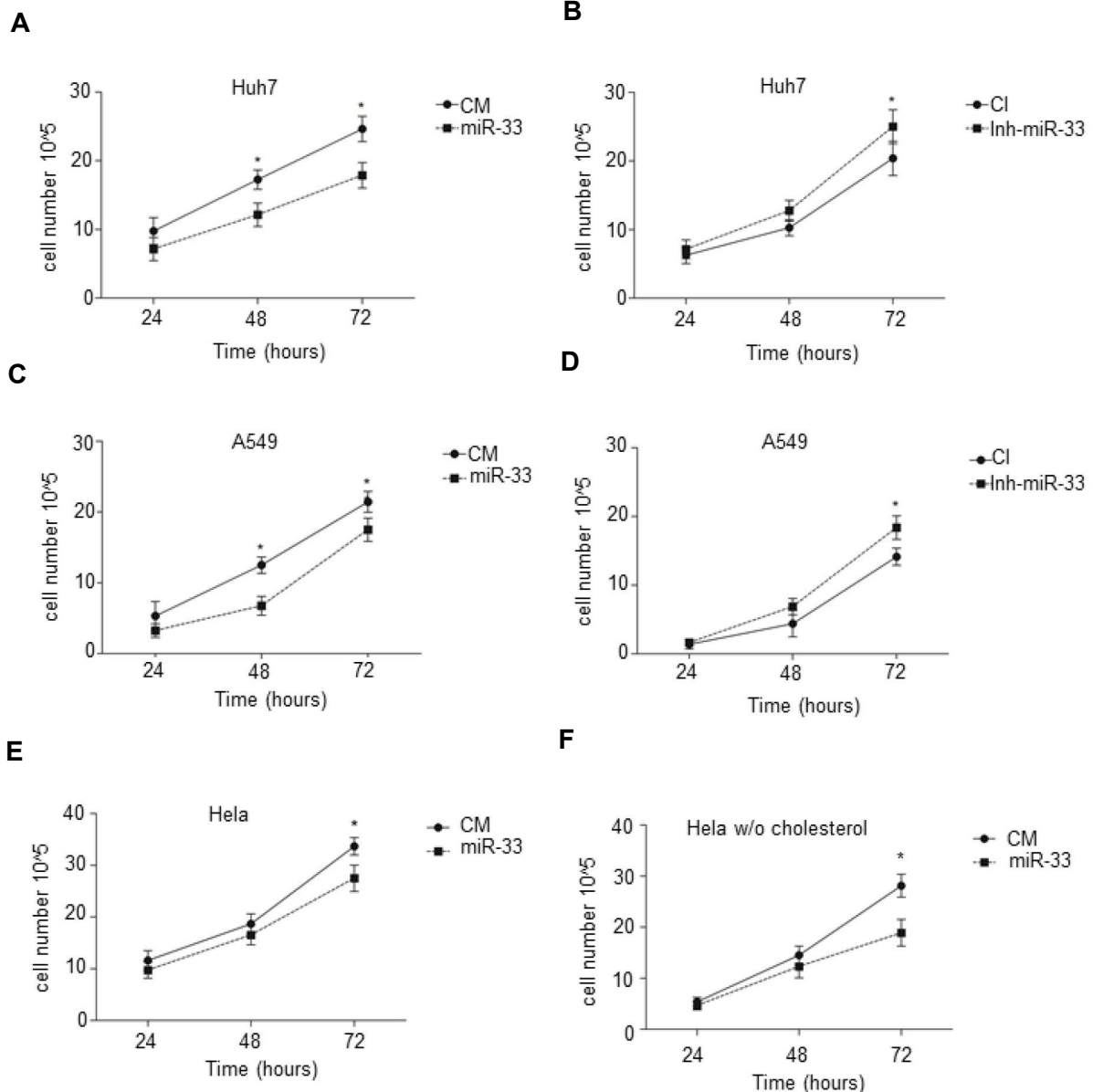

Figure 11. miR-33 inhibits cell proliferation. Time course analysis of the effects of overexpression (**A**, **C**, **E** & **F**) or inhibition (**B** & **D**) of miR-33 on cell proliferation. Huh7, A549 and HeLa cells were cultured in cholesterol (**E**) or cholesterol-free (**A-D** & **F**) medium and transfected with CM, miR-33, CI and Inh-miR-33.

At the indicated times, the viable cells were counted. Data correspond to means ± SEM and are representative of ≥ 3 experiments. * p ≤ 0.05.

To verify these observations, in collaboration with Angel Baldán´s group from St Louis University (UCLA, USA), cell growth was assessed by Crystal Violet Staining and MTTassay in HeLa and MCF7 cells transfected with miR-33 with a lentivirus transfection system.
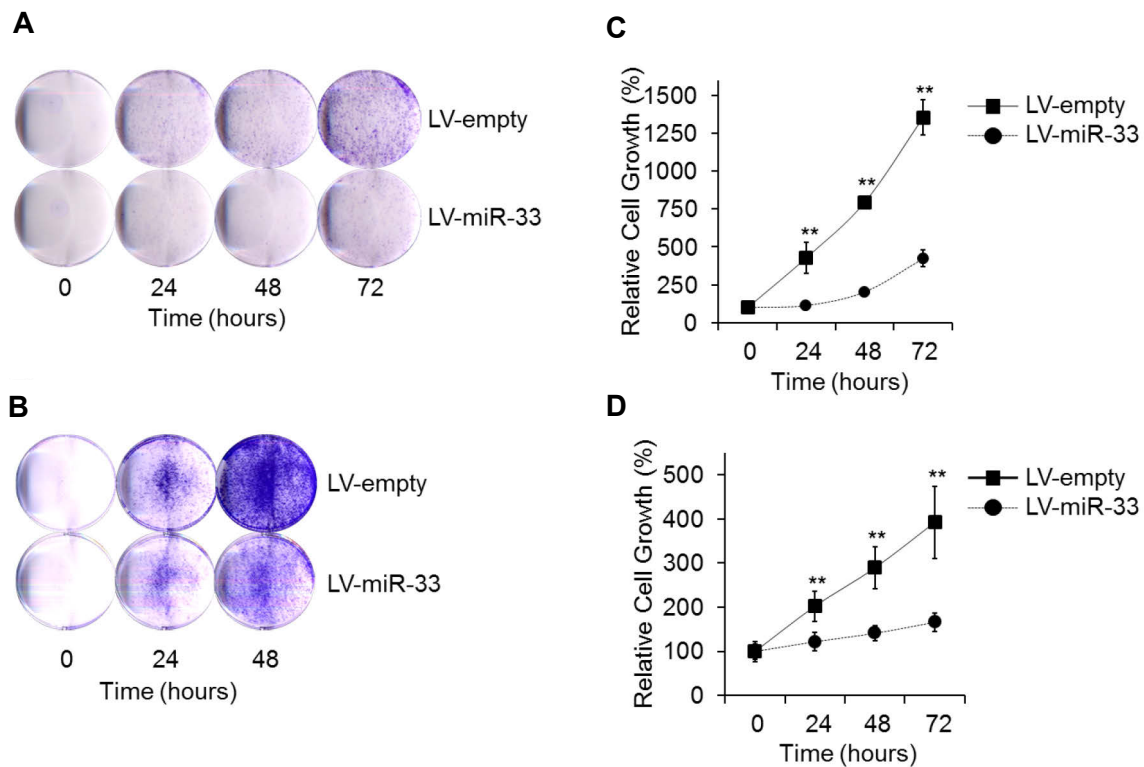

Figure 12. Proliferation ability decreases with miR-33. HeLa (**A** & **C**) and MCF-7 (**B** & **D**) cells stably transduced with empty or miR-33 overexpression lentiviral vectors were serum starved for 48 h in DMEM supplemented with 0.2% BSA. In two independent experiments, growing following the return serum was assayed at 24, 48 and 72 h qualitatively by Crystal Violet Staining (**A** & **B**) and quantitatively by MTT assay (Cayman Chemical Inc.) (**C** & **D**). Data are represented as mean ± SEM. ** p ≤ 0.01.

As illustrated in **Figure 12**, HeLa (**Fig. 12A** and **12C**) as well as MCF7 cells (**Fig. 12B** and **12D**) showed a reduced cell growth when transfected with miR-33 compared to empty control vector. Those results were ascertained by the Crystal Violet Staining as well as by MTT-assay.

Further, stably transfected HeLa cells were used to study the impact of miR-33 overexpression on the cellular response to mitogenic stimuli. Hence, the cells were serum-starved for 72 h and serum was reintroduced, as described in Methods 2.3.8. As shown in **Figure 13** (upper panel), the expression of CDK6 and CCND1 was induced

when cells were switched form BSA to serum, and the expression of both genes was reduced in cells overexpressing miR-33 as compared to controls. Of note, miR-33–dependent repression of these targets resulted in increased mRNA levels of *CDK4*, *CCND2* and *CCND3* (**Fig. 13,** bottom panel).

The exact molecular events that lead to these compensatory changes remain obscure, though; these results demonstrate that miR-33 regulates cell proliferation via targeting CDK6 and CCND1. Most of the mitogenic pathways result in the transcriptional induction of D-type cyclins and the subsequent activation of cyclin-dependent kinases (CDKs) such as CDK4 and CDK6. The active CDK4/6-cyclin D complexes then inactivate the RB, leading to the EF-dependent transcription of specific cell cycle genes and progression throughout the cell cycle.
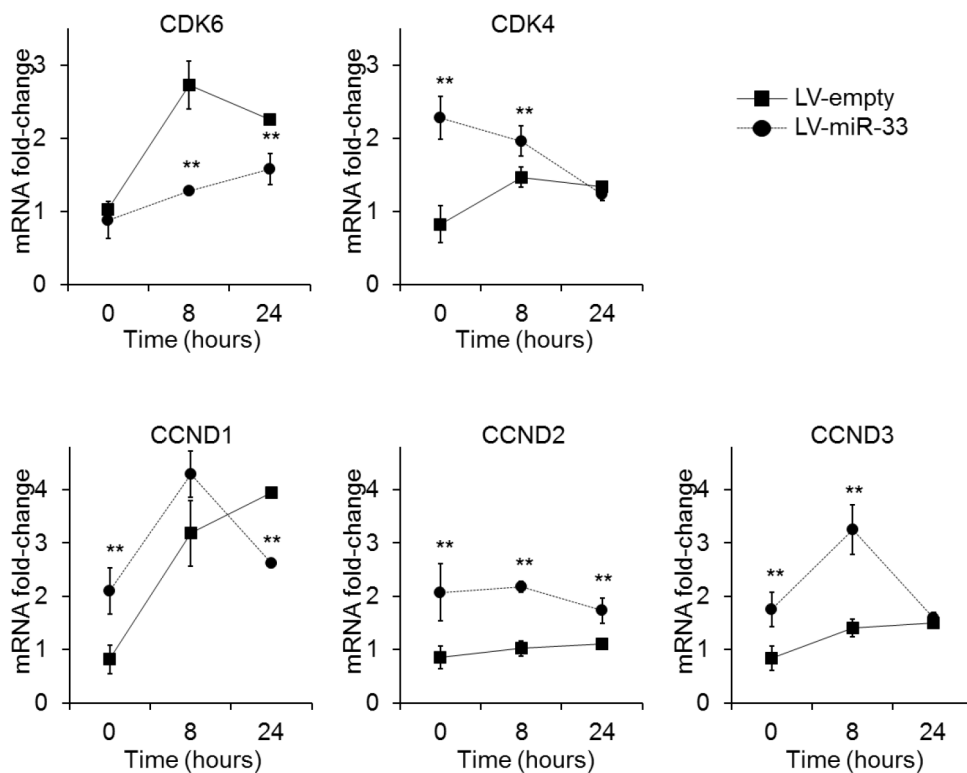

Figure 13. Compensatory effects of miR-33 inhibition. HeLa cells stably transduced with empty (LV-empty) or miR-33 overexpression (LV-miR-33) lentiviral vectors were serum starved for forty-eight hours in DMEM supplemented with 0.2% BSA. mRNA levels of CDK6, CDK4, CCND1, CCND2, and CCND3 were determined at the end of the 48 h starvation, as well as at 8 and 24 h following the return of serum (DMEM supplemented with 10%FBS). Data are represented as mean ± SEM. ** $p \leq 0.05$.

3.6 miR-33 induces G1 arrest

To assess the effect of miR-33 on cell cycle progression, Huh7 cells were transfected with CM or mIR-33 and further synchronized in mitosis by nocodazole treatment during 24 h. As seen in **Figure 14** control cells were released from G1 phase, as showed by a progressing lower relative amount of diploid cells (2N). Contrary, cells transfected with miR-33 were arrested in G1 phase after release from mitosis, suggesting an important role of miR-33 in regulating the G1/S transition.
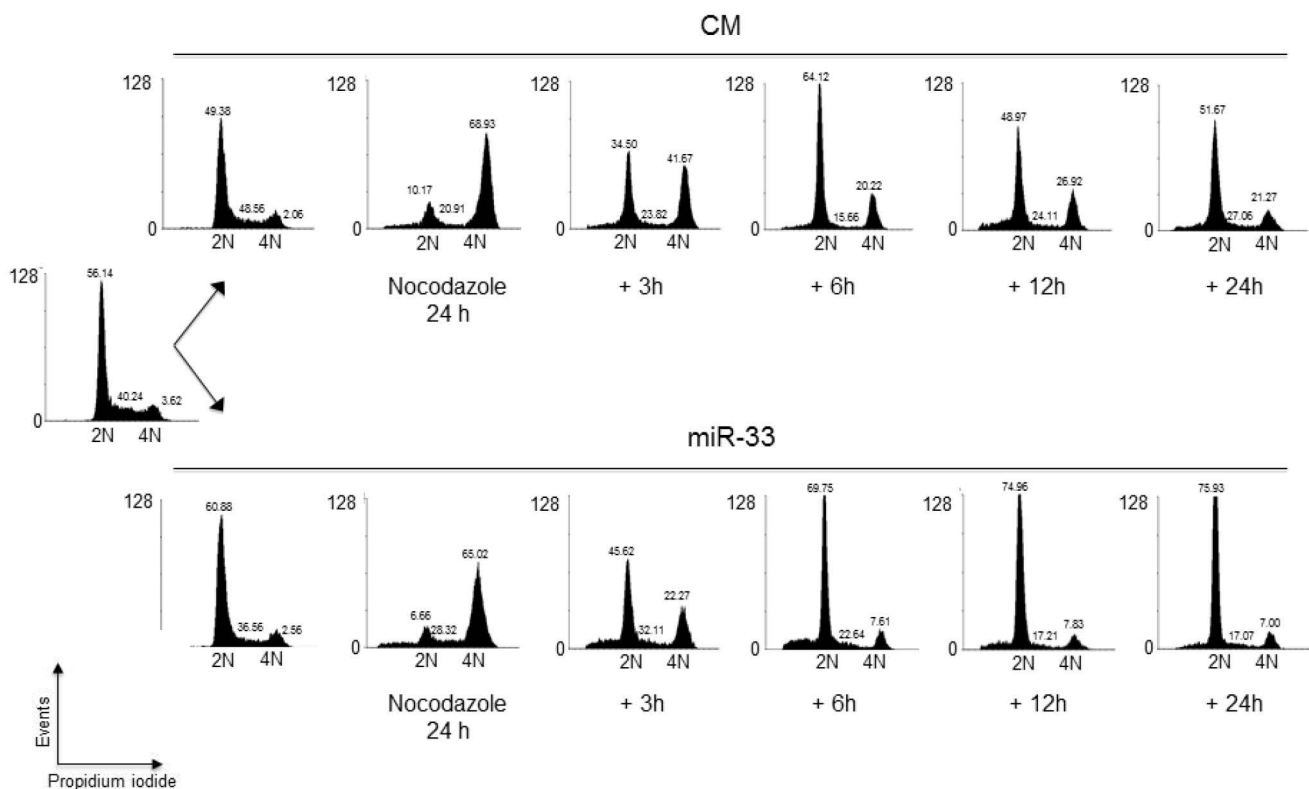

Figure 14. miR-33 induces G1-arrest. Cell cycle distribution of Huh7 cells transfected with CM or miR-33 and synchronized in G2/M with nocodazole. After 24 h of treatment with nocodazole, cells were washed and released of the G2/M cell cycle arrest. At the indicated times, cells were stained with propidium iodide and analyzed by flow cytometry. 2N: cells have diploid DNA content (G0/G1 phase); 4N (G2/M): cells have tetraploid DNA content. Data correspond to a representative experiment among three that gave similar results. FL2-A corresponds to the fluorescence emitted by propidium iodide bound to DNA, which is measured by cytometry in channel 2 (FL2). To avoid the eventual presence of doublets, among the parameters given by the cytometer area (FL2-A) is preferred in order to quantify the amount of DNA present in the cell.

The kinetics of miR-33 mRNA expression during cell cycle progression was analyzed as next after 4, 8, 12 and 24 h in nocodazole synchronized Huh7 cells. As shown in **Fig. 15A** and **15B**, *miR-33a*, *miR-33b*, *SREBP1* and *SREBP2* levels decreased after releasing the cells from mitosis. The results emphasize once more the functional role of miR-33 in regulating the expression of *CDK6*, *CCND1* and *ABCA1*. Indeed, *miR-33* levels were inversely correlated with the expression of *CDK6*, *CCND1* (**Fig. 15D**) and *ABCA1* (**Fig. 15C**), suggesting a functional role for miR-33 in regulating the expression of these genes. Moreover, miR-16 is a marker for G1 phase and inversely correlates with miR-33 expression (**Fig. 15A**). The inhibition of *ABCA1* and the increased expression of genes involved in cellular cholesterol uptake (low-density lipoprotein receptor, LDLr) and cholesterol biosynthesis (3-hydroxy-3methylglutaryl coenzyme A reductase, HMGCR) (**Fig. 15E**) resulted in an increase in cellular cholesterol levels (**Fig. 15F**).
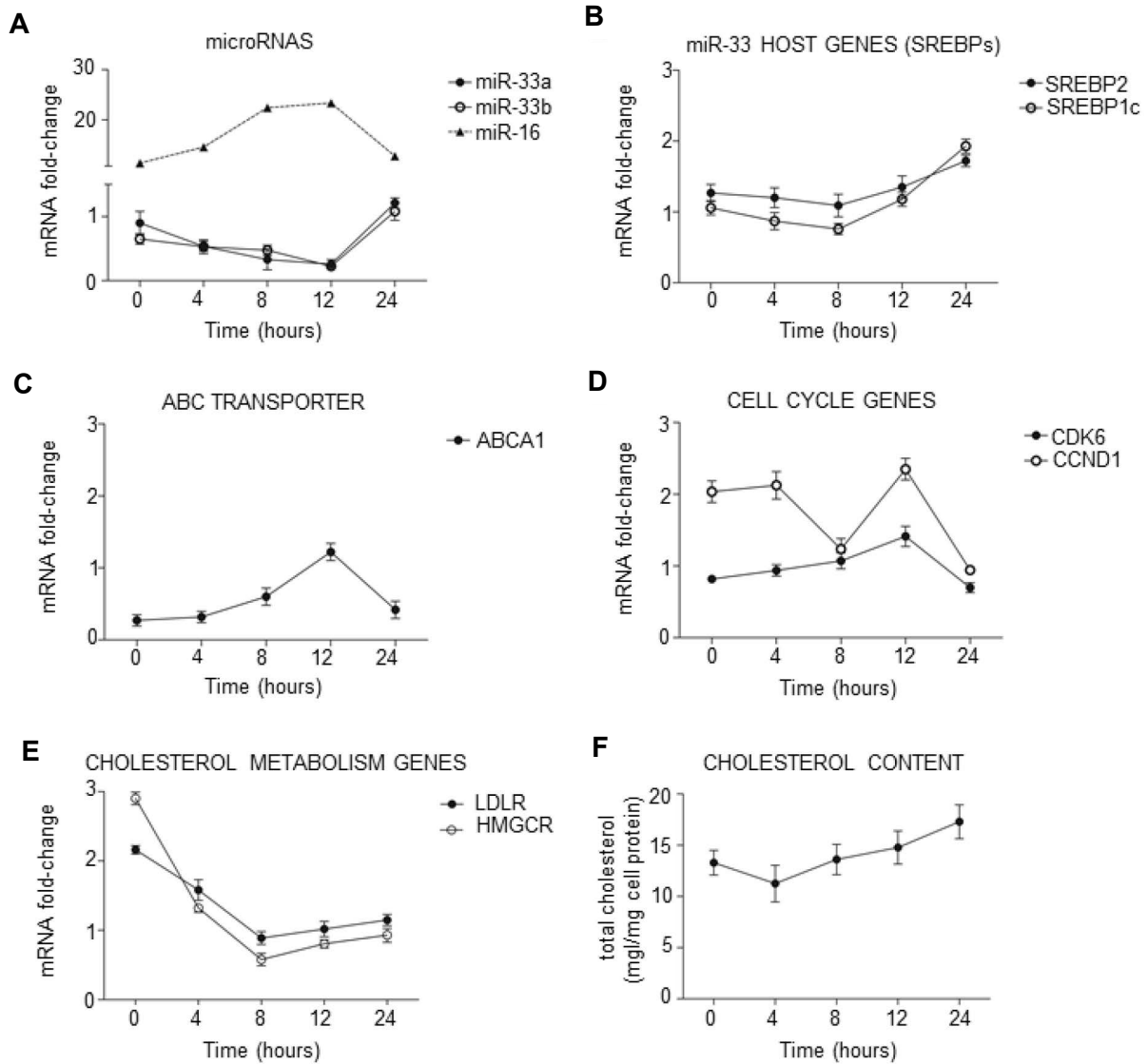
Figure 15. **mir-33 expression levels correlate inversely with its predicted target genes during cell cycle progression**. (**A** to **E**) Quantitative RT-PCR analysis of *miR-33a/b*, *SREBP-2*, *SREBP-1*, *ABCA1*, *CDK6*, *CCND1*, *LDLR* and *HMGCR* in human hepatic Huh7 cells synchronized with nocodazole for 24 h. (**F**) Total cholesterol content was measured at 0, 4, 8, 12 and 24h after nocodazole release. Data are the mean ± SEM and are representative of ≥ 3 experiments which gave similar results.

3.7 Antagonism of miR-33 in mice promotes liver regeneration

The liver is pivotally positioned in the regulation of the body´s metabolic homeostasis of lipids, carbohydrates and vitamins. Consequently, the liver has evolved complex regenerative mechanisms to respond to chemical, traumatic or infectious injuries [113]. One of the most extensively characterized model systems to study liver regeneration is the partial hepatectomy (2/3 PH) in rodents. In this model, the left and medial lobes of the liver are excised, resulting in removal of 70% of the hepatic mass. Within minutes, hepatocytes then undergo a coordinated cellular activation termed the acute phase response. As a result of the acute response, the hepatocyte initiates the transcription of more than 100 early genes, accumulates triacylglycerol and cholesterol esters in intracellular lipid droplets, and progresses through the cell cycle. Lipid droplet formation is an essential part of the proliferative response during liver regeneration. By compensatory hyperplasia, the regenerative process reestablishes the original liver mass in approximately 1 week, after which hepatocytes return to a quiescent state.

To analyze the role of miR-33 in a physiological model of cellular proliferation and regeneration 2/3 PH was performed in mice and Ki67 expression (**Fig. 17**) as well as lipid accumulation (**Fig. 18**) were assessed as markers for proliferation and regeneration, respectively (following the time course shown in **Fig. 16**).
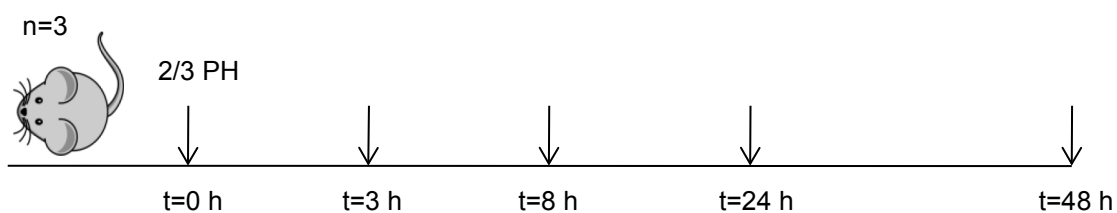

Figure 16. Experimental outline of liver regeneration after 2/3 PH. Time-course analysis from liver of mice (n=3) subjected to 2/3 PH. Samples were analyzed at 0, 3, 8, 24 and 48 h after 2/3 PH.

As seen in **Fig. 17**, a significant number of Ki67 positive cells were observed in sections of livers at 48h following 2/3 PH. Cell cycle entry and progression of hepatocytes after 2/3 PH occurred not only rapidly, but also in a synchronized dependent fashion. Most hepatocytes have entered S phase by 72 hours after 2/3 PH in adult C57BL/6 mice. Confirming our previous findings, 2/3 PH in such mice caused decreased mir-33 expression that was detectable at 8 hours, peaked between 8 and 24 hours, and returned to almost normal levels by 72 hours after the surgery (**Fig. 19**). The timing of the miR-33 decay suggests a role in the regulation of cell cycle events preceding the S phase.
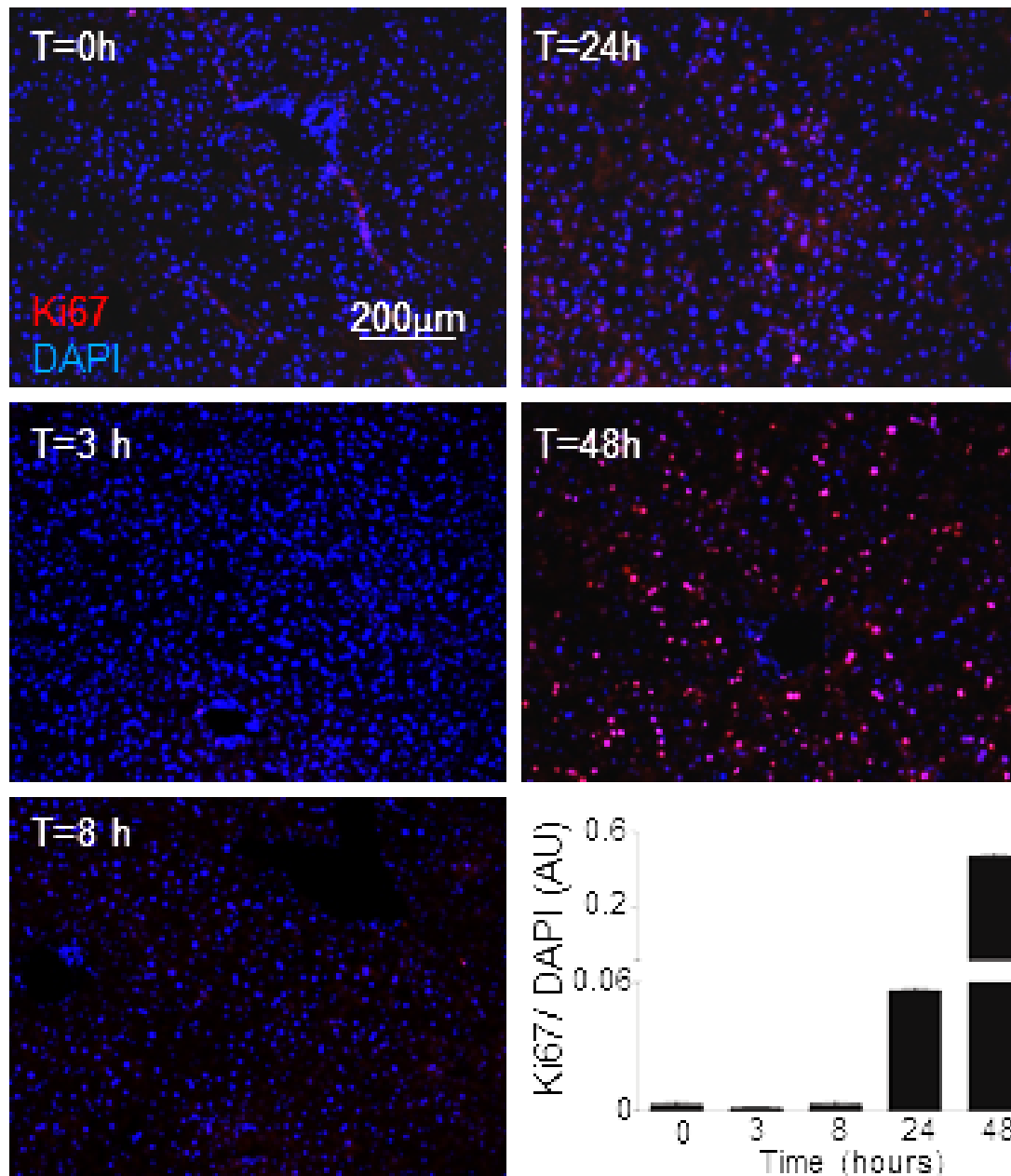
Figure 17. Liver regeneration after 2/3 PH. Time course analysis of Ki67 positive cells from liver sections of mice subjected to 2/3 PH. The computed assisted quantification of the proliferating cells (red) vs. the total number of cells (blue) is shown at the graph. Data are mean ± SEM (n=6 mice).

In agreement with the proliferation status and the Ki67 staining (**Fig. 17**), the accumulation of lipid-droplets was similar in the liver after 2/3 PH. After partial hepatectomy, the levels of fatty acids in the plasma increase several fold, leading to the intracellular accumulation of lipids and the formation of numerous cytosolic lipid droplets [114]. Eight hours after partial hepatectomy, the hepatocytes of mice accumulated enlarged lipid droplets in the cytosol (**Fig. 18**), confirming the data shown by Glende *et al.*
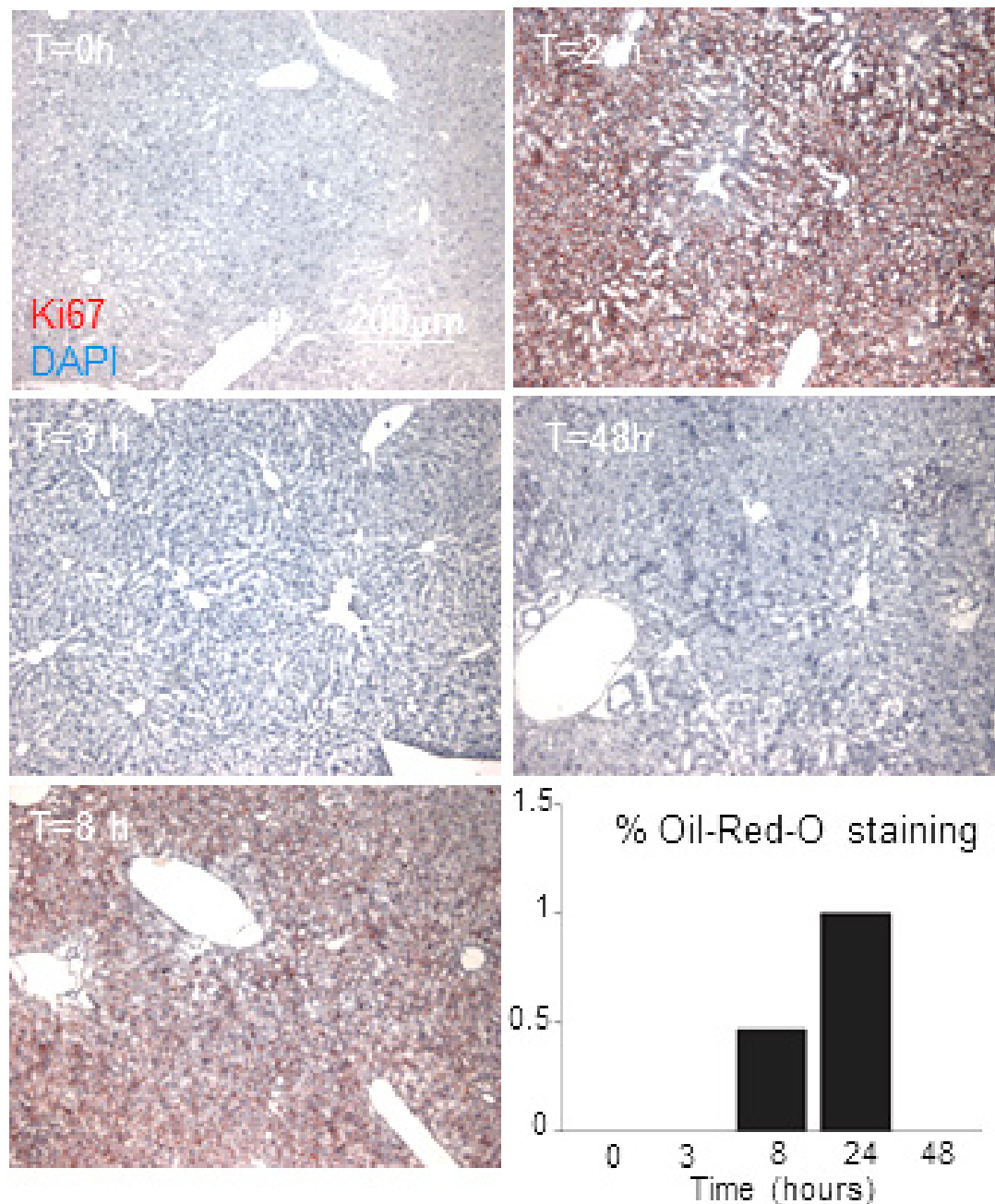
Figure 18. Intracellular lipid accumulation in the liver after 2/3 PH. Time course analysis of Oil-red-O positive cells from liver sections of mice subjected to 2/3 PH. The computed assisted quantification of the lipid droplets (red) *vs.* the total number of cells (blue) is shown in the graph. Data are mean ± SEM (n=6 mice).

To determine whether or not miR-33 plays a role during liver regeneration, *miR-33*, *SREBP2*, *CDK6* and *CCDND1* levels were measured in the same 2/3 PH model. The expression of *miR-33* (**Fig. 19**, upper panel) correlated inversely with both the proliferative status of the liver (**Fig. 17**) and the mRNA expression of *CDK6* and *CCND1* (**Fig. 19**, middle panel), thus suggesting a role for miR-33 in regulating liver regeneration.

Similar results were obtained when the expression of proliferating cell-nuclear antigen (PCNA) in liver lysates was analyzed by Western blot (**Fig.19**, bottom panel).
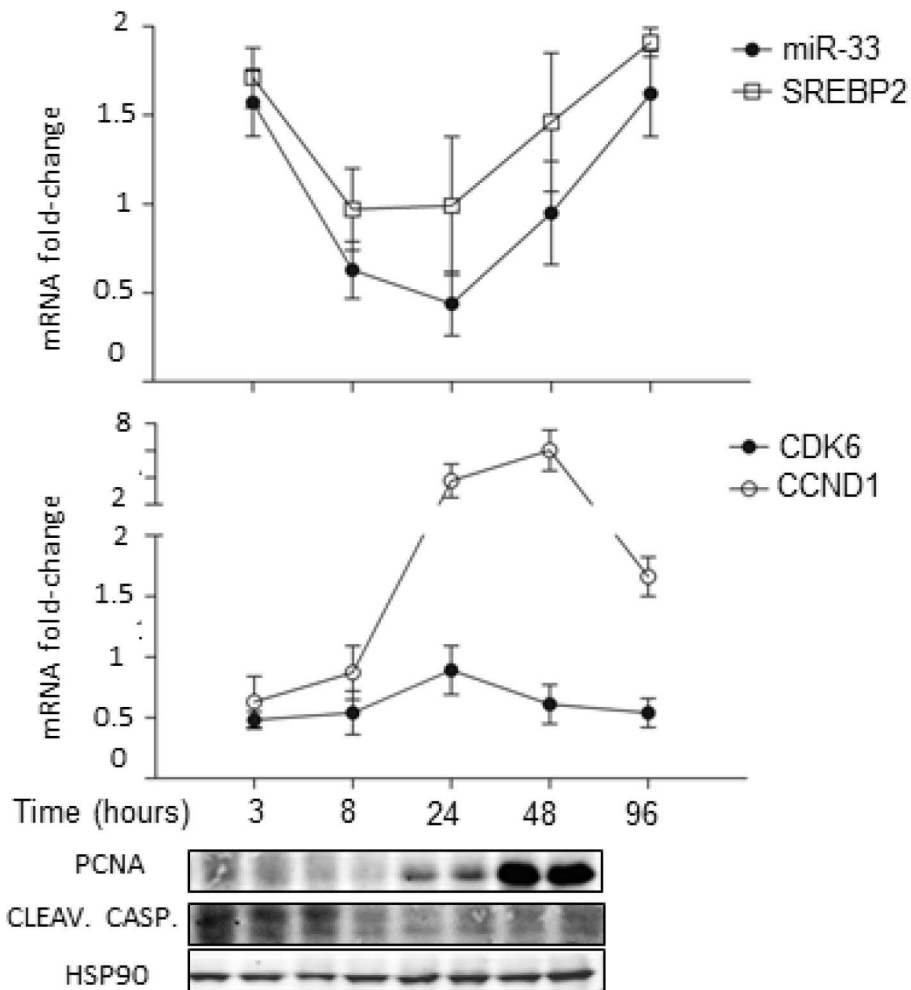

Figure 19. Liver regeneration after 2/3 PH causes a rapid induction of CCND1 expression and miR-33 downregulation. Time course mRNA expression analysis of miR-33, SREBP-2 (upper), CDK6 and CCND1 (middle) and Western blot analysis (bottom) of PCNA and cleaved caspase 3 expression from liver lysates of mice subjected to 2/3 PH. Data are mean ± SEM (n=6 mice).

To assess the effects of inhibiting *miR-33* in the 2/3 PH model, C57BL/6 mice were treated with 10 mg/Kg of 2'fluoro/methoxyethyl-modified (2'F/MOE- modified) phosphorothioate backbone antisense miR-33 oligonucleotides (miR-33-ASO), control anti-miR (Control-ASO) or PBS (untreated) once a week for one month. The experimental outline of miR-33-therapy is illustrated in **Figure 20**.
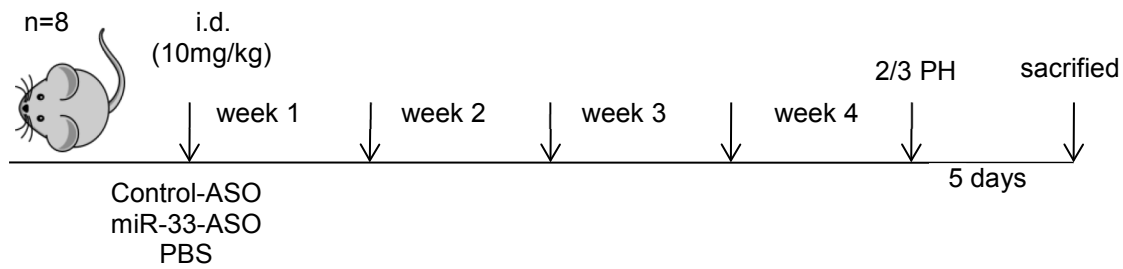
Figure 20. Experimental outline of miR-33-ASO, Control-ASO or PBS treatment in mice. C57BL/6 mice (n = 8 per group) were treated for one month prior 2/3 PH. The analysis was done at day 0 (before 2/3 PH) and at day 5 (after 2/3 PH).

This subcutaneous or intraperitoneal antisense therapy has been used successfully in mice to inhibit the function of various miRNAs and to increase expression of their target genes, with no apparent toxicity [105]. To determine the efficacy of the anti-miR-33 treatment, the hepatic expression of miR-33 and its target genes (*Cdk6*, *Ccnd1* and *Abca1*) were measured after 4 weeks of treatment (see **Figure 21A** and **21C**). Levels of miR-33, detected by qRT-PCR, were decreased by more than 50% in anti-miR-33-treated mice (miR-33-ASO) compared with controls (Control-ASO) (data not shown). Consistent with these results, the expression of ABCA1, CDK6 and CCND1 was increased in the livers of the mice treated with anti-miR-33 before the 2/3 PH (t=0, **Fig. 21B**) and during liver regeneration (t=5 days after 2/3 PH, **Fig. 21D**). Of note, the expression of the proliferative marker PCNA was also increased in mice treated with anti-miR-33 (**Fig. 21B** and **21D**).
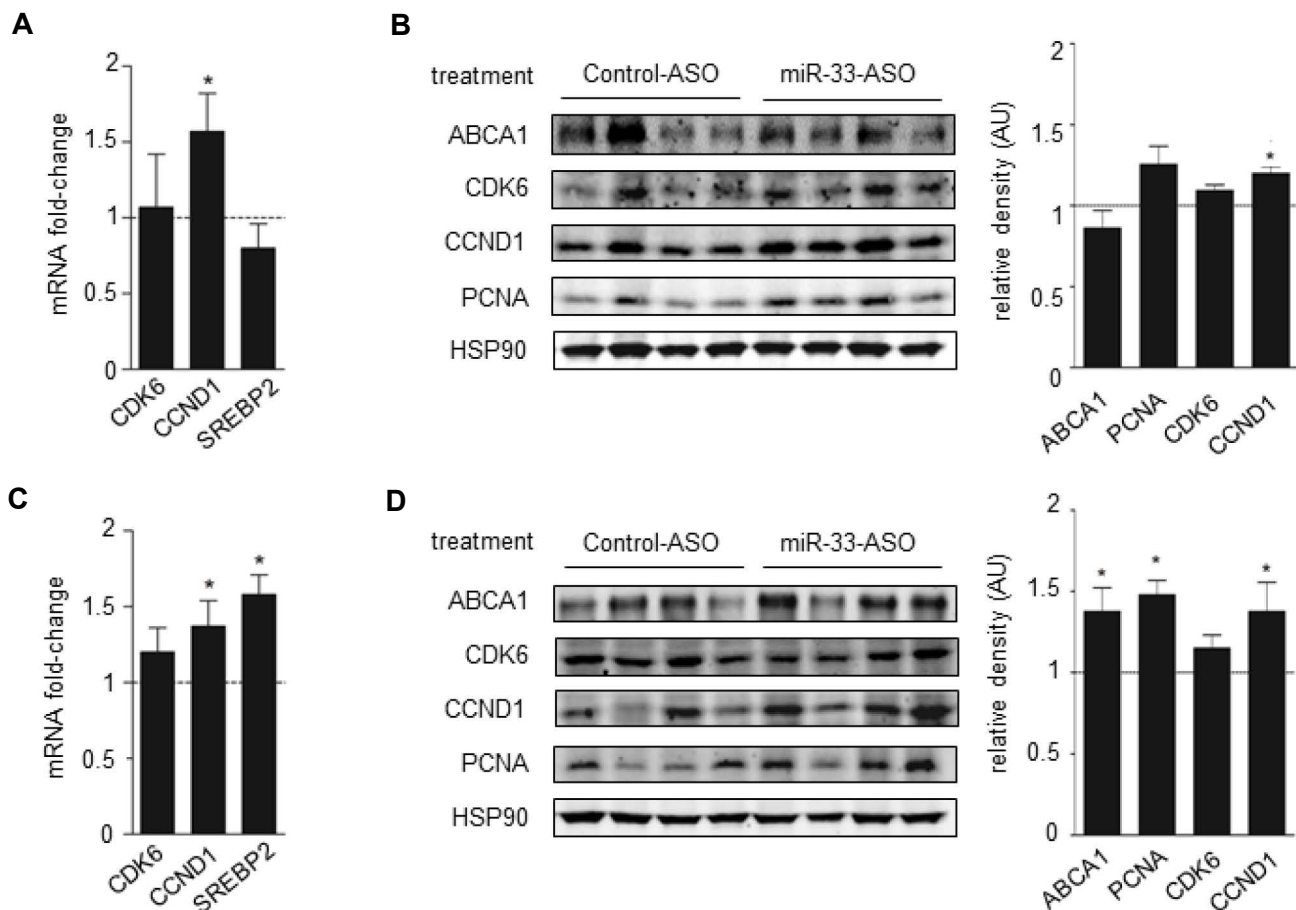
Figure 21. **Anti-miR-33 treatment reduces miR-33 expression in the liver and causes derepression of its target genes.** Mice were treated for 4 weeks with PBS (no treatment) or control anti-miR (Control-ASO) or anti-miR-33 2'F/MOE oligonucleotides (miR-33-ASO). Expression of miR-33 target genes (ABCA1, CDK6, CCND1), and proliferation marker (PCNA) and miR-33 host gene (*Srebp2*) in the liver was quantified by RT-PCR (**A**) and by Western blot (**B**) at time 0 (**A** and **B**) and 5 days after (**C** and **D**) 2/3 PH. The representative Western Blot analysis (**B** and **D**) shows that the inhibition of miR-33 in vivo for 4 weeks increased the expression of PCNA, CDK6, CCND1 and ABCA1. Relative density analysis is shown in the right part. Dotted line positioned at one represents the normalized values of control mice. The data are presented as the mean ± SEM and are representative of 3 experiments * $p < 0.05$.

Further, the effects of anti-miR-33 oligonucleotides in liver regeneration after 2/3 PH were investigated (**Fig. 22**). Mice treated with miR-33-ASO have significantly more proliferating hepatocytes at day 5 after 2/3 PH as compared to controls (**Fig. 22A**). The regeneration index, given as the increase in the liver-to-body mass ratio, was calculated as described in Methods 2.6.2. As seen in **Fig. 22B**, mice treated with anti-miR-33 oligonucleotides showed an accelerated liver regeneration suggesting that anti-miR-33 therapy might be useful for treating liver disease.

A

B
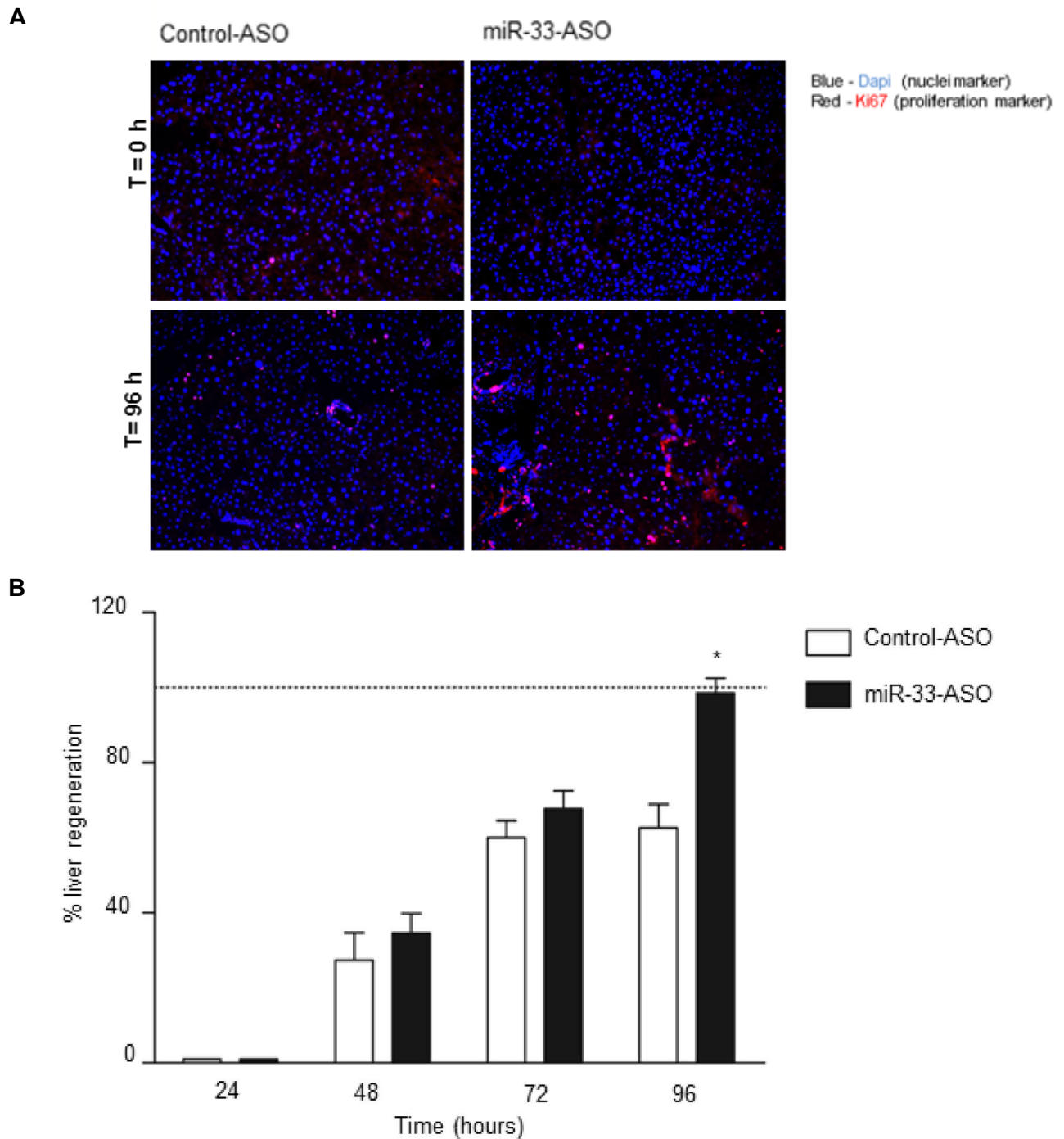
Figure 22. Inhibition of miR-33 with miR-33-ASO *in vivo* increases liver regeneration. Mice treated with miR-33-ASO proliferated more that the mice treated with ASO Control after 2/3 PH (**A**) as shown by Ki67 staining, a proliferation marker. (**B**) Effect of miR-33-ASO treatment on liver regeneration after partial hepatectomy. The body weight recovery was used to calculate the percentage of liver regeneration after 2/3 PH vs. control animals (dotted line indicates 100% liver regeneration). The data are presented as the mean ± SEM and are representative of 8 experiments * $p < 0.05$

In the presented liver regeneration model, miR-33 inversely correlated with CDK6, CCD1 and PCNA expression and anti-miR-33 therapy provoked an increased of those targets.

Taken together, these results suggest that miR-33 is involved in cell cycle progression and cellular proliferation via the regulation of multiple proteins. **Figure 23** is a pontential working hypothesis for miR-33.
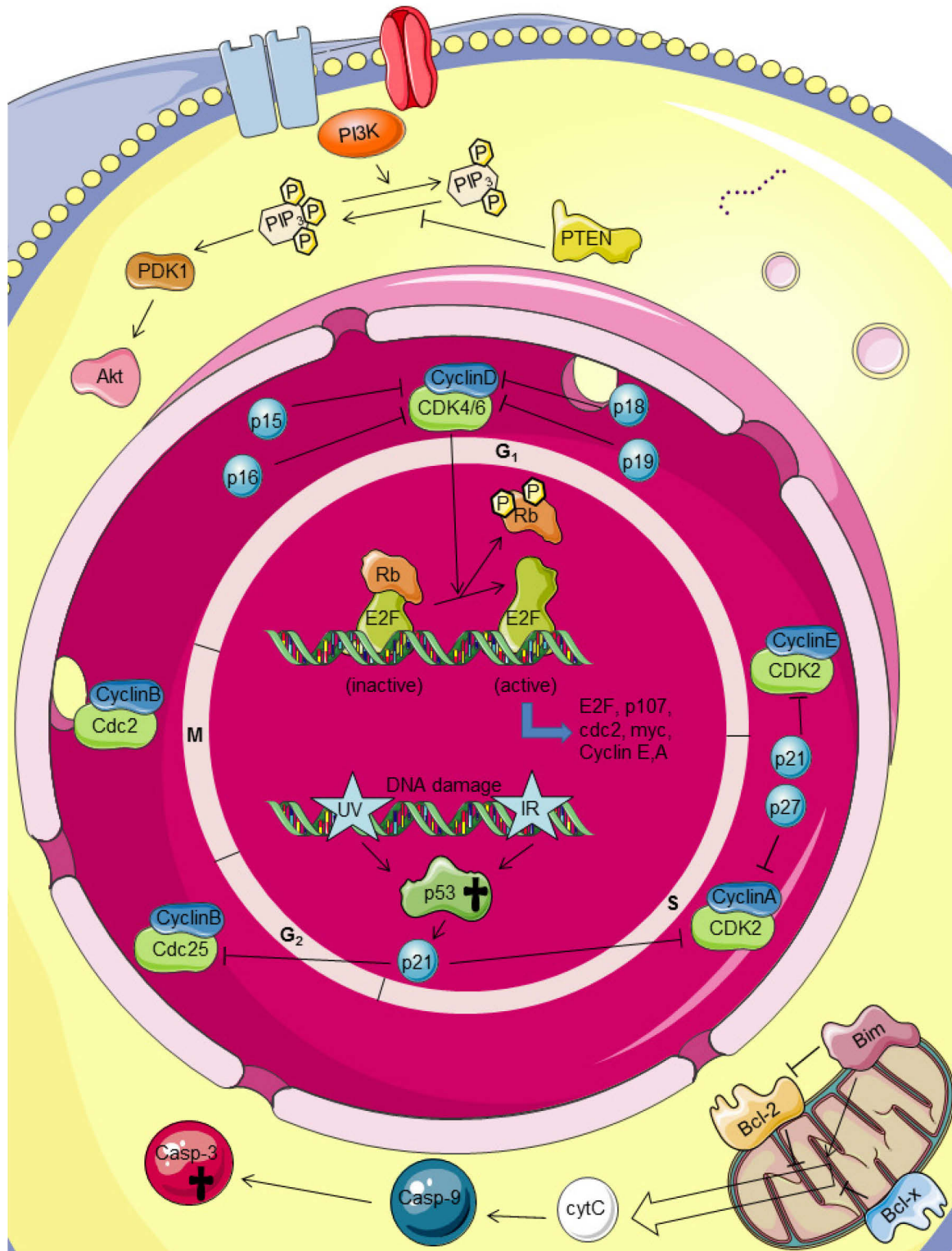

Figure 23. A model for miR-33-mediated regulation of cell proliferation and cell cycle progression. miR-33 induces a G1 arrest through negative effects on cell cycle related proteins including CDK6 and CCND1. Other

molecules (e.g. p53, PTEN, Bcl-2) involved in the cell cycle are targets or predicted targets for miR-33. (Modified from Cirera-Salinas *et al.*)

3.8 Construction of a conditional miR-33 knockout

To further explore the functions of mir-33, a conditional knockout mouse model was designed and generated. A targeting vector was created to "flox" the miR-33 genomic coding region in the intron 17 of the *Srebf2* gene. This vector contained a neomycin selection cassette flanked by site-specific flippase recognition target (FRT) recombination sites in intron 17 (**Fig. 24**). To clone the left and right homologous recombination regions, genomic intron 17 from *Srebf2* gene sequences were obtained by PCR of genomic DNA from BAC clones library (CHORI Hospital, BACPAC Resources Center, USA). The miR-33 genomic coding region and the flanking regions were step-wise inserted into a vector backbone already containing the appropriate loxP recombination sites (pEZ-Frt-lox-DT). As next the neomycin selection cassette flanked by FRT sites and the genomic miR-33 coding region flanked by the loxP sites were first excised from pEZ-Frt-lox-DT and then inserted into the right homologous recombination region in the intron 17.

After integration into the *Srebf2* locus, this construct gave rise to a bicistronic mRNA that is transcribed from the endogenous expression of *Srebf2* promoter. Thus the expression of the neomycin selection gene depended on the endogenous expression of *Srebf2* in embrionic stem (ES) cells. The selection cassette could be removed *in vivo* from the conditional allele with a site-specific flippase recombinase by crossing animals harboring the modified conditional miR-33 allele with a FLP expression deleter strain, as described by Farley *et al.* [115]. After the correct removal of the neomycin selection cassette, genomic miR-33 coding region was flanked by only two loxP sites in the intron 17; termed flox allele (flox).
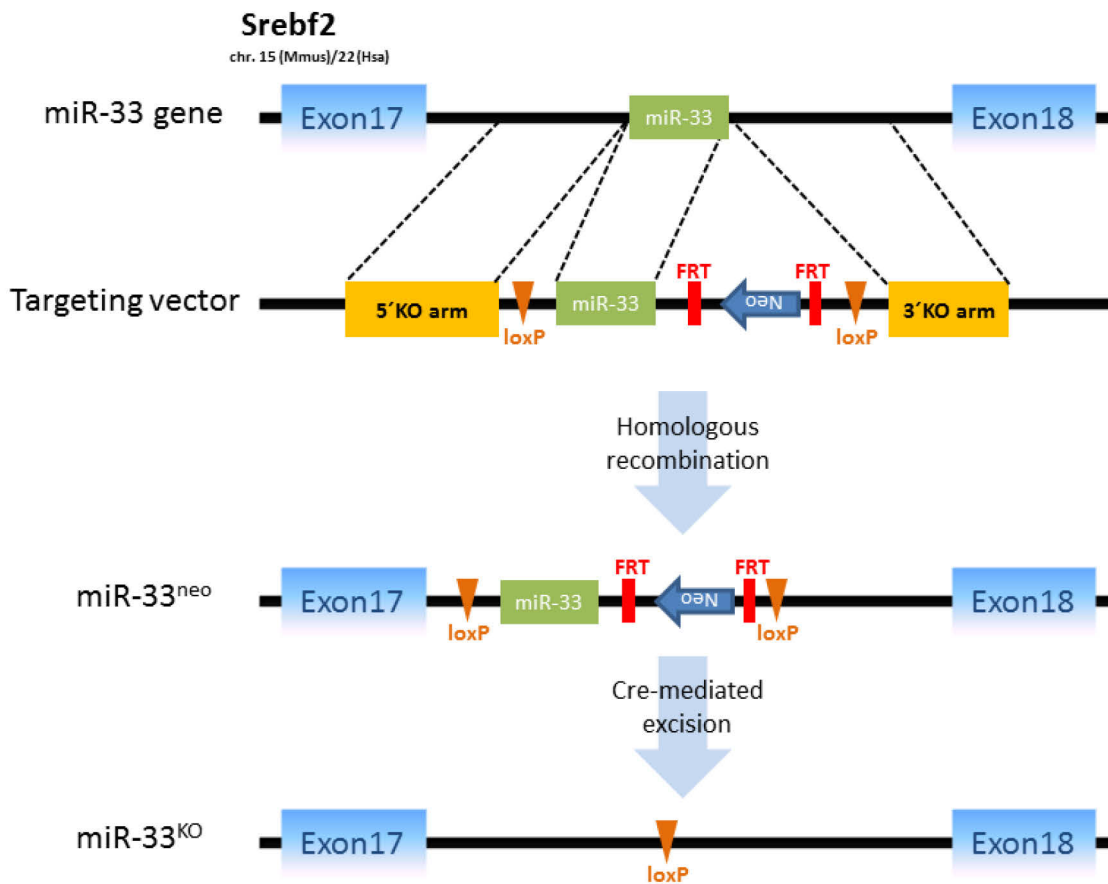
Figure 24. Strategy to generate a miR-33 conditional knockout mouse by homologous recombination. The loxP and the FRT sites flanking the neomycin cassette were inserted into the intron 17 of the *Srebf2* gene flanking the miR-33 genomic coding region. Neomycin cassette was removed in the mouse germ line by crossing heterozygous mice to a recombinase-flippase transgenic mouse.

3.9 Generation of conditional knockout mice

Mouse-derived ES cells (JM8.A3) were transfected with the targeting vector, selected with neomycin and grown in culture. Positive ES cell clones were identified by PCR, using different primers combinations located upstream and downstream of the integration site. After selection, a properly targeted ES cell clone was injected in C57BL/6 blastocysts to generate chimeras. Several chimeric males were obtained and crossed with C57BL/6 females. PCR-based genotyping of their agouti progenies showed successfully transmission of the mutant allele to the germ line. To remove the neo selection cassette, animals carrying the miR-33$^{neo/+}$ allele were bred with expressing deleter mice, as described by Rodriguez *et*

al. [116]. To detect the flox and the wild type (wt) allele, the progenies were genotyped by PCR. As expected, miR-33 was flanked by loxP sites and a single FRT remained in intron 17. The miR-33$^{flox/+}$ animals were further intercrossed and bred till homozygosity (flox/flox). These miR-33$^{flox/flox}$ mice were phenotypically normal and fertile, indicating that the loxP sites did not interfere with the normal processing of the miR-33 mRNA. Finally, it was very important to prove that miR-33 can be deleted by introducing a Cre recombinase in vivo. The Cre-mediated excision of miR-33 resulted in deletion of the miR-33.

In summary, a conditional miR-33 mouse model was generated. The selection cassette was successfully removed *in vivo*. Homozygous animals for the floxed miR-33 allele (miR-33$^{flox/flox}$) develop normally, indicating that the loxP sites did not interfere with the function of miR-33 or its host gene *Srebf2*. Floxed miR-33 could be deleted *in vivo* by crossing with early Cre-deleter mice. The tool to further study the role of miR-33 *in vivo* was thus established in our laboratory.

4 DISCUSSION

Since the discovery of the first miRNA, lin-4, in 1993 [60, 61], this family of previously unknown molecules has earned a superordinate position among the central mechanisms of gene activity regulation. Computational analyses predicted that the expression of 40-60% of all genes is regulated by miRNAs and they are involved in the control of all biological processes [117]. The present work aimed to characterize the relation between miR-33, cholesterol, fatty acid oxidation and carbohydrate metabolism, as well as to identify the regulatory properties of miR-33 in the cell cycle.

4.1 miR-33 modulates cholesterol, fatty acid oxidation and carbohydrate homeostasis

Our understanding of cholesterol homeostasis has significantly advanced over the past years. Much insight has been gained into the transport pathways that regulate sterol trafficking and distribution within cells and much progress has been made in understanding the regulatory mechanisms that control cholesterol uptake and efflux. In this context, recent studies indicated that miRNAs, particularly miR-33a and miR-33b, play a significant role in regulating cholesterol and fatty acid metabolism [101, 105].

In previous studies, Fernández-Hernando´s laboratory and others provided for the first time the identification of a miRNA family, miR-33, highly conserved from Drosophila to humans. They determined that miR-33 is an intronic miRNA located within the SREBPs gene, key transcription factors regulating cholesterol biosynthesis and transport. It was shown that miR-33 inhibited HDL biogenesis in the liver and cellular cholesterol efflux by targeting multiple genes regulating cholesterol homeostasis, including *Abca1*, *Abcg1* and *Npc1* [101]. Antagonism of miR-33 *in vitro* and *in vivo* significantly increased ABCA1 expression, promoted cholesterol efflux to Apo-A1 and increased HDL plasma levels in mice [99-104].

Furthermore, Fernández-Hernando´s and Gerin´s group identified in 2010 new targets of miR-33 involved in fatty acid metabolism including *Cpt1a*, *Crot* and *Hadhb*. Overexpression

of miR-33 lead to the accumulation of triglycerides in human hepatic cells and in the fat body of miR-33 transgenic flies [105]. Previous work also revealed an interesting role for miR-33 in glucose metabolism, as miR-33 overexpression reduced IRS2 levels and inhibited activation of downstream messenger cascades, including PI3/Akt pathway [105]. Consistent with these findings, miR-33b overexpression reduced insulin-induced 2-deoxyglucose (2-DOG) uptake in hepatic cells, suggesting that miR-33 plays a key role in regulating insulin signaling [105].

miRNAs represent an elegant layer above transcriptional control for both fine-tuning and dramatically altering activity and output of cell signaling. In addition, miRNAs may serve as points of crosstalk between signaling pathways by integrating transcriptional inputs or by their functional regulatory output on different gene networks. The dysregulation of many siRNAs and miRNAs has been linked to the development and progression of disease and, consequently, these non-coding RNAs have gained considerable attention as therapeutic targets [118]. The results obtained highlight the use of anti-miR-33 therapies in the treatment of a number of metabolic disorders, such as dyslipidemias, atherosclerosis, type II diabetes and metabolic syndrome. Inhibition of miRNA expression can be achieved using anti sense oligonucleotides, termed "antagomirs", or their chemically modified versions, 2´ O-methyl (2´-Ome)-oligonucleotides and locked nucleic acid (LNA), termed "anti-miRs". Additionally, the production of the mature forms can also be disrupted at the processing level [119-122]. Using anti-miR-33 treatment to elevate ABCA1 levels and increase HDL levels would hold tremendous potential for the treatment and/or the prevention of coronary artery disease (CAD), in which an underlying risk factor is low levels of HDL. Moreover, inhibition of miR-33 would result in increased fatty acid oxidation and reduced accumulation of fat stores in the liver, suggesting that antagonism of endogenous miR-33 may also be used to treat metabolic syndrome and non-alcoholic fatty liver disease (NAFLD). While there are still unanswered questions surrounding miRNA therapeutics, the promise demonstrated by the use of anti-miRs in preclinical studies raised the possibility that miR-33 may become a viable therapeutic target in the future [104,105,149].

4.2 miR-33 is a novel regulator of cell cycle progression and proliferation

This venture led to conclusive mechanistic evidence for miR-33 as a very versatile regulator of cell cycle progression, cell proliferation and liver regeneration. The data presented herein constitutes the first example of a single miRNA with the ability to influence major pathways of metabolism and cell cycle and fills another piece of the puzzle linking lipid synthesis, cell cycle, SREBPs and miR-33, hinting a regulatory role for cholesterol in cell cycle progression.

Since SREBPs have been implicated in the regulation of cell cycle [123], we decided to investigate the link between miR-33 and cell cycle progression as well as cell proliferation. Using bioinformatics approaches, potential miR-33 binding sites were predicted in genes involved in cell cycle progression and cell proliferation. Indeed, the overexpression of miR-33 *in vitro* reduced CDK6 and CCND1 at the mRNA and the protein level, consequently reducing cell proliferation and notably arresting cell cycle in the G1 phase. Conversely, inhibiting miR-33 increased expression of CDK6 and CCND1 and promoted proliferation. miR-33 overexpression reduced cell proliferation and retarded cell cycle progression from the late G1 into the S phase in human hepatic cells.

Since we observed that the 3'UTR of human and mouse *CCND1* harbors one putative site recognized by miR-33, and more importantly, *miR-33* and *CCND1* expression seemed to be inversely correlated in several experiments, we hypothesized that CCND1 may be directly regulated by miR-33 at the posttranscriptional level. By a luciferase-based reporter assay, we showed that one predicted miR-33 targeting site in the 3′UTR of *CCND1* is functional, and the expression of miR-33 caused a significant decrease, both at the mRNA and the protein level. Comparatively, the same was observed for the *CDK6* human and mouse 3′UTR. In this case, the 3′UTR of *CDK6* harbored three putative sites for miR-33. The same luciferase-based reporter assay confirmed that the three predicted miR-33 binding sites were functional. In particular, the second binding site seemed to be the most important for the repression of *CDK6*, since the 3′UTR activity of *CDK6* decreased by 40% when transfected

with miR-33 as compared to the control. Similarly, the mRNA and protein levels of CDK6 decreased significantly when miR-33 was overexpressed.

Cell cycle progression involves the sequential activation of different cyclin-dependent kinases. The expression of cyclins and other regulators of CDKs vary during cell cycle progression [32]. CDK6 and CCND1 have been shown to be essential for the regulation of cell cycle progression during G1/S phase transition [124]. Our study indicated miR-33 to inhibit proliferation and to cause cell cycle arrest at the G1 phase in different cell lines and the mechanism involved the downregulation of CCND1 and CDK6 by direct binding of miR-33.

In addition to miR-33, many miRNAs have been shown to play a role in regulating proliferation and cell cycle progression [125]. The miR-15a-16-1 cluster (*miR-15a* and *miR-16-1* are transcribed as a cluster residing in the 13q14 chromosomal region) may induce cell cycle arrest at the G1 phase by targeting critical cell cycle regulators such as CDK1, CDK2 and CDK6, as well as their partner cyclins CCND1, CCND2 and CCNE1 [84, 126, 127]. Indeed, the major cell cycle kinase complexes are regulated by several other miRNAs. Thus, the 3´UTR of CDK6 mRNA is also targeted by miR-24, miR-34a, miR-124, miR-125b, miR-129, miR-137, miR-195, miR-449 and let7 family members. Likewise, the levels of D-type cyclins are downregulated by let-7, miR-15 family, miR-17, miR-19a, miR-20a and miR-34 [125].

A variety of tumor types are associated with inappropriate miRNA expression or structural alterations of miRNA genes, demonstrating the oncogenic or tumor-suppressive potential of specific miRNAs [128, 129]. Herrera-Merchán *et al.* in 2010 demonstrated the action of miR-33 upstream of p53. In fact, they showed how important miRNAs are in tumorigenesis when miR-33 can replace p53-loss in the classic oncogenic cooperation assays with oncogenic Ras [108]. Although, it is becoming increasingly clear that the majority of the miRNAs target multiple genes with related functions and thereby exert strong effects on a particular regulatory pathway, the so called fine tuners. As described by the aforementioned group,

miR-33 functions to influence tumor-suppressor networks by suppressing p53, essential regulators of cell survival [108]. Given that *p53* is frequently downregulated in cancers and that the *p53* gene itself is not mutated, it would be very interesting, from a clinical point of view, to investigate whether miR-33-p53 dysregulation represents a novel mechanism for cellular transformation in certain types of cancer.

4.3 miR-33 involvement during liver regeneration

This study furthermore showed that *in vivo* inhibition of miR-33 using antisense oligonucleotides improved liver regeneration after partial hepatectomy. The *in vitro* findings were then verified in an *in vivo* model of liver regeneration induced by a 70% resection of the liver. The recovery of the liver function after hepatectomy is promoted by a variety of signals that lead to a prompt re-establishment of liver mass by upregulating cell growth and/or proliferation [130, 131]. Several proteins involved in regulating cell cycle progression play a key role during hepatocyte replication and liver growth [124, 132, 133]. Indeed, transient expression of CCND1 is sufficient to promote hepatocyte replication and liver growth *in vivo* [132]. D-and E- type cyclins and their CDK partners CDK4/6 regulate cell cycle progression through G1 to S phase [134]. Activation of the CCND1/CDK6 complex phosphorylates and inactivates the retinoblastoma protein, a repressor that in turn, inhibits the E2F transcription factor and recruits chromatin-remodeling complexes that lead to the repression of specific targeted genes.

In the normal adult liver, hepatocytes are highly differentiated and rarely undergo cell division, but they retain a remarkable ability for proliferation in response to an acute or chronic injury if necessary [113]. Previous studies have suggested that CCND1 is a critical mediator of G1 progression in hepatocytes. Similarly, CDK4/CDK6 regulate cell cycle progression in hepatoma cells. Accordingly, Huh7 and HepG2 cells, both human hepatocellular liver carcinoma cell lines, treated with PD_0332991, a potent inhibitor of these kinases, arrested the cells in the G1 phase [135].

In the present work, it was demonstrated that miR-33 targeted CCND1 and CDK6 and consequently regulated hepatocyte proliferation. In addition to CCND1 and CDK6, it has previously been reported that miR-33 also targets p53 and Pim-1. p53 activates the transcription of genes that induce cell cycle arrest, apoptosis and senescence in response to several stress conditions, including DNA damage. In our work, we did not find differences in the number of apoptotic cells when miR-33 was overexpressed or inhibited, suggesting that the effect of miR-33 on p53 and cell viability may be cell type-specific. On the other hand, Thomas M. *et al.* 2012 have recently shown that miR-33 also targets the serine/threonine-protein kinase Pim-1 and inhibits proliferation in K562 and LS174T cells [109].

The overall impact of miRNAs on liver regeneration has been studied by generating mice with hepatocyte-specific miRNA deficiency [136]. Song *et al.* addressed this question by 2/3 partial hepatectomy (PH) on mice with hepatocyte-specific inactivation of DiGeorge syndrome critical region gene 8 (DGCR8), an essential component of the miRNA processing pathway. These mice were viable and developed normally until adulthood. However, whereas miRNA-deficient hepatocytes readily exited the G0 phase of the cell cycle, they failed transition into the S phase by 36h after PH, suggesting a key role of miRNA in regulating liver regeneration. Examination of livers of wildtype mice after 2/3 PH revealed differential expression of a subset of miRNAs, notably an induction of miR-21 and repression of miR-378. It was further discovered that miR-21 directly inhibited Btg2, a cell cycle inhibitor that prevents activation of forkhead box M1 (FoxM1), which is essential for DNA synthesis in hepatocytes after 2/3 PH. In addition, miR-378 was found to directly inhibit ornithine decarboxylase (Odc1), which is known to promote DNA synthesis in hepatocytes after 2/3 PH [137].

The whole process of liver regeneration has three clearly distinct phases: an initiation stage, a proliferation stage and a termination stage [138]. Most research has focused on the first two stages. However, the participants at the stage of termination have not been well characterized so far. Most of the studies have focused on the anti proliferative role of transforming growth factor (TGF)-β1 [130]. However, the fact that transgenic mice displayed

a complete, although delayed, liver regeneration suggests that other mediators must be involved in this process [139]. In this context, our results support the idea that miR-33 may have a significant role in mediating the termination signal in the process of liver regeneration. These new findings could open new therapeutic perspectives to stimulate liver regeneration in chronic liver disease or after liver resection in patients affected by hepatocellular carcinoma.

4.4 miR-33: one miRNA, many targets

Currently, an important question in the miRNA field is whether these small regulatory molecules achieve their physiological impact through repression of a single or a few cardinal targets, or via the cumulative impact of impairing the expression of large sets of targets [145]. Whereas most experimental evidence supports the latter option, there are some reported cases where siRNA-mediated downregulation of one single gene resembled miRNA-mediated phenotypes. Namely, a specific knockdown of phosphatidylinositol-3,4,5-trisphosphate 5-phosphatase 1 (SHIP1) in the murine hematopoietic system following retroviral delivery of a miR-155-formatted siRNA against SHIP1 resulted in a myeloproliferative disorder, with striking similarities to the one observed in miRNA-155 overexpressing mice [146]. According to the data presented here, two critical cell cycle progression genes, whose expression is impaired simultaneously and directly by miR-33, could be identified. Importantly, as determined by gene-specific knockdown experiments, *Cdk6* gene was not capable by itself of phenocopying the liver regeneration effect of anti-miR-33 treatment in its whole magnitude. This supports the idea that the effect mediated by miR-33 is rather the consequence of a multiple synergistic small changes in the expression levels of various genes, than being attributable to the impaired expression of one single master gene.

4.5 Conditional miR-33 knockout

To understand the physiological role of miR-33 *in vivo*, a miR-33 conditional deficient mouse model was generated. Typically Cre-loxP mice are produced by using transgenic technology [140-142]. We used the Cre-loxP and the FLP-FRT systems as a genetic tool to enable cell type specific and/or inducible deletion of miR-33. The loxP and the FRT sites were placed in cis (same DNA strand) and the same directional orientation. This is a common approach, which results in a simple excision of the flanked element (**Fig. 24**). There are several advantages using this technique. First, in comparison to shRNA or siRNA experiments, the floxed gene or element will be completely deleted. Second, the model will provide an *in vivo* system spatial and temporally specific. Many mice carrying a Cre recombinase under the control of a tissue-specific promoter can be used to knock out the miR-33 in a "guided" manner. For example, albumin-Cre mice [143] will be crossed with miR-33$^{flox/flox}$ to enable access to a liver-specific miR-33 knock-out. Moreover, it facilitates the construction of a variety of Cre-mediated mouse models and Cre-inducible mice. This approach allowed us to study the effect of miR-33 in various and different tissues and models, *in vitro* and *in vivo*.

The targeting vector was constructed to flank the miR-33 genomic coding region (76bp) in intron 17 of the *Srebf2* gene with loxP recombination sites and to insert a neomycin selection cassette flanked by FRT sites (**Fig. 24**). We obtained chimeras and the mutated allele was successfully transmitted into the germ line. The selection cassette from the conditional allele was removed *in vivo*, with FLP-deleter mice as shown in **Fig. 24** [115, 116]. The sequence of the floxed miR-33 allele was confirmed by PCR-screening. miR-33$^{flox/flox}$ animals were fertile and appeared phenotypically normal. This suggests that the integrated loxP sites did not interfere with miR-33 transcription. Deletion of the floxed miR-33 genomic coding region was achieved with Cre-recombinase *in vivo* and *in vitro*. This Cre-mediated excision resulted in a complete loss of function of miR-33. No functional miR-33 was produced and this lead to a complete null phenotype. miR-33 was first deleted *in vivo* by crossing miR-33$^{flox/flox}$ mice with

an early Cre-expressing deleter EIIa-Cre strain [144]. This line carried a Cre transgene under the control of the adenovirus EIIa promoter that targets expression of Cre recombinase to the early mouse embryo. *Cre* expression is thought to occur prior implantation in the uterine wall. The deletion of miR-33 by the Cre-recombinase resulted in no phenotype.

4.6 Concluding remarks and outlook

Our data suggests a model in which miR-33a and miR-33b work in concert with their host genes *Srebf-2* and *Srebf-1*, respectively, to ensure a balanced metabolic state in the cell. During low cholesterol conditions miR-33a and miR-33b coexpressed with their host genes boost intracellular cholesterol levels by targeting ABCA1, reduce insulin signaling by targeting IRS2, and increase fatty acid levels by targeting a variety of fatty acid oxidation enzymes. Given that the abnormal regulation of these pathways leads to diseases such as atherosclerosis, metabolic syndrome and NAFLD, miR-33 could then represent an ideal target for future therapies [107].

In particular, the development of novel therapies to exploit the atheroprotective properties of HDL is an area of intense investigation. In randomized clinical trials raising plasma HDL by augmenting ApoA-1 levels or treating with niacin have shown direct benefits in patients with coronary artery disease, including reduced cardiovascular event rates and plaque volume [147, 148]. Previous studies have shown that inhibition of miR-33a in mice is an effective strategy to raise plasma HDL [99-101], and to enhance reverse cholesterol transport and regress atherosclerotic plaques [104]. Although promising, these studies in mice are limited in their translational insight due to the lack of miR-33b expression, which may contribute substantially to miR-33 levels in humans. Rayner *et al.* recently published in Nature a study regarding this feature, showing for the first time in non-human primates that inhibiting both, miR-33a and miR-33b, has a profound and sustained effect on circulating plasma HDL levels [149]. Importantly, this study also established that miR-33 antagonism markedly suppresses plasma VLDL triglyceride levels, in part attributable to the regulation of key genes involved in

fatty acid oxidation and synthesis [103, 105]. As low HDL and high VLDL triglycerides are commonly associated with metabolic syndrome [150], miR-33 inhibitors may have clinical utility for the treatment of this growing health concern. These findings in non-human primates support the development of antagonists of miR-33 as potential therapeutics for dyslipidemia, atherosclerosis, and related metabolic diseases.

Furthermore, our results revealed that the decreased expression of miR-33 during liver regeneration causes proliferation in hepatocytes. This raises the possibility of using anti-oligonucleotides of miR-33 for therapy in liver failure. They may be effective in accelerating progression of hepatocytes through G1 and into S phase, which is critical for survival after liver injury [151].

REFERENCES

1. Brown, M.S. and J.L. Goldstein, *Receptor-mediated control of cholesterol metabolism.* Science, 1976. 191(4223): p. 150-4.
2. Chen, H.W., H.J. Heiniger, and A.A. Kandutsch, *Relationship between sterol synthesis and DNA synthesis in phytohemagglutinin-stimulated mouse lymphocytes.* Proc Natl Acad Sci U S A, 1975. 72(5): p. 1950-4.
3. Chen, H.W., A.A. Kandutsch, and C. Waymouth, *Inhibition of cell growth by oxygenated derivatives of cholesterol.* Nature, 1974. 251(5474): p. 419-21.
4. Fernandez, C., et al., *Cholesterol is essential for mitosis progression and its deficiency induces polyploid cell formation.* Exp Cell Res, 2004. 300(1): p. 109-20.
5. Glass, C.K. and J.L. Witztum, *Atherosclerosis. the road ahead.* Cell, 2001. 104(4): p. 503-16.
6. Maxfield, F.R. and I. Tabas, *Role of cholesterol and lipid organization in disease.* Nature, 2005. 438(7068): p. 612-21.
7. Grundy, S.M., *Absorption and metabolism of dietary cholesterol.* Annu Rev Nutr, 1983. 3: p. 71-96.
8. Bloch, K., *Summing up.* Annu Rev Biochem, 1987. 56: p. 1-19.
9. Brown, M.S. and J.L. Goldstein, *A receptor-mediated pathway for cholesterol homeostasis.* Science, 1986. 232(4746): p. 34-47.
10. Goldstein, J.L. and M.S. Brown, *Regulation of the mevalonate pathway.* Nature, 1990. 343(6257): p. 425-30.
11. Brown, M.S. and J.L. Goldstein, *The SREBP pathway: regulation of cholesterol metabolism by proteolysis of a membrane-bound transcription factor.* Cell, 1997. 89(3): p. 331-40.
12. Sakakura, Y., et al., *Sterol regulatory element-binding proteins induce an entire pathway of cholesterol synthesis.* Biochem Biophys Res Commun, 2001. 286(1): p. 176-83.
13. Horton, J.D., J.L. Goldstein, and M.S. Brown, *SREBPs: activators of the complete program of cholesterol and fatty acid synthesis in the liver.* J Clin Invest, 2002. 109(9): p. 1125-31.
14. Osborne, T.F., *Sterol regulatory element-binding proteins (SREBPs): key regulators of nutritional homeostasis and insulin action.* J Biol Chem, 2000. 275(42): p. 32379-82.
15. Eberhard, Y., et al., *Inhibition of SREBP1 sensitizes cells to death ligands.* Oncotarget, 2011. 2(3): p. 186-96.
16. Peet, D.J., B.A. Janowski, and D.J. Mangelsdorf, *The LXRs: a new class of oxysterol receptors.* Curr Opin Genet Dev, 1998. 8(5): p. 571-5.
17. Tall, A.R., et al., *HDL, ABC transporters, and cholesterol efflux: implications for the treatment of atherosclerosis.* Cell Metab, 2008. 7(5): p. 365-75.
18. Tall, A.R., *Cholesterol efflux pathways and other potential mechanisms involved in the athero-protective effect of high density lipoproteins.* Journal of internal medicine, 2008. 263(3): p. 256-73.
19. Linsel-Nitschke, P. and A.R. Tall, *HDL as a target in the treatment of atherosclerotic cardiovascular disease.* Nat Rev Drug Discov, 2005. 4(3): p. 193-205.
20. Moore, K.J., et al., *microRNAs and cholesterol metabolism.* Trends Endocrinol Metab, 2010. 21(12): p. 699-706.
21. Coller, H.A., *What's taking so long? S-phase entry from quiescence versus proliferation.* Nat Rev Mol Cell Biol, 2007. 8(8): p. 667-70.
22. Pardee, A.B., *A restriction point for control of normal animal cell proliferation.* Proc Natl Acad Sci U S A, 1974. 71(4): p. 1286-90.
23. Planas-Silva, M.D. and R.A. Weinberg, *The restriction point and control of cell proliferation.* Curr Opin Cell Biol, 1997. 9(6): p. 768-72.

24.   Mac Auley, A., Z. Werb, and P.E. Mirkes, *Characterization of the unusually rapid cell cycles during rat gastrulation.* Development, 1993. 117(3): p. 873-83.

25.   Savatier, P., et al., *Contrasting patterns of retinoblastoma protein expression in mouse embryonic stem cells and embryonic fibroblasts.* Oncogene, 1994. 9(3): p. 809-18.

26.   Thomson, J.A., et al., *Embryonic stem cell lines derived from human blastocysts.* Science, 1998. 282(5391): p. 1145-7.

27.   Varmuza, S., et al., *Polytene chromosomes in mouse trophoblast giant cells.* Development, 1988. 102(1): p. 127-34.

28.   Morgan, D.O., *Cyclin-dependent kinases: engines, clocks, and microprocessors.* Annu Rev Cell Dev Biol, 1997. 13: p. 261-91.

29.   Murray, A.W., *Recycling the cell cycle: cyclins revisited.* Cell, 2004. 116(2): p. 221-34.

30.   Hadwiger, J.A., et al., *A family of cyclin homologs that control the G1 phase in yeast.* Proc Natl Acad Sci U S A, 1989. 86(16): p. 6255-9.

31.   Nash, R., et al., *The WHI1+ gene of Saccharomyces cerevisiae tethers cell division to cell size and is a cyclin homolog.* EMBO J, 1988. 7(13): p. 4335-46.

32.   Sanchez, I. and B.D. Dynlacht, *New insights into cyclins, CDKs, and cell cycle control.* Semin Cell Dev Biol, 2005. 16(3): p. 311-21.

33.   Bates, S., et al., *Absence of cyclin D/cdk complexes in cells lacking functional retinoblastoma protein.* Oncogene, 1994. 9(6): p. 1633-40.

34.   Matsushime, H., et al., *Identification and properties of an atypical catalytic subunit (p34PSK-J3/cdk4) for mammalian D type G1 cyclins.* Cell, 1992. 71(2): p. 323-34.

35.   Meyerson, M. and E. Harlow, *Identification of G1 kinase activity for cdk6, a novel cyclin D partner.* Mol Cell Biol, 1994. 14(3): p. 2077-86.

36.   Dulic, V., E. Lees, and S.I. Reed, *Association of human cyclin E with a periodic G1-S phase protein kinase.* Science, 1992. 257(5078): p. 1958-61.

37.   Gudas, J.M., et al., *Cyclin E2, a novel G1 cyclin that binds Cdk2 and is aberrantly expressed in human cancers.* Mol Cell Biol, 1999. 19(1): p. 612-22.

38.   Koff, A., et al., *Formation and activation of a cyclin E-cdk2 complex during the G1 phase of the human cell cycle.* Science, 1992. 257(5077): p. 1689-94.

39.   Lauper, N., et al., *Cyclin E2: a novel CDK2 partner in the late G1 and S phases of the mammalian cell cycle.* Oncogene, 1998. 17(20): p. 2637-43.

40.   Leone, G., et al., *Collaborative role of E2F transcriptional activity and G1 cyclindependent kinase activity in the induction of S phase.* Proc Natl Acad Sci U S A, 1999. 96(12): p. 6626-31.

41.   Zariwala, M., J. Liu, and Y. Xiong, *Cyclin E2, a novel human G1 cyclin and activating partner of CDK2 and CDK3, is induced by viral oncoproteins.* Oncogene, 1998. 17(21): p. 2787-98.

42.   Coverley, D., et al., *Chromatin-bound Cdc6 persists in S and G2 phases in human cells, while soluble Cdc6 is destroyed in a cyclin A-cdk2 dependent process.* J Cell Sci, 2000. 113 (Pt 11): p. 1929-38.

43.   Petersen, B.O., et al., *Phosphorylation of mammalian CDC6 by cyclin A/CDK2 regulates its subcellular localization.* EMBO J, 1999. 18(2): p. 396-410.

44.   Yan, Y., et al., *Ablation of the CDK inhibitor p57Kip2 results in increased apoptosis and delayed differentiation during mouse development.* Genes Dev, 1997. 11(8): p. 973-83.

45.   Girard, F., et al., *Cyclin A is required for the onset of DNA replication in mammalian fibroblasts.* Cell, 1991. 67(6): p. 1169-79.

46.   Pagano, M., et al., *Cyclin A is required at two points in the human cell cycle.* EMBO J, 1992. 11(3): p. 961-71.

47.   Furuno, N., N. den Elzen, and J. Pines, *Human cyclin A is required for mitosis until mid prophase.* J Cell Biol, 1999. 147(2): p. 295-306.

48.   den Elzen, N. and J. Pines, *Cyclin A is destroyed in prometaphase and can delay chromosome alignment and anaphase.* J Cell Biol, 2001. 153(1): p. 121-36.

49.   Minshull, J., et al., *The A- and B-type cyclin associated cdc2 kinases in Xenopus turn on and off at different times in the cell cycle.* EMBO J, 1990. 9(9): p. 2865-75.

50.   Draetta, G., et al., *Cdc2 protein kinase is complexed with both cyclin A and B: evidence for proteolytic inactivation of MPF.* Cell, 1989. 56(5): p. 829-38.

51.   Obaya, A.J. and J.M. Sedivy, *Regulation of cyclin-Cdk activity in mammalian cells.* Cell Mol Life Sci, 2002. 59(1): p. 126-42.

52.   Wheatley, S.P., et al., *CDK1 inactivation regulates anaphase spindle dynamics and cytokinesis in vivo.* J Cell Biol, 1997. 138(2): p. 385-93.

53.   Sherr, C.J. and J.M. Roberts, *CDK inhibitors: positive and negative regulators of G1-phase progression.* Genes Dev, 1999. 13(12): p. 1501-12.

54.   Silver, D.L. and D.J. Montell, *A new trick for Cyclin-Cdk: activation of STAT.* Dev Cell, 2003. 4(2): p. 148-9.

55.   Satyanarayana, A. and P. Kaldis, *Mammalian cell-cycle regulation: several Cdks, numerous cyclins and diverse compensatory mechanisms.* Oncogene, 2009. 28(33): p. 2925-39.

56.   Ambros, V., *The functions of animal microRNAs.* Nature, 2004. 431(7006): p. 350-5.

57.   Ambros, V., *MicroRNA pathways in flies and worms: growth, death, fat, stress, and timing.* Cell, 2003. 113(6): p. 673-6.

58.   Bartel, D.P., *MicroRNAs: target recognition and regulatory functions.* Cell, 2009. 136(2): p. 215-33.

59.   Filipowicz, W., S.N. Bhattacharyya, and N. Sonenberg, *Mechanisms of post-transcriptional regulation by microRNAs: are the answers in sight?* Nat Rev Genet, 2008. 9(2): p. 102-14.

60.   Lee, R.C., R.L. Feinbaum, and V. Ambros, *The C. elegans heterochronic gene lin-4 encodes small RNAs with antisense complementarity to lin-14.* Cell, 1993. 75(5): p. 843-54.

61.   Wightman, B., I. Ha, and G. Ruvkun, *Posttranscriptional regulation of the heterochronic gene lin-14 by lin-4 mediates temporal pattern formation in C. elegans.* Cell, 1993. 75(5): p. 855-62.

62.   Hendrickson, D.G., et al., *Concordant regulation of translation and mRNA abundance for hundreds of targets of a human microRNA.* PLoS Biol, 2009. 7(11): p. e1000238.

63.   Friedman, R.C., et al., *Most mammalian mRNAs are conserved targets of microRNAs.* Genome Res, 2009. 19(1): p. 92-105.

64.   Griffiths-Jones, S., et al., *miRBase: tools for microRNA genomics.* Nucleic Acids Res, 2008. 36(Database issue): p. D154-8.

65.   Bushati, N. and S.M. Cohen, *microRNA functions.* Annu Rev Cell Dev Biol, 2007. 23: p. 175-205.

66.   Chang, T.C. and J.T. Mendell, *microRNAs in vertebrate physiology and human disease.* Annu Rev Genomics Hum Genet, 2007. 8: p. 215-39.

67.   Esquela-Kerscher, A. and F.J. Slack, *Oncomirs - microRNAs with a role in cancer.* Nat Rev Cancer, 2006. 6(4): p. 259-69.

68.   Krutzfeldt, J. and M. Stoffel, *MicroRNAs: a new class of regulatory genes affecting metabolism.* Cell Metab, 2006. 4(1): p. 9-12.

69.   Lynn, F.C., *Meta-regulation: microRNA regulation of glucose and lipid metabolism.* Trends Endocrinol Metab, 2009. 20(9): p. 452-9.

70.   Suarez, Y. and W.C. Sessa, *MicroRNAs as novel regulators of angiogenesis.* Circ Res, 2009. 104(4): p. 442-54.

71.   Kim, V.N., J. Han, and M.C. Siomi, *Biogenesis of small RNAs in animals.* Nat Rev Mol Cell Biol, 2009. 10(2): p. 126-39.

72.   Kim, Y.K. and V.N. Kim, *Processing of intronic microRNAs.* EMBO J, 2007. 26(3): p. 775-83.

73.   Okamura, K., et al., *The mirtron pathway generates microRNA-class regulatory RNAs in Drosophila.* Cell, 2007. 130(1): p. 89-100.

74.   Ruby, J.G., C.H. Jan, and D.P. Bartel, *Intronic microRNA precursors that bypass Drosha processing.* Nature, 2007. 448(7149): p. 83-6.

75.   Cheloufi, S., et al., *A dicer-independent miRNA biogenesis pathway that requires Ago catalysis.* Nature, 2010. 465(7298): p. 584-9.

76. Cifuentes, D., et al., *A novel miRNA processing pathway independent of Dicer requires Argonaute2 catalytic activity.* Science, 2010. 328(5986): p. 1694-8.

77. Rasmussen, K.D., et al., *The miR-144/451 locus is required for erythroid homeostasis.* J Exp Med, 2010. 207(7): p. 1351-8.

78. Forman, J.J. and H.A. Coller, *The code within the code: microRNAs target coding regions.* Cell Cycle, 2010. 9(8): p. 1533-41.

79. Lytle, J.R., T.A. Yario, and J.A. Steitz, *Target mRNAs are repressed as efficiently by microRNA-binding sites in the 5' UTR as in the 3' UTR.* Proc Natl Acad Sci U S A, 2007. 104(23): p. 9667-72.

80. Orom, U.A., F.C. Nielsen, and A.H. Lund, *MicroRNA-10a binds the 5'UTR of ribosomal protein mRNAs and enhances their translation.* Mol Cell, 2008. 30(4): p. 460-71.

81. Rigoutsos, I., *New tricks for animal microRNAS: targeting of amino acid coding regions at conserved and nonconserved sites.* Cancer Res, 2009. 69(8): p. 3245-8.

82. Calin, G.A., et al., *Human microRNA genes are frequently located at fragile sites and genomic regions involved in cancers.* Proc Natl Acad Sci U S A, 2004. 101(9): p. 2999-3004.

83. Raveche, E.S., et al., *Abnormal microRNA-16 locus with synteny to human 13q14 linked to CLL in NZB mice.* Blood, 2007. 109(12): p. 5079-86.

84. Linsley, P.S., et al., *Transcripts targeted by the microRNA-16 family cooperatively regulate cell cycle progression.* Mol Cell Biol, 2007. 27(6): p. 2240-52.

85. Chen, Y. and R.L. Stallings, *Differential patterns of microRNA expression in neuroblastoma are correlated with prognosis, differentiation, and apoptosis.* Cancer Res, 2007. 67(3): p. 976-83.

86. Welch, C., Y. Chen, and R.L. Stallings, *MicroRNA-34a functions as a potential tumor suppressor by inducing apoptosis in neuroblastoma cells.* Oncogene, 2007. 26(34): p. 5017-22.

87. He, L., et al., *A microRNA component of the p53 tumour suppressor network.* Nature, 2007. 447(7148): p. 1130-4.

88. Chang, T.C., et al., *Transactivation of miR-34a by p53 broadly influences gene expression and promotes apoptosis.* Mol Cell, 2007. 26(5): p. 745-52.

89. Raver-Shapira, N., et al., *Transcriptional activation of miR-34a contributes to p53-mediated apoptosis.* Mol Cell, 2007. 26(5): p. 731-43.

90. Tarasov, V., et al., *Differential regulation of microRNAs by p53 revealed by massively parallel sequencing: miR-34a is a p53 target that induces apoptosis and G1-arrest.* Cell Cycle, 2007. 6(13): p. 1586-93.

91. Liu, M., et al., *miR-137 targets Cdc42 expression, induces cell cycle G1 arrest and inhibits invasion in colorectal cancer cells.* Int J Cancer, 2011. 128(6): p. 1269-79.

92. Brown, M.S. and J.L. Goldstein, *Suppression of 3-hydroxy-3-methylglutaryl coenzyme A reductase activity and inhibition of growth of human fibroblasts by 7-ketocholesterol.* J Biol Chem, 1974. 249(22): p. 7306-14.

93. Martinez-Botas, J., et al., *Cholesterol starvation decreases p34(cdc2) kinase activity and arrests the cell cycle at G2.* FASEB J, 1999. 13(11): p. 1359-70.

94. Crick, D.C., D.A. Andres, and C.J. Waechter, *Geranylgeraniol promotes entry of UT-2 cells into the cell cycle in the absence of mevalonate.* Exp Cell Res, 1997. 231(2): p. 302-7.

95. Martinez-Botas, J., et al., *Dose-dependent effects of lovastatin on cell cycle progression. Distinct requirement of cholesterol and non-sterol mevalonate derivatives.* Biochim Biophys Acta, 2001. 1532(3): p. 185-94.

96. Bengoechea-Alonso, M.T. and J. Ericsson, *Cdk1/cyclin B-mediated phosphorylation stabilizes SREBP1 during mitosis.* Cell Cycle, 2006. 5(15): p. 1708-18.

97. Inoue, N., et al., *Lipid synthetic transcription factor SREBP-1a activates p21WAF1/CIP1, a universal cyclin-dependent kinase inhibitor.* Mol Cell Biol, 2005. 25(20): p. 8938-47.

98.   Nakakuki, M., et al., *A transcription factor of lipid synthesis, sterol regulatory element-binding protein (SREBP)-1a causes G(1) cell-cycle arrest after accumulation of cyclin-dependent kinase (cdk) inhibitors.* FEBS J, 2007. 274(17): p. 4440-52.

99.   Marquart, T.J., et al., *miR-33 links SREBP-2 induction to repression of sterol transporters.* Proc Natl Acad Sci U S A, 2010. 107(27): p. 12228-32.

100. Najafi-Shoushtari, S.H., et al., *MicroRNA-33 and the SREBP host genes cooperate to control cholesterol homeostasis.* Science, 2010. 328(5985): p. 1566-9.

101. Rayner, K.J., et al., *MiR-33 contributes to the regulation of cholesterol homeostasis.* Science, 2010. 328(5985): p. 1570-3.

102. Horie, T., et al., *MicroRNA-33 encoded by an intron of sterol regulatory element-binding protein 2 (Srebp2) regulates HDL in vivo.* Proc Natl Acad Sci U S A, 2010. 107(40): p. 17321-6.

103. Gerin, I., et al., *Expression of miR-33 from an SREBP2 intron inhibits cholesterol export and fatty acid oxidation.* J Biol Chem, 2010. 285(44): p. 33652-61.

104. Rayner, K.J., et al., *Antagonism of miR-33 in mice promotes reverse cholesterol transport and regression of atherosclerosis.* J Clin Invest, 2011. 121(7): p. 2921-31.

105. Davalos, A., et al., *miR-33a/b contribute to the regulation of fatty acid metabolism and insulin signaling.* Proc Natl Acad Sci U S A, 2011. 108(22): p. 9232-7.

106. Hardie, D.G. and D.A. Pan, *Regulation of fatty acid synthesis and oxidation by the AMP-activated protein kinase.* Biochem Soc Trans, 2002. 30(Pt 6): p. 1064-70.

107. Ramirez, C.M., L. Goedeke, and C. Fernandez-Hernando, *"Micromanaging" metabolic syndrome.* Cell Cycle, 2011. 10(19): p. 3249-52.

108. Herrera-Merchan, A., et al., *miR-33-mediated downregulation of p53 controls hematopoietic stem cell self-renewal.* Cell Cycle, 2010. 9(16): p. 3277-85.

109. Thomas, M., et al., *The proto-oncogene Pim-1 is a target of miR-33a.* Oncogene, 2012. 31(7): p. 918-28.

110. van Rooij, E., et al., *Control of stress-dependent cardiac growth and gene expression by a microRNA.* Science, 2007. 316(5824): p. 575-9.

111. Kaartinen, V. and A. Nagy, *Removal of the floxed neo gene from a conditional knockout allele by the adenoviral Cre recombinase in vivo.* Genesis, 2001. 31(3): p. 126-9.

112. Mitchell, C. and H. Willenbring, *A reproducible and well-tolerated method for 2/3 partial hepatectomy in mice.* Nat Protoc, 2008. 3(7): p. 1167-70.

113. Fausto, N., *Liver regeneration and repair: hepatocytes, progenitor cells, and stem cells.* Hepatology, 2004. 39(6): p. 1477-87.

114. Glende, E.A., Jr. and W.S. Morgan, *Alteration in liver lipid and lipid fatty acid composition after partial hepatectomy in the rat.* Exp Mol Pathol, 1968. 8(2): p. 190-200.

115. Farley, F.W., et al., *Widespread recombinase expression using FLPeR (flipper) mice.* Genesis, 2000. 28(3-4): p. 106-10.

116. Rodriguez, C.I., et al., *High-efficiency deleter mice show that FLPe is an alternative to Cre-loxP.* Nat Genet, 2000. 25(2): p. 139-40.

117. Bartel, D.P. and C.Z. Chen, *Micromanagers of gene expression: the potentially widespread influence of metazoan microRNAs.* Nat Rev Genet, 2004. 5(5): p. 396-400.

118. Fernandez-Hernando, C., et al., *MicroRNAs in lipid metabolism.* Curr Opin Lipidol, 2011. 22(2): p. 86-92.

119. Krutzfeldt, J., et al., *Silencing of microRNAs in vivo with 'antagomirs'.* Nature, 2005. 438(7068): p. 685-9.

120. Elmen, J., et al., *Antagonism of microRNA-122 in mice by systemically administered LNA-antimiR leads to up-regulation of a large set of predicted target mRNAs in the liver.* Nucleic Acids Res, 2008. 36(4): p. 1153-62.

121. Esau, C., et al., *miR-122 regulation of lipid metabolism revealed by in vivo antisense targeting.* Cell Metab, 2006. 3(2): p. 87-98.

122. Elmen, J., et al., *LNA-mediated microRNA silencing in non-human primates.* Nature, 2008. 452(7189): p. 896-9.

123. Munoz, M.A., et al., *The E3 ubiquitin ligase EDD regulates S-phase and G(2)/M DNA damage checkpoints.* Cell Cycle, 2007. 6(24): p. 3070-7.
124. Boylan, J.M. and P.A. Gruppuso, *D-type cyclins and G1 progression during liver development in the rat.* Biochem Biophys Res Commun, 2005. 330(3): p. 722-30.
125. Bueno, M.J. and M. Malumbres, *MicroRNAs and the cell cycle.* Biochim Biophys Acta, 2011. 1812(5): p. 592-601.
126. Takeshita, F., et al., *Systemic delivery of synthetic microRNA-16 inhibits the growth of metastatic prostate tumors via downregulation of multiple cell-cycle genes.* Mol Ther, 2010. 18(1): p. 181-7.
127. Wang, F., et al., *Down-regulation of the cyclin E1 oncogene expression by microRNA-16-1 induces cell cycle arrest in human cancer cells.* BMB Rep, 2009. 42(11): p. 725-30.
128. Lee, Y.S. and A. Dutta, *MicroRNAs in cancer.* Annu Rev Pathol, 2009. 4: p. 199-227.
129. Mayr, C., M.T. Hemann, and D.P. Bartel, *Disrupting the pairing between let-7 and Hmga2 enhances oncogenic transformation.* Science, 2007. 315(5818): p. 1576-9.
130. Michalopoulos, G.K., *Liver regeneration.* J Cell Physiol, 2007. 213(2): p. 286-300.
131. Overturf, K., et al., *Serial transplantation reveals the stem-cell-like regenerative potential of adult mouse hepatocytes.* Am J Pathol, 1997. 151(5): p. 1273-80.
132. Hanse, E.A., et al., *Cdk2 plays a critical role in hepatocyte cell cycle progression and survival in the setting of cyclin D1 expression in vivo.* Cell Cycle, 2009. 8(17): p. 2802-9.
133. Kato, A., et al., *Relationship between expression of cyclin D1 and impaired liver regeneration observed in fibrotic or cirrhotic rats.* J Gastroenterol Hepatol, 2005. 20(8): p. 1198-205.
134. Nurse, P., *Checkpoint pathways come of age.* Cell, 1997. 91(7): p. 865-7.
135. Rivadeneira, D.B., et al., *Proliferative suppression by CDK4/6 inhibition: complex function of the retinoblastoma pathway in liver tissue and hepatoma cells.* Gastroenterology, 2010. 138(5): p. 1920-30.
136. Song, G., et al., *MicroRNAs control hepatocyte proliferation during liver regeneration.* Hepatology, 2010. 51(5): p. 1735-43.
137. Song, G., et al., *MicroRNAs control hepatocyte proliferation during liver regeneration.* Hepatology (Baltimore, Md.), 2010. 51(5): p. 1735-43.
138. Michalopoulos, G.K. and M.C. DeFrances, *Liver regeneration.* Science, 1997. 276(5309): p. 60-6.
139. Sanderson, N., et al., *Hepatic expression of mature transforming growth factor beta 1 in transgenic mice results in multiple tissue lesions.* Proc Natl Acad Sci U S A, 1995. 92(7): p. 2572-6.
140. Nagy, A., *Cre recombinase: the universal reagent for genome tailoring.* Genesis, 2000. 26(2): p. 99-109.
141. Sadowski, P.D., *The Flp recombinase of the 2-microns plasmid of Saccharomyces cerevisiae.* Prog Nucleic Acid Res Mol Biol, 1995. 51: p. 53-91.
142. Sauer, B. and N. Henderson, *Site-specific DNA recombination in mammalian cells by the Cre recombinase of bacteriophage P1.* Proc Natl Acad Sci U S A, 1988. 85(14): p. 5166-70.
143. Dirkx, R., et al., *Absence of peroxisomes in mouse hepatocytes causes mitochondrial and ER abnormalities.* Hepatology, 2005. 41(4): p. 868-78.
144. Schwenk, F., U. Baron, and K. Rajewsky, *A cre-transgenic mouse strain for the ubiquitous deletion of loxP-flanked gene segments including deletion in germ cells.* Nucleic Acids Res, 1995. 23(24): p. 5080-1.
145. Wallach, D. and A. Kovalenko, *12th international TNF conference: the good, the bad and the scientists.* Cytokine Growth Factor Rev, 2009. 20(4): p. 259-69.
146. O'Connell, R.M., et al., *Inositol phosphatase SHIP1 is a primary target of miR-155.* Proc Natl Acad Sci U S A, 2009. 106(17): p. 7113-8.
147. Degoma, E.M. and D.J. Rader, *Novel HDL-directed pharmacotherapeutic strategies.* Nat Rev Cardiol, 2011. 8(5): p. 266-77.

148. Chyu, K.Y., A. Peter, and P.K. Shah, *Progress in HDL-based therapies for atherosclerosis.* Curr Atheroscler Rep, 2011. 13(5): p. 405-12.

149. Rayner, K.J., et al., *Inhibition of miR-33a/b in non-human primates raises plasma HDL and lowers VLDL triglycerides.* Nature, 2011. 478(7369): p. 404-7.

150. Alberti, K.G., et al., *Harmonizing the metabolic syndrome: a joint interim statement of the International Diabetes Federation Task Force on Epidemiology and Prevention; National Heart, Lung, and Blood Institute; American Heart Association; World Heart Federation; International Atherosclerosis Society; and International Association for the Study of Obesity.* Circulation, 2009. 120(16): p. 1640-5.

151. Clavien, P.A., et al., *Strategies for safer liver surgery and partial liver transplantation.* N Engl J Med, 2007. 356(15): p. 1545-59.

ACKNOWLEDGEMENTS

First and foremost, I would like to say that I had a great time at the DRFZ and NYU Medical Center and would like to thank all of you who made this time so pleasant and scientifically fruitful.

This work would not have been possible without the generous intellectual and unconditional emotional support provided by innumerous colleagues, friends and my family. Now that I am about to seal this important phase of my life, I feel this uncontrollable necessity of expressing my deepest gratitude and respect to all of you.

In particular, I wish to express my deep gratitude to **Carlos Fernández-Hernando** and **Enric Esplugues**, my principle supervisors, who supported me and my work in Berlin and New York with tremendous efforts. Without your encouragement and guidance, I could have never conducted this dissertation. You gave me the change to become a self-confident researcher and fully supported my work. Dear Carlos and dear Enric, thank you so much for this wonderful years in Berlin and New York.

Likewise, special thanks go to **Yajaira Suárez** for her excellent support and for sharing all her expert knowledge with me.

Thank you to **Prof. Kloetzel** for the supervision of my thesis as a representative for the faculty of biology, and to the other members of my PhD thesis committee, **Prof. Theuring**, **Prof. Hauser, Prof. Sommer, Prof. Grimm** and **Dr. Or-Guil**, for kindly accepting to be part of the evaluation process. Special thanks go to **Prof. Franken** for accepting and being my Vorsitzender.

I would like to express my sincere gratitude to all my colleagues in **Fernández-Hernando´s** and **Suárez´s** lab which all contributed to this work. Thanks go to **Cristina Ramírez-Hidalgo** and **Leigh Goedecke** for your helpful comments and discussion, teaching me techniques

APPENDIX

PUBLICATIONS

1. Dávalos A, Goedeke L., Smibert P, Ramírez C.M.., Warrier N. P., Andreo U., <u>Cirera-Salinas D.</u>, Rayner K, Suresh U., Pastor-Pareja JC., Esplugues E., Fishera E.A., Penalva L.O. , Moore K J., Suárez Y., Lai E. C., Fernández-Hernando C*.,"miR-33a/b contribute to the regulation of fatty acid metabolism and insulin signaling"*. 2011. ***Proc. Nat. Aca. Sci***.

2. Ramírez C.M., Dávalos A, Goedeke L., Salerno AG., <u>Cirera-Salinas D.</u>, Suárez Y., Fernández-Hernando C*.,"miR-758 regulates chol.estherol efflux thourhh post-transcriptional repression of ABCA1".* 2011. ***Arteriosc. Thromb. And Vasc. Biol.***

3. <u>Cirera-Salinas D</u>, Pauta M, Allen RM, Salerno AG, Ramírez CM, Chamorro-Jorganes A, Wanschel AC, Lasuncion MA, Morales-Ruiz M, Suarez Y, Baldan A, Esplugues E, Fernández-Hernando C., "**Mir-33 regulates cell proliferation and cell cycle progression**". 2012. ***Cell Cycle***.

4. Ramírez C.M., Rotllan N., Vlassov A.V., Dávalos A., Li M., Goedeke L., <u>Cirera-Salinas D.</u>, Kim J., Araldi E., Yoon H., Salerno A., Wanschel A., Nelson P.T., Castrillo A., Kim J., Suárez Y. and Fernández-Hernando C*.,"Control of cholesterol metabolism and plasma HDL levels by miR-144"*. 2012. ***Cell Metabolism (Under Revision)***.

5. Goedeke L, Fenstermaker M, <u>Cirera-Salinas D</u>, Vales F, Chamorro-Jorganes A, Suárez Y and Fernández-Hernando, C. "**A regulatory role for miRNA-33* in controlling lipid metabolism gene expression**". 2012. **Science Signaling** *(Submitted)*.

COMMUNICATIONS AND CONGRESS

- 7th Annual ELSO Meeting (ELSO & EMBO), 30 August- 2 September 2008, Nice (France). Analyzing the *in vivo* function of Plakophilin 4 (Pkp4/p0071). Daniel Cirera-Salinas, Markus Irgang, Jörg Isensee, Henning Witt and Patricia Ruiz Noppinger.

- RCIS Berlin Immunology Day November 12th 2009

- NeuroCure Retreat 2009 (November 26th-27th, 2009 in Hermannswerder, Potsdam, Germany)

- T cells - Subsets and Functions (June 30th-July 1st, 2010 in Marburg, Germany)

- Ramírez C.M., Dávalos A, Goedeke L., Salerno AG., Cirera-Salinas D., Suárez Y., Fernández-Hernando C.,"miR-758 regulates cholestherol efflux thourhh post-transcriptional repression of ABCA1". DEUEL conference of Lipids 2011.NAPA, California.

- Goedeke L., Dávalos A., Smibert P, Ramírez C.M., Warrier N. P., Andreo U., Cirera-Salinas D., Rayner K, Esplugues E., Fishera E.A., Moore K J., Suárez Y., Lai E. C., Fernández-Hernando C.,"miR-33a/b contribute to the regulation of fatty acid metabolism and insulin signaling". Deul Conference on Lipids, Poster Session, Nappa Valley CA, 2011.

- Th17 cells in Health and Disease. Organizers: Cheng Dong, Vijay K. Kuchroo, Jay K. Kolls and Brigitta Stockinger. (February 5-10, 2012; Keystone Resort, Keystone, Colorado, USA).

- 8th Spring School on Immunology, 11.-16.03.2012, Ettal (Germany). Organizing Committee: Friederike Berberich-Siebelt (Würzburg), Christine Falk (Hannover), Robert Jack (Greifswald), Michael Lohoff (Marburg), Fritz Melchers (Berlin), Andreas Radbruch (Berlin), Hendrik Schulze-Koops (München). Deutsche Gesellschaft für Immunologie.

- **miR-33 connects cholesterol to the cell cycle**. Inukai S, Slack FJ. Departament of Molecular, Cellular and Developmental Biology, Yale University, New Haven, CT, USA. Comment on: Cirera-Salinas D, *et al*. ***Cell Cycle*** 2012; 11:922-33.

- **A role of miR-33 for cell cycle progression and cell proliferation**. Iwakiri Y. Section of Digestive Diseases, Department of Internal Medicine, Yale University, New Haven, CT, USA. Comment on: Cirera-Salinas D, *et al*. ***Cell Cycle*** 2012; 11:922-33.

- **miR-33 regulates cell proliferation and cell cycle progression.** Riedmann EM. Landes Highlights. Comment on: Cirera-Salinas D, et al. ***RNA Biol.*** 2012;9(3)

HONORS AND AWARDS

- Invited guest speaker 22nd Annual Conference of the German Society for Cytometry.(Bonn, Germany. 2012)

- Invited guest speaker "Next Generation Sequencing - Application cases and bioinformatics development". German-Italian Dialogue (Naples, Italy. 2012)

- Travel grant award. 7th Annual ELSO/EMBO Meeting (Nice, France. 2008)

- Research Fellowship ARGO (ARGO/DE/0752/1) (2008-2009)

EIDESSTATTLICHE ERKLÄRUNG

Hiermit erkläre ich, dass ich die vorliegende Dissertation selbständig und nur unter Verwertung der angegebenen Hilfsmittel erarbeitet und verfasst habe. Diese Arbeit wurde keiner anderen Prüfungsbehörde vorgelegt.

Berlin,

Daniel Cirera Salinas